SEA GRANT PROJECT OFFICE

THE APPLICATION OF HYDROACOUSTIC METHODS FOR AQUATIC BIOMASS MEASUREMENTS

BY
J. B. LOZOW
J. B. SUOMALA, JR.

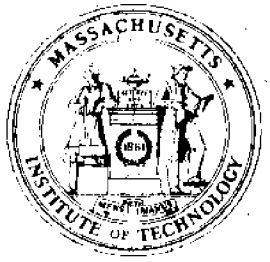

Massachusetts Institute of Technology

Cambridge, Massachusetts 02139

Report No. MITSG 72-8
March 1, 1972

The Application of Hydroacoustic Methods For Aquatic Biomass Measurements

A Note on Echo Envelope Sampling and Integration

by

J. B. Lozow

J. B. Suomala, Jr.

Report No. MITSG 72-8
Index No. 72-608-V1k

MASSACHUSETTS INSTITUTE OF TECHNOLOGY
CAMBRIDGE, MASS. 02139

SEA GRANT PROJECT OFFICE

ADMINISTRATIVE STATEMENT

Acoustic methods have long been thought to be important in establishing the fishery resources of the open oceans. Accurate acoustic methods, however, have as yet not been developed although there is considerable research now underway. This report addresses a particular set of research questions that must be answered in the development of accurate acoustic sensing techniques. The analysis pertains to somewhat idealized conditions, namely down-looking sonar without doppler capability and in the absence of noise, surface and bottom reverberation and multiple target scattering. Nonetheless, valuable insights are gained into the fundamentals of fish density assessment as may be approached with sonar systems. Extensions to more realistic conditions will no doubt be necessary, but the results attained thus far will have, we believe, an important place in the developing technology of fishery assessment sonar.

The study contained in this report was supported by the National Marine Fisheries Service. The printing and distribution of this report was organized by the M.I.T. Sea Grant Project Office under a project established to expedite dissemination of important research results developed at M.I.T. under other than Sea Grant support. This related reports publication effort is made possible with funds from a grant by Henry L. and Grace Doherty Charitable Foundation, Inc., to the M.I.T. Sea Grant Program.

Ira Dyer
Associate Director

March 1, 1972

ROOM 3-282 (617) 864-6900 EXT. 7041

Original Work Sponsored

by

National Marine Fisheries Service
National Oceanic and Atmospheric Administration

under

Contract No. 14-17-007-1125

and

reported by

The Charles Stark Draper Laboratory
Massachusetts Institute of Technology

Technical Report R-712
August 1971

R-712

THE APPLICATION OF HYDROACOUSTIC METHODS FOR AQUATIC BIOMASS MEASUREMENTS

A NOTE ON ECHO ENVELOPE SAMPLING AND INTEGRATION

ABSTRACT

A detailed analysis of basic fish abundance estimation techniques and their respective errors is presented. (No attempt is made to include hardware implementation in this note.) Echo sampling and integration schemes approach unbiased population estimates if the following details are known: a) the average target strength of the aggregation, b) the approximate "shape" or geometry of the fish aggregation, and c) the transducer directivity function, source level, voltage response, etc. It is shown that unbiased estimates of dense populations demand a priori knowledge of the geometry and distribution of the randomly assembled targets with respect to the transducer's effective volume coverage. Two typical geometries are examined; they may be loosely described as 1) thick layer of infinite expanse, and 2) thin layer of infinite expanse. The effect of the random phase components on the variance of the population estimate is demonstrated and the autocorrelation of the echo intensity is given.

By Jeffrey B. Lozow
John B. Suomala

August 1971

PREFACE

This note is directed to persons engaged in or contemplating aquatic biomass measurements employing hydroacoustical techniques.

We have limited the scope of this note to the minimum level of complexity required to describe the behavior of a single hydroacoustical pulse propagated vertically from a projector, its return from fish targets as an echo, and the information contained in the echo signal.

This has been done because the pulsed echo sounder is a fundamental device and is the most common component in hydroacoustical intrumentation currently available for fisheries research.

We have started with the fundamental engineering principals of hydroacoustics. Furthermore, we have diligently avoided simplifying assumptions or procedures which can lead to erroneous conclusions concerning the applicability of hydroacoustics for aquatic biomass measurements.

We have combined a discussion of the physical concepts with the pertinent mathematics involved, however, since the subject is somewhat complicated it would be unrealistic to suggest that a detailed understanding of the technical content of this note does not require a certain degree of mental effort.

We would also suggest that any attempt to apply pulsed hydroacoustical signals for aquatic biomass or resource assessment measurements which does not, at the very least, properly account for all the factors set forth in this note can hardly be expected to yield useful results. Indeed, it is not clear at this time that the explicit hydroacoustical signal processing methods which we have developed in this note can be practically applied to aquatic resource assessment without precise experimental verification.

This note is the result of the efforts of the authors, but it must be noted that a number of individuals contributed their thoughtful comments which have helped greatly to bring us to this point in time.

We would particularly like to mention R. Edwards, M. Greenwood, M. Grosslein, R. Hennemuth, J. Posgay, J. Slavin, K. Smith, A. Stevenson, W. Stevenson, and P. Twohig of the National Marine Fisheries Service; L. Midttun

and O. Nakken at the Institute of Marine Research, Bergen, Norway; L. Boerema, D. Raitt, and S. Olsen at the Food and Agricultural Organization, Department of Fisheries, Rome, Italy; H. Lampe and S. Saila at the University of Rhode Island; V. Suskan of AtlantNIRO, Kaliningrad, U.S.S.R.; and A. Borud at Simrad AS., Horten, Norway.

Here at M.I.T. we must mention our colleagues, J. Scholten, R. Scholten, and R. Werner who reviewed our work, Miss Martha Ploetz who prepared the manuscript, and W. Eng and D. Farrar who provided the illustrations. To these people we express our gratitude for their help. Nevertheless, we take full responsibility for the contents of this note.

J. B. L. and J. B. S., Jr.

TABLE OF CONTENTS

1.0 INTRODUCTION

The subject of this paper is a detailed analytical investigation of the information content inherent in a single acoustical pulse scattered by an assembly of independent random scatterers. Since current echo-sounding systems produce simple monochromatic pulses for transmission, this analysis will be restricted to such.

Information in the recieved echo from a pulsed transmission may be contained (assuming high signal-to-noise ratio) in variations of phase, amplitude, pulse duration, and time delay between transmission and reception. Physical considerations regarding the propagation of sound in the sea, as well as our limited knowledge of the mechanism of scattering from fish targets rule out, on any practical basis, any kind of phase processing. Thus, we are left with the envelope of the received echo, its total duration, its frequency content, and its travel time to and from the target(s). We must somehow interpret these quantities in a manner that is consistent with some physical model of the entire acoustical link.

First, and foremost, it is necessary to construct the geometry of a stationary echo-sounder positioned over a region containing fish targets. In Fig. 1 we have depicted a closed volume V_T (which may be infinite) of arbitrary shape, said to contain all targets of interest. The transducer emits a pressure pulse (possibly a train of pulses) which in time envelops each of the targets contained in V_T. Obviously, the positions of the various targets within V_T greatly affects the characteristics of the net echo produced by all the scattering members. For example, if the targets were all clustered about a particular point within V_T, we would expect the echo envelope to exhibit a large amplitude for a duration on the order of a pulselength. However, if the targets were uniformly distributed throughout V_T, we would expect a long drawn out echo envelope of many pulselengths in duration, since all targets would be contributing to the echo at different times. A reasonable approach to mathematically modeling this type of occupancy problem (if the packing density is not too great) is to assume that the individual positions of the scatterers within V_T are a random phenomena obeying a three-dimensional Poisson probability law. This has the advantage of rendering the mathematics involved tractable. Certainly, however, experimental verification is needed to truly verify the Poisson law assumption. We state below some conditions under which we would expect the target positions to obey a three-dimensional Poisson probability law. Suppose we arbitrarily select a small subvolume "V" of V_T. Let there exist a positive quantity "ρ" such that the

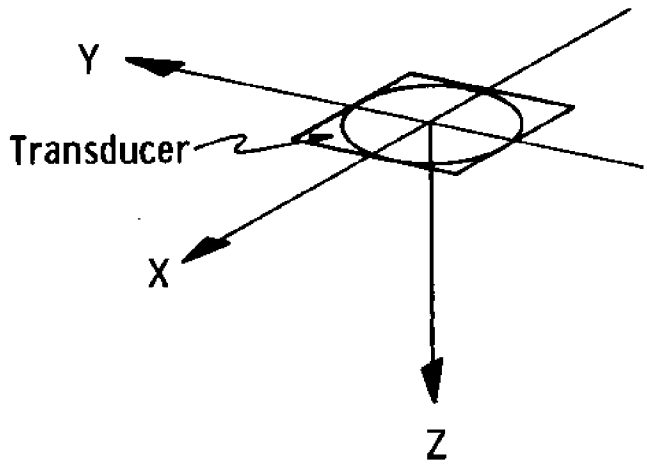

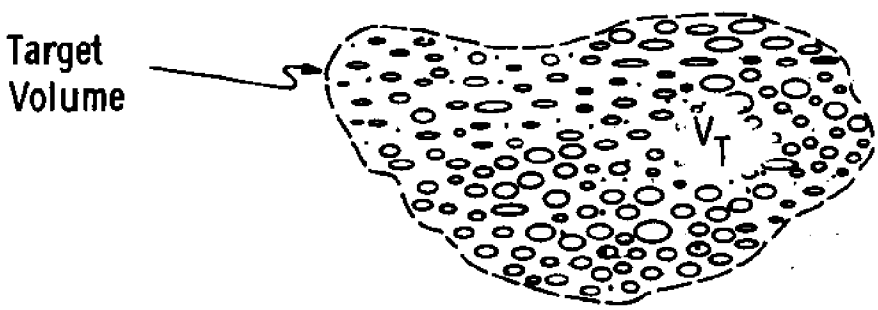

Figure 1 Geometry of Transducer and Target Volume

following conditions are approximately true:

A) the probability that exactly one target will occur in V is approximately equal to the product ρV.

B) the probability that exactly no targets occur in V is approximately equal to $1 - \rho V$.

C) if V is arbitrarily subdivided into smaller portions: $\Delta V_1, \Delta V_2, \ldots \Delta V_i \ldots \Delta V_M$, such that $V = \sum_{i=1}^{M} \Delta V_i$, the occupancy of any ΔV_i by one or more targets is independent of that of any other portion ΔV_j $(j \neq i)$.

In other words, if the targets are uniformly and independently dispersed throughtout a volume such that a quantity ρ may be interpreted as the mean rate at which the targets occur per unit volume, we assume that these occurrences are a kind of random phenomena described by the three-dimensional Poisson probability law (with parameter ρ). More precisely, the probability that exactly n targets occupy a volume, V, is equal to

$$\underline{P}\left\{ \text{exactly n targets in V} \right\} = \frac{e^{-\rho V} (\rho V)^n}{n!} \quad . \tag{1}$$

The assumption of independent behavior on the part of the targets (fish) at higher densities is doubtful. Most certainly, the validity of the model of fish as isolated geometric points becomes questionable if the mean distance between fish decreases to a level of the order of a fish length. On the other hand, if the mean distance between fish is great enough, the assumption of mutual independence seems reasonable. It can be demonstrated (see Appendix A) that the relationship between the density parameter ρ of a three-dimensional Poisson process and the mean distance, D, between a point and its nearest neighbor is given by

$$D = \frac{(1/3)!}{(4/3\pi\rho)^{1/3}} \approx \frac{.55}{\rho^{1/3}} \tag{2}$$

However, for the non-probabalistic case of densely packed spheres of diameter, D, occupying a volume with density ρ,

$$D \approx \frac{1.2}{\rho^{1/3}} \quad , \tag{3}$$

where D is also the distance between sphere centers. Relationship (3) may apply in the highly dense case, where (2) may apply in low to moderate densities if the random phenomena obeys the Poisson law.

In any case, if we accept the concept of average target density as meaningful and applicable to most situations which arise in abundance estimation, then the question of actual target distribution, be it Poisson or any other, would not influence an unbiased estimate based on average effects. However, the error models associated with the estimates are, in fact, dependent on the exact distribution assumed.

2.0 BASIC CONCEPTS

2.1 ECHO SIGNAL – SINGLE TARGET

In this section some basic concepts and equations are presented from which simple estimation schemes are derived based on the average density model. To begin with, we start with the basic echo sounding equation for a single target (see Reference 3).

$$V_{rms}^2 = ZK^2 I_o \frac{\sigma}{4\pi} \cdot \frac{1}{R^4} e^{-2\alpha R} \cdot G^2(\theta,\phi) \quad (4)$$

V_{rms}	~	rms voltage produced at transducer terminals
Z	~	specific acoustic impedance of fluid ($g/cm^2 sec$)
K	~	transducer voltage response ($volt \cdot cm^2/dyne$)
I_o	~	source level ($dyne/cm \cdot sec$)
$G(\theta,\phi)$	~	transducer directivity function
(θ,ϕ)	~	directional spherical coordinates relative to reference coordinates fixed at transducer
σ	~	ratio of power scattered in direction of transducer per unit solid angle to the incident intensity at target
α	~	path attenuation loss due to combined effects of scattering and absorption
R	~	range to target (meters)

It is generally more convenient to define two auxiliary variables I_R and TS such that

$$I_R \equiv \frac{V_{rms}^2}{ZK^2}, \qquad TS \equiv \frac{\sigma}{4\pi}, \qquad (5A)$$

and thus expression (4) becomes

$$I_R = I_o TS \frac{e^{-2\alpha R}}{R^4} G^2(\theta,\phi) \quad . \qquad (5B)$$

The quantities I_R and TS are designated as the equivalent received intensity level and the equivalent (plane wave) target strength. In general I_R is not really an intensity as its units ($watts/meter^2$) seem to imply. The true intensity incident

at the transducer aperture is actually given by the ratio $I_R/G(\theta,\phi)$, although in analysis one usually deals directly with the term I_R rather than the ratio I_R/G. The target strength parameter, TS, refers to the echo produced by an object in the path of a plane acoustic wave. Mathematically it is the ratio of the intensity of the local echo (at one meter from the object) to the incident intensity.* In general, target strength is a function of the target orientation with respect to the transducer. Except for isotropic reflectors such as rigid spheres, irregular bodies have target strengths which are complicated functions of their orientation to the sound source/receiver.

The term $e^{-2\alpha R}/R^4$ is a consequence of the two way spreading and absorption losses characteristic of wave propagation in a lossy medium. For frequencies in the 100 kilo-hertz region "α" is about 6.3×10^{-3} or the equivalent of 0.055 decibels per meter.

The function $G(\theta,\phi)$ specifies the directional characteristics of the transducer on a three dimensional basis. If we imagine a coordinate system fixed to the effective center of the transducer as in Fig. 2, the angles (θ,ϕ) are the reference polar coordinates. The direction (0,0) is ordinarily taken to be the direction of maximum response/projection. The directivity function $G(\theta,\phi)$ is normalized to the maximum so that $G(\theta,\phi) \leq G(0,0) = 1$ for any combination of θ and ϕ. Typical directivity functions include those of the circular and rectangular plate transducers. For the circular aperture transducer

$$G(\theta,\phi) = G(\phi) = \left| \frac{2J_1(\frac{\pi d}{\lambda}\sin\phi)}{\frac{\pi d}{\lambda}\sin\phi} \right|^2 , \qquad (6A)$$

where $J_1(\,)$ ~ 1st order Bessel function

d ~ diameter of aperture

λ ~ wavelength ,

and for the rectangular plate

$$G(\theta,\phi) = \left[\frac{\sin(\frac{\pi a}{\lambda}\sin\phi\cos\theta)}{\frac{\pi a}{\lambda}\sin\phi\cos\theta} \cdot \frac{\sin(\frac{\pi b}{\lambda}\sin\phi\sin\theta)}{\frac{\pi b}{\lambda}\sin\phi\sin\theta} \right]^2 \qquad (6B)$$

where a, b ~ dimension of rectangular aperture

λ ~ wavelength .

The associated geometry is shown in Figs. 3A and 3B. Note that the directivity function of the circular plate transducer is not a function of the rotational angle θ

*Some authors define target strength in decibel form, i.e. 10 LOG (TS). Also, target strength is sometimes referenced to one yard rather than one meter.

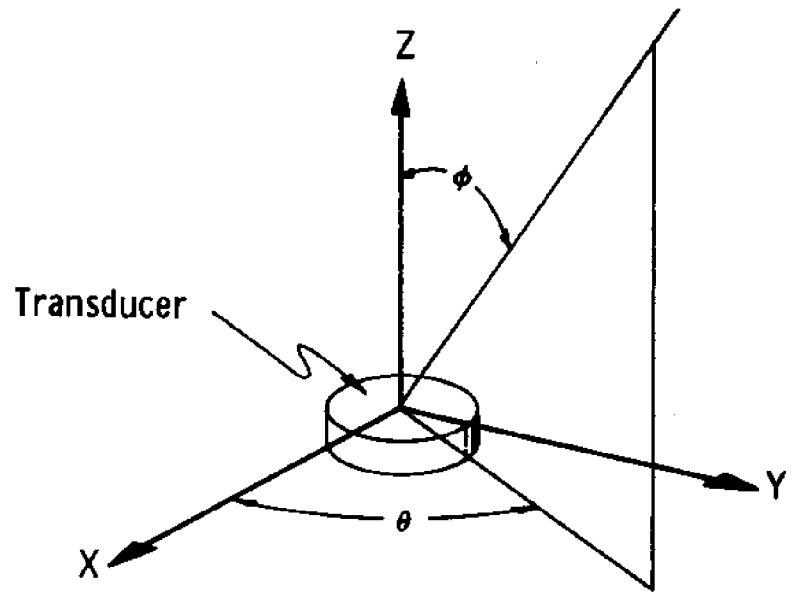

Figure 2 Transducer Directional Coordinate Reference

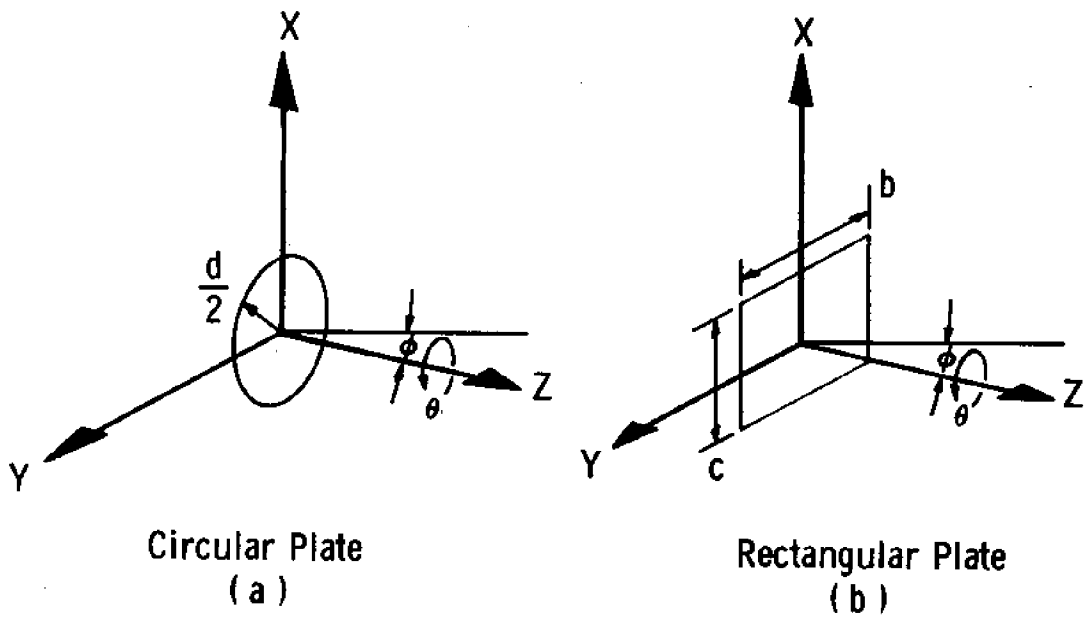

Figure 3 Transducer Directivity Function Coordinates

which may be called a condition of "circular symmetry." In practice, analytical expressions for the $G(\theta, \phi)$ of a particular transducer might not be available and laboratory measurements would be necessary for its determination.

2.2 ECHO SIGNAL-MULTIPLE TARGETS

Equations (4) and (5) are expressions of rms voltage and intensity respectively. They express the time averaged effects of the physics of the transducer-target-transducer link. For multiple targets, the time dependent form of the received signal need be examined. Let the pulse returns from N distinct targets be incident simultaneously at the aperture of the transducer at some arbitrary time $t = t^1$ seconds.* From (5) let the intensity level of the i^{th} echo be given as

$$(I_R)_i = I_o \, TS_i \, \frac{e^{-2\alpha R}}{R^4} G^2(\theta_i, \phi_i) \quad , \tag{7}$$

The rms voltage, $(V_{rms})_i$, associated with the i^{th} target, if the echo were isolated from the other n-1 returns is given by

$$(V_{rms})_i = K \left[Z (I_R)_i \right]^{1/2} \quad , \tag{8}$$

where K ~ voltage response of transducer .

The instantaneous voltage $v_i(t)$ that (8) represents may be expressed as a cosine function of duration equal to one pulselength "τ". It is given by

$$v_i(t) = \sqrt{2} \, (V_{rms})_i \cos(\omega_c t + \Phi_i) \; ; \; t^1 < t < (t^1 + \tau) \tag{9}$$

where t^1 ~ arrival time
ω_c ~ carrier frequency
Φ_i ~ signal phase
τ ~ pulse length.

The net transducer terminal voltage at $t^1 < t < (t^1 + \tau)$ is given by the sum

$$v_n(t) = \sum_{i=1}^{n} v_i(t) \quad . \tag{10}$$

* Assumes identical ranges to all n targets.

The instantaneous squared voltage thus may be expressed as

$$v_n^2(t) = \sum_{i=1}^{n} v_i^2(t) + \sum_{\substack{i=1 \\ i \neq j}}^{n} \sum_{j=1}^{n} v_i(t) v_j(t) \; ; \; t^1 < t < (t^1 + \tau) \quad . \quad (11)$$

Generally it is the square of the net voltage that is the quantity of interest since on the average it will be shown to be directly proportional to the number of targets contributing to the echo at any particular time. Substitution of equation (9) into (11) yields for $t^1 < t < (t^1 + \tau)$

$$v_n^2(t) = \mathcal{E}(t) + \sum_{i=1}^{n} (V_{rms}^2)_i + \sum_{\substack{i=1 \\ i \neq j}}^{n} \sum_{j=1}^{n} (V_{rms})_i (V_{rms})_j \cos(\phi_i - \phi_j). \quad (12)$$

It is easily shown that the term $\mathcal{E}(t)$ in (12) behaves as "cos $(2\omega_c t)$" or varies with time at twice the carrier frequency. The mean squared value of $v_n^2(t)$, S, is given by averaging $v_n^2(t)$ over a cycle of oscillation. If all other terms in expression (12) vary slowly in time relative to $\mathcal{E}(t)$ then

$$S = \langle v_n^2(t) \rangle = \sum_{i=1}^{n} (V_{rms}^2)_i + \sum_{\substack{i=1 \\ i \neq j}}^{n} \sum_{j=1}^{n} (V_{rms})_i (V_{rms})_j \cos(\phi_i - \phi_j), \quad (13)$$

$$\text{since} \qquad \langle \mathcal{E}(t) \rangle = \langle \cos(2\omega_c t) \rangle = 0,$$

where the "$\langle \; \rangle$" indicates time averaging over a cycle period $\frac{2\pi}{\omega_c}$.

Expression (13) reflects the significance of the phase relationships $(\phi_i - \phi_j)$ between the n signals. As a trivial example consider the net mean squared voltage produced by two identical scatterers at nearly identical positions with respect to the transducer. In this case n = 2 and (13) becomes

$$S_{(2)} = 2V_{rms}^2 \left[1 + \text{Cos} \, (\phi_1 - \phi_2) \right] \quad . \quad (14)$$

A plot of (14) (see Fig. 4) illustrates the possible variation of $S_{(2)}$ as a function of phase difference $(\phi_1 - \phi_2)$. Note that the net mean squared voltage fluctuates between 0 and twice the mean squared voltage available from one echo, i.e., V_{rms}^2. The two extremes are total reinforcement when $\phi_1 - \phi_2$ = integer x 2π, and total cancellation when $\phi_1 - \phi_2$ = π + integer x 2π. Obviously, the respective phases ϕ_1 and ϕ_2 play a dominant role in the effective voltage produced at the transducer terminals.

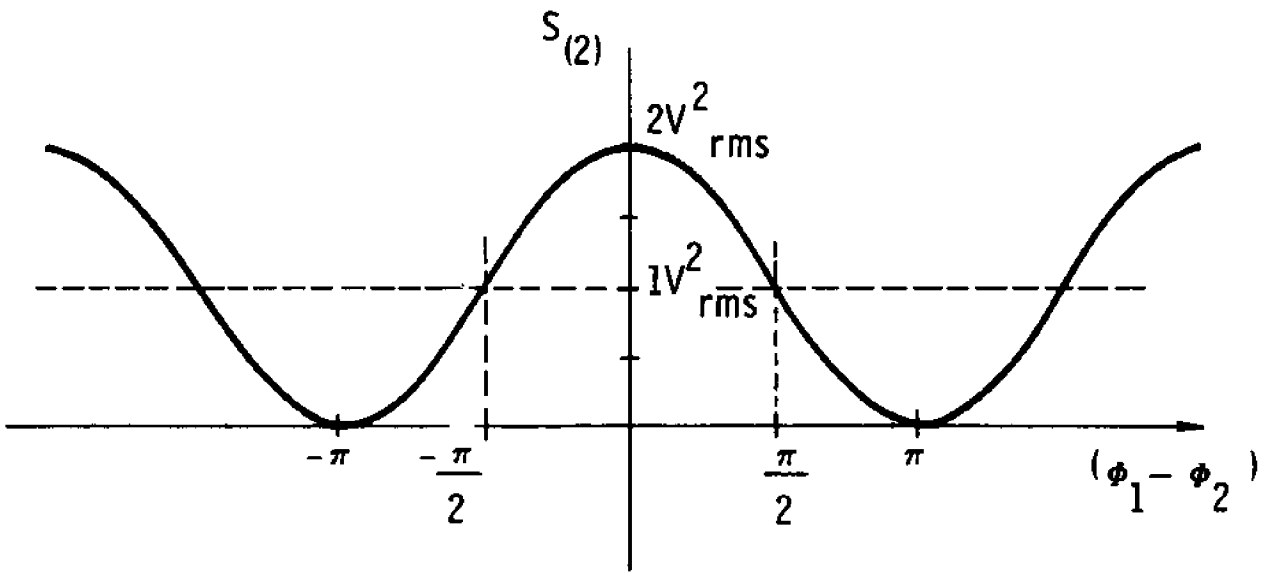

Figure 4 Variation of Instantaneous Value of the Net Mean Squared Voltage From Two Targets as a Function of Phase Difference

It is generally assumed that the ocean perturbs the phase of an acoustical wave in a random fashion, especially at longer ranges. In addition, even a slight range difference between one target and any other changes their echo phase relationship when this difference is comparable to a wavelength. These considerations among others, lead to the postulation of random, uniformly distributed phases for each of the signal components. This assumption is common to most analyses dealing with echoes from assemblies of scatterers whether the scattering be of acoustical or electromagnetic nature (e.g., radar echoes from rain drops, chaff, etc.)

Suppose equation (12) is rewritten in a random variable sense regarding the individual voltage or signal as an independent random variable:

$$\tilde{S} = \sum_{i=1}^{n} (\tilde{V}^2_{rms})_i + \sum_{\substack{i=1 \\ i \neq j}}^{n} \sum_{j=1}^{n} (\tilde{V}_{rms})_i (\tilde{V}_{rms})_j \cos(\tilde{\phi}_i - \tilde{\phi}_j) \quad , \qquad (15)$$

where the $\sim$ symbol over a quantity designates it as a random variable, (r.v.). It is a direct consequence of the central limit theorem in probability that the first order statistics of $\tilde{S}$ are described by a Rayleigh probability distribution of power* (if n is sufficiently large). More specifically the probability that $\tilde{S}$ lies between S and S + dS is given by

$$P\left\{ S < \tilde{S} < S + dS \right\} \approx 1/\bar{S}\ e^{-S/\bar{S}}\ dS \qquad \text{(for large n)} \qquad (16)$$

$$\text{where} \qquad \bar{S} \equiv \sum_{i=1}^{n} (\bar{V}^2_{rms})_i \quad .$$

The mean or expected value of $\tilde{S}$ is given by the integral

$$E\left\{ \tilde{S} \right\} = \int_0^{\infty} (1/\bar{S})\ S e^{-S/\bar{S}}\ dS = \bar{S} \quad . \qquad (17)$$

The variance of $\tilde{S}$, $\sigma^2_{\tilde{S}}$ is given by

$$\sigma^2_{\tilde{S}} = \left(\int_0^{\infty} \frac{1}{\bar{S}} S^2\, e^{-S/\bar{S}}\, dS \right) - \bar{S}^2 = \bar{S}^2 \quad . \qquad (18)$$

The usual measure of fluctuation is the value of the standard deviation σ_S. Taking the square root of (18) yields a σ_S which is equal to $\bar{S}$. Note that the fluctuation is large as its value is 100% of the mean. This fact is true as long as the number of components is sufficiently large (say $N \geq 5$). The fact that the average value of the net mean squared voltage $\bar{S}$ is equal to the sum of the

*Also called the exponential distribution. (See Reference 4)

averaged component mean square voltages is somewhat intuitive. However, the fact that such a large fluctuation is inherent to the mean squared voltage (neglecting noise or any other spurious inputs) is surprising. It should be noted that the Rayleigh power distribution holds regardless of the distributions of $(\tilde{V}_{rms})_i$, the individual component amplitudes. That is, there is no requirement that the second moments $(\bar{V}^2_{rms})_i$ be equal or have the same distribution functions.

The probability density function as given by (16) describes the statistical behavior of fluctuation (at any arbitrary point in time) of the echo signal produced by "n" scatterers located at roughly the same range from the transducer. Generally, however, the real situation will be that depicted in Fig. 1 where targets will be somehow distributed over a volume such that it is not very likely that all, if any, targets are located at identical ranges.

Suppose a number of targets are uniformly dispersed over a large volume with density " ρ ". Also, assume a transducer is situated over this volume and sends out one pulse of length τ seconds. The shape and duration of the echo (mean squared voltage) as a function of time, will depend on the transducer directivity pattern, and the depth and extent of the target volume. More specifically, assume a hypothetical scattering layer of infinite expanse located at a depth R_o (see Fig. 5). The pulse is viewed as a bundle of energy contained in a hemispherical shell of thickness $c\tau$ and radius ct (where c is the speed of sound in the sea and t is the time starting when the leading edge of the pulse left the transducer). Any objects in the path of the pulse shell at range "R" will scatter energy, a fraction of which will be incident on the transducer aperture at time $t = 2R/c$. The echo signal should start to build at time equal to $2R_o/c$ and not die out until the pulse shell has passed the lower boundary of the layer. After this point in time, the hemisphere shell intersects the layer only at large angles from the direction of maximum transducer response. In Fig. 6 a sketch of mean echo level vs. time is presented, The distinct levels (A), (B), (C), (D) and (E) correspond to the spatial positions of the propagating pulse as shown in Fig. 5.

At point (A) the pulse shell has not yet come in contact with the scattering layer and thus the echo level is zero. Point (B) corresponds to the initial echoes as the pulse shell begins to merge with the layer. The level stays relatively constant, point (C), until portions of the pulse shell emerge from the lower boundary, point (D). As the pulse shell propagates through the layer further the echo level diminishes, point (E). Figs. (5) and (6) represent a graphical interpretation of the echo level received from a simple assemblage of scatterers, i.e., thick uniform scattering layer.

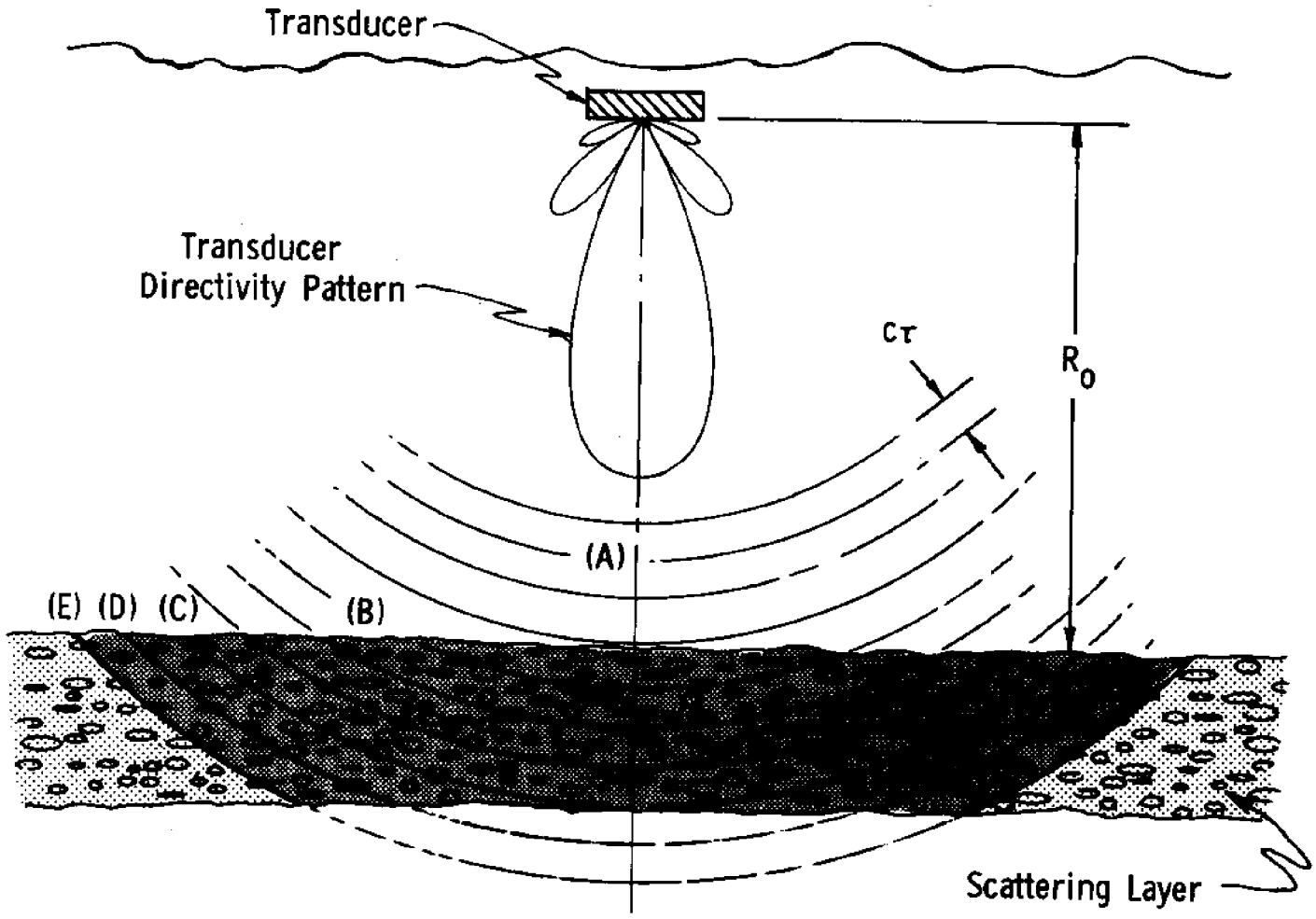

Figure 5 Spherically Spreading Acoustical Pulse Propagating Through Scattering Layer

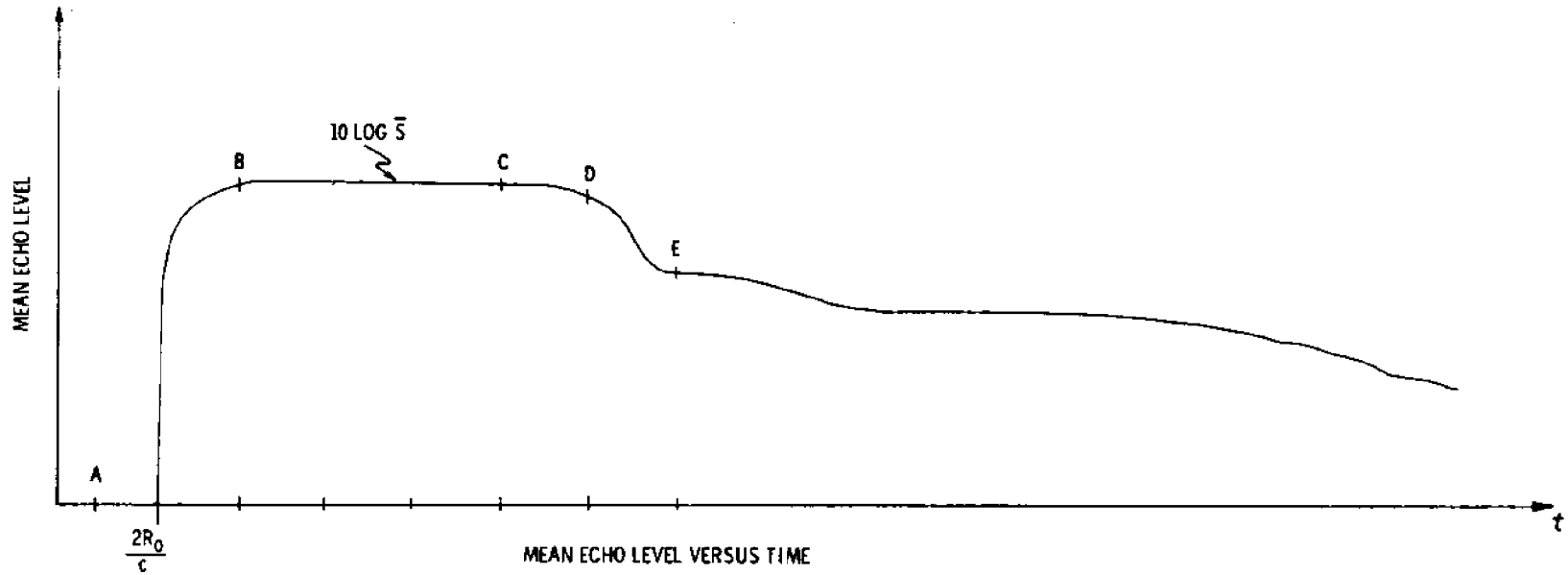

Figure 6 Sketch of Mean Echo Versus Time From Figure 5

2.3 CORRELATION

Figure 6 depicts a representation of the mean received echo (voltage envelope) level vs. time. As has been shown in equations (15) through (18), the fluctuation about the mean level is likely to be large at any point on the echo level vs. time curve. Thus, the curve will exhibit irregular fluctuation in level as the pulse shell propagates through the scattering layer. If a curve possesses coherency it means that if at any instant the level is high, it is likely that the level will remain high for a while whereas if it is low, it is not likely to become large in a short time. The degree of coherence between two distinct points on a curve is described in terms of the correlation coefficient $r(t_1, t_2)$. If $\tilde{S}(t_1)$ is the value of the mean square voltage (echo level) at time t_1 and $\tilde{S}(t_2)$ is the corresponding value at time t_2 then $r(t_1, t_2)$ is defined

$$r(t_1, t_2) \triangleq \frac{\overline{\left[\tilde{S}(t_1) - \bar{S}(t_1)\right]\left[\tilde{S}(t_2) - \bar{S}(t_2)\right]}}{\left[\overline{\left[\tilde{S}(t_1) - \bar{S}(t_1)\right]^2}\ \overline{\left[\tilde{S}(t_2) - \bar{S}(t_2)\right]^2}\right]^{1/2}} \quad . \tag{19}$$

It can be shown that the following inequality holds:

$$-1 \leq r(t_1, t_2) \leq 1 \quad . \tag{20}$$

If, on the same echo level curve, $r(t_1, t_2) \approx 1$, a high value of $\tilde{S}(t_1)$ is likely to be associated with a high value of $\tilde{S}(t_2)$; if $r(t_1, t_2) \approx 0$, a given value of $\tilde{S}(t_1)$ gives no information about the level of $\tilde{S}(t_2)$; and if $r(t_1, t_2) \approx -1$ a high value of $\tilde{S}(t_1)$ is likely to be associated with a low value of $\tilde{S}(t_2)$. It will be shown in Appendix B that for the "thick" scattering layer, the correlation coefficient is given by

$$r(t_1, t_2) = \begin{cases} \left(1 - \dfrac{|t_1 - t_2|}{\tau}\right)^2 & |t_1 - t_2| \leq \tau \\ 0 & \text{OTHERWISE} \end{cases} \tag{21}$$

From (21) it is seen that $r(t_1, t_2)$ depends only on the value $|t_1 - t_2|$.

2.4 TIME AVERAGING

In the regions where the expected value of $\tilde{S}(t)$ (written $E\{\tilde{S}(t)\}$ or $\overline{S(t)}$) is constant, the process $\tilde{S}(t)$ is said to be "stationary in the wide sense." For

thick scattering layers a large portion of the echo pulse might be stationary, e.g., the region between points (C) and (D) in Fig. 6. If we know that a significant portion of $\tilde{S}(t)$, the echo level vs. time curve, is stationary, time averaging may be employed to smooth out the fluctuations caused by the random phase components. Time averaging along $\tilde{S}(t)$, the echo level vs. time curve, will smooth the data without bias error if $\tilde{S}(t)$ is stationary. In the sketch of Fig. 7, we depict a typical echo vs. time curve for a thick scattering layer. The symbol $\tilde{S}(t)$ represents a possible echo, whereas the symbol $\bar{S}(t)$ depicts the "average" of $\tilde{S}(t)$. Note that after an initial rise time t_r, the average is almost constant until some time t_f when the echo begins to die out. The time interval $t_f - t_r$ naturally depends on the thickness of the scattering layer. For example, we could represent $\tilde{S}(t)$ between t_r and t_f by a running average $\langle S \rangle_t$,

$$\langle S \rangle_t \equiv \frac{1}{\Delta t} \int_{t-\Delta t}^{t} \tilde{S}(t')\, dt' \quad . \tag{22}$$

Note that $\langle S \rangle_t$ is itself a function of time t. It is assumed that the goal is to reduce the fluctuation inherent in $\tilde{S}(t)$ in order to get a better estimate of the statistical mean or expected value of $\tilde{S}(t)$. More precisely, if Δt is sufficiently small so that the expected value of $\tilde{S}(t)$ changes slowly over the interval $(t - \Delta t,\ t)$ then

$$E\{\langle S \rangle_t\} = \frac{1}{\Delta t} \int_{t-\Delta t}^{t} E\left\{\tilde{S}(t')\right\} dt' \approx \bar{S}(t). \tag{23}$$

Thus, $\langle S \rangle_t$ is practically an unbiased estimate of the statistical mean, $\bar{S}(t)$.

It can be shown, (Ref. 1), by implementing equation (21) that the variance of the estimate is given by

$$\sigma^2_{\langle S \rangle_t} = \begin{cases} \bar{S}^2(t)\left[1 - \frac{2}{3}\frac{\Delta t}{\tau} + \frac{1}{6}\left(\frac{\Delta t}{\tau}\right)^2\right] & \Delta t \leq \tau \\ \frac{\bar{S}^2(t)}{2}\left(\frac{\tau}{\Delta t}\right)^2 & \Delta t > \tau \end{cases} \tag{24}$$

This result should be compared with expression (18) where

$$\sigma^2_{\tilde{S}} = \bar{S}^2 \tag{18}$$

If, for example Δt were set equal to τ, the variance of the fluctuation would be reduced by 1/2 (i.e. $\sigma^2_{\langle S \rangle_t} = \bar{S}^2/2$). It is desirable to make Δt, the averaging

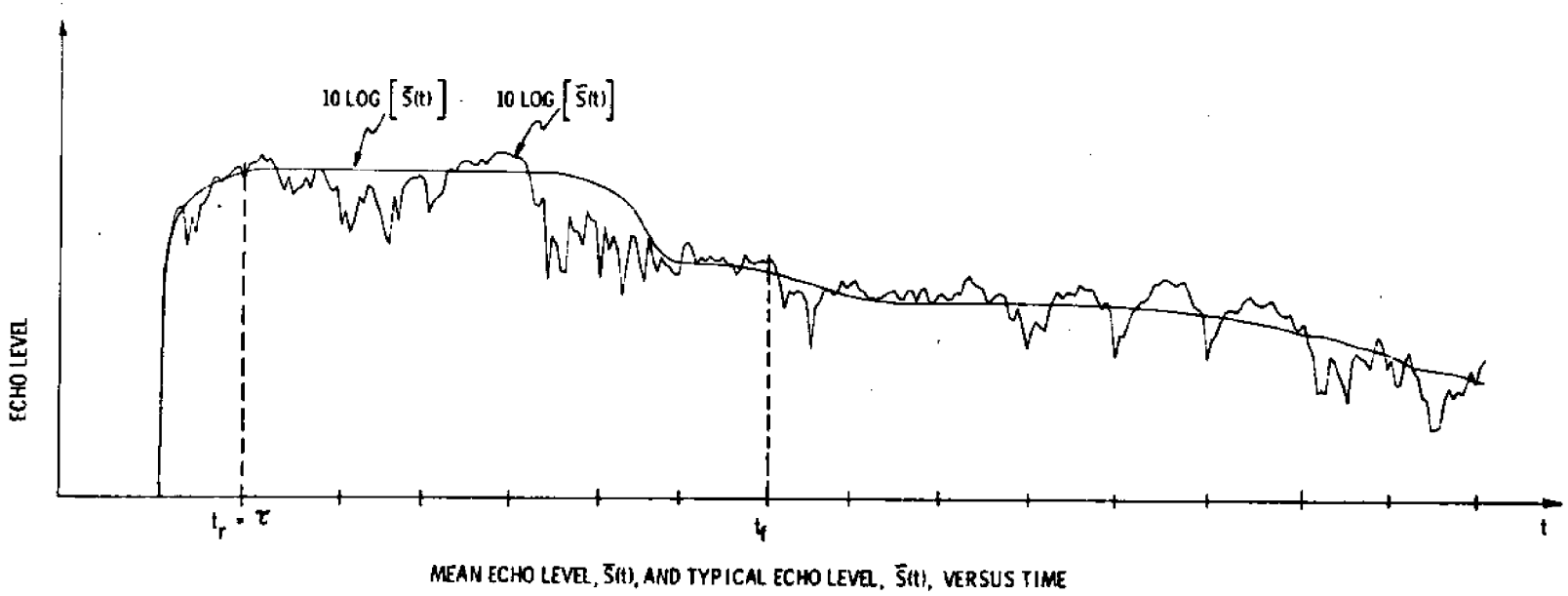

Figure 7 Variation Between Mean and Typical Intensity Level Versus Time

interval, as large as possible since expression (24) indicates that $\sigma^2_{\langle S \rangle_t}$ diminishes rapidly with increasing Δt. On the other hand, too large a Δt would result in a large bias error since $E\{\langle S \rangle_t\}$ would not be close to $\overline{S}(t)$.

From the results above it is reasonable to conclude that in the thick scattering layer case, where the echo level approximates a stationary random process, smoothing or time averaging reduces the fluctuations caused by the random phases of the component echoes.

3.0 ABUNDANCE ESTIMATION

This section will be concerned with some methods of target counting or abundance estimation along with their associated errors. The analyses will be carried out on a single ping basis. That is, the echo signal will be assumed to be the result of a single acoustical pulse projected from a stationary transducer. The extension of these techniques to a moving transducer projecting a burst of pulses will be discussed in a later paper.

3.1 THICK SCATTERING LAYER

The geometric characteristics which a target volume must possess in order to fall into this category are 1) target volume has a lateral expanse greater than the effective range of the transducer, and 2) a vertical thickness greater than one half a pulselength or $c\tau/2$. A cross section of a thick scattering layer is shown in Fig. 8. The term R_o is the depth to the layer from the working face of the transducer. The term δ refers to the average thickness. Figure 8 is an idealized model in that the target volume or layer is depicted as an infinite region bounded by parallel planes. The fish are assumed to be dispersed throughout the scattering layer. We restrict the analysis to layers through which the targets are homogeneously distributed.* We fix a coordinate system at the transducer to which the spherical coordinates (R, θ, ϕ) will be referred. If the transducer projects a pulse at time $t = 0$, the sound backscattered from the layer should not be received until $t_0 = 2R_o/c$. From this time onward, backscattered energy should be significant until the pulse shell has passed through the lower boundary directly below the transducer at time $t = 2(R_o + \delta)/c$. It may be shown** that the average value, $\bar{S}$, of the net mean squared voltage (from "n" scatterers) at the receiving terminals is equal to the sum of the averaged component mean squared voltage, or

$$\bar{S} = \sum_{i=1}^{n} \bar{S}_i \quad , \qquad (25)$$

$$\text{where} \quad \bar{S} = \overline{V^2_{rms}}$$

$$\bar{S}_i = \overline{(V^2_{rms})_i} \quad .$$

As it is more convenient to work in intensity levels at this point we use relationship (8) to transform (25) to

*We assume in this discussion that the effects of multiple scattering are negligible.

**By taking the expected value of both sides of (15) and noting that $E\{\cos(\tilde{\phi}_i - \tilde{\phi}_j)\} = 0$.

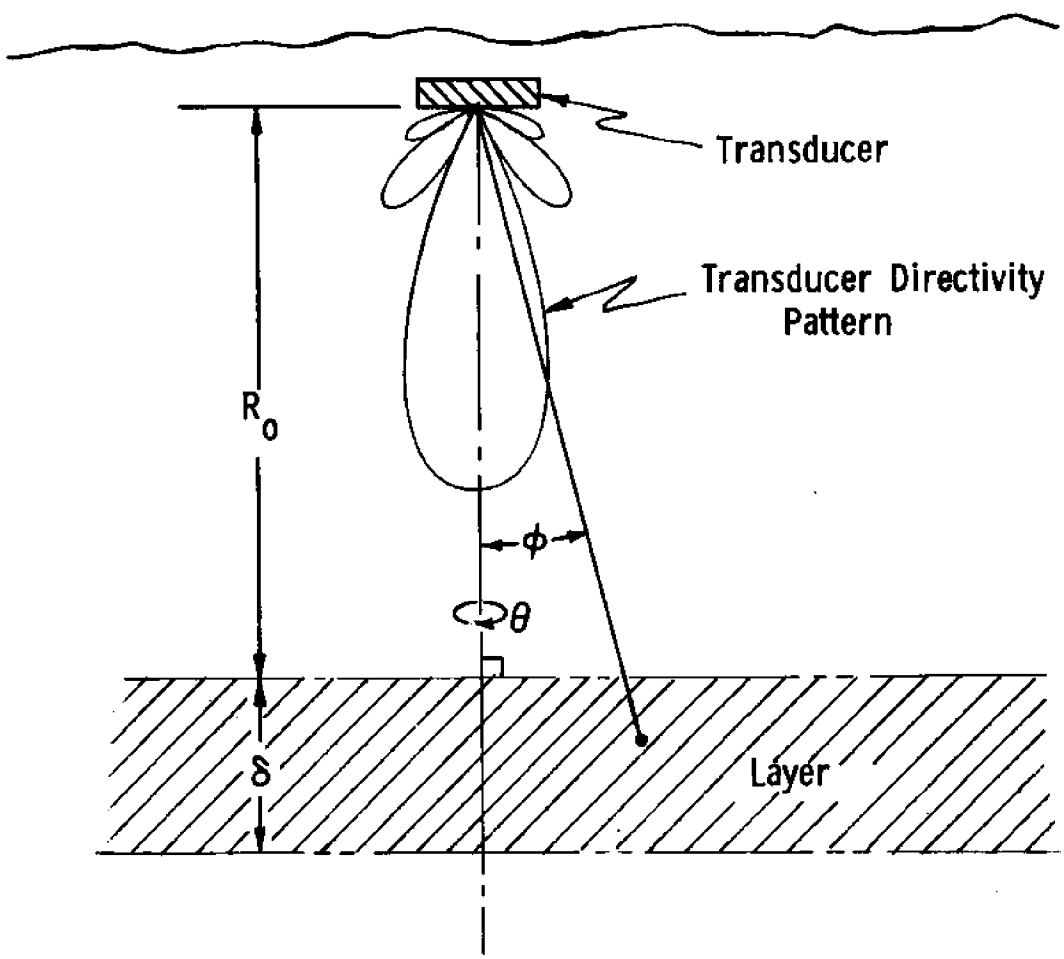

Figure 8 Idealized Model of Transducer and Scattering Layer

$$\bar{I}_R = \sum_{i=1}^{n} (\bar{I}_R)_i \quad ,$$

where $$(\bar{I}_R)_i = \frac{\bar{S}_i}{K^2 Z} \quad . \tag{26}$$

Taking any arbitrary time during reception, say t, the intensity level will be made up of the contribution from the pulse shell whose range boundaries fall within $c(t-\tau)/2$ and $c\tau/2$. As a first approximation we will consider the scatterers within this shell to be located at some intermediate range R, where

$$\bar{R} \equiv \frac{1}{2}\left[\frac{ct}{2} + \frac{c}{2}(t-\tau)\right] = c\left(t - \frac{\tau}{2}\right)/2 \quad . \tag{27}$$

Suppose we determine the average incremental intensity $\Delta\bar{I}_R$ produced by a portion of the pulse shell ΔV (Fig. 9). If there are on the average ρ scatterers per unit volume, then the average number of scatterers, $\overline{\Delta n}$, in ΔV is given by

$$\overline{\Delta n} = \rho \Delta V \quad . \tag{28}$$

If the scatterers in ΔV have roughly the same average target strengths, then by equations (7) and (26)

$$\Delta\bar{I}_R = \sum_{i=1}^{\overline{\Delta n}} (\bar{I}_R)_i = \overline{\Delta n}\left(I_o \overline{TS}\, \frac{e^{-2\alpha\bar{R}}}{\bar{R}^4} G^2(\theta,\phi)\right) , \tag{29}$$

$$= \rho \Delta V I_o \overline{TS}\, \frac{e^{-2\alpha\bar{R}}}{\bar{R}^4} G^2(\theta,\phi) \quad .$$

The quantity ΔV can be written in terms of the differential angles $d\phi$ and $d\theta$ as

$$\Delta V = \frac{c\tau}{2}\bar{R}^2 \sin\phi\, d\phi\, d\theta \quad . \tag{30}$$

Thus, in terms of the calculus, the differential of the average intensity, $d\bar{I}_R$, can be written as

$$d\bar{I}_R = \rho\left(\frac{c\tau}{2}\bar{R}^2 \sin\phi\, d\phi\, d\theta\right)\left(I_o \overline{TS}\, \frac{e^{-2\alpha\bar{R}}}{\bar{R}^4} G^2(\theta,\phi)\right), \tag{31}$$

$$= \rho \frac{c\tau}{2} \overline{TS}\, I_o\, \frac{e^{-2\alpha\bar{R}}}{\bar{R}^2} G^2(\phi,\theta) \sin\phi\, d\phi\, d\theta \quad .$$

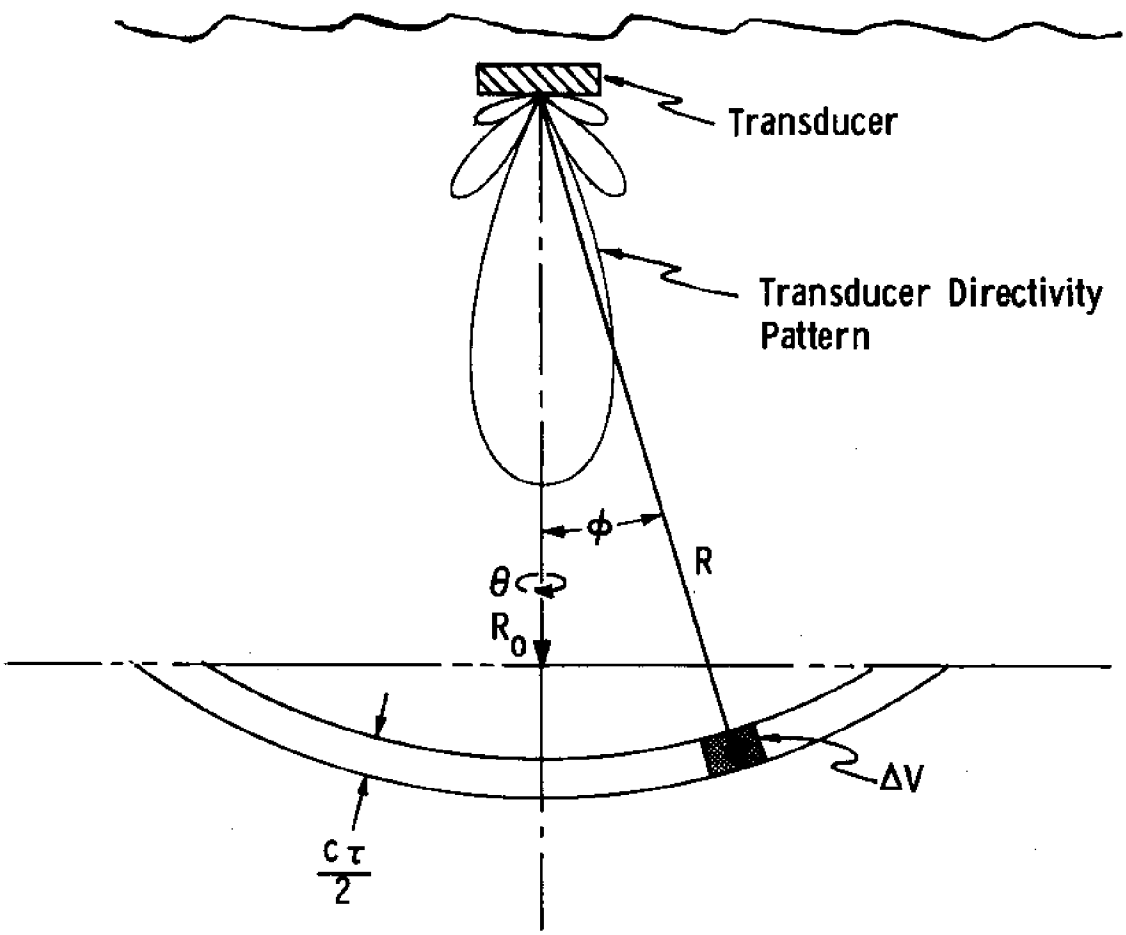

Figure 9 Incremental Scattering Volume in Pulse Shell

The average intensity of the pulse shell at the transducer may be expressed as the integral

$$\overline{I}_R = \int_0^{\overline{I}_R} \overline{dI}_R = \rho I_o \overline{TS} \frac{c\tau}{2} \frac{e^{-2\alpha \overline{R}}}{\overline{R}^2} \int_0^{2\pi} \int_0^{\mathrm{Cos}^{-1}(R_o/\overline{R})} G^2(\theta,\phi)\,\mathrm{Sin}\phi\, d\phi\, d\theta . \tag{32}$$

Relationship (32) holds for all ranges, R, falling within the limits

$$R_o \leq \overline{R} \leq R_o + \delta \tag{33}$$

$\overline{I}_R$ can be written as an explicit function of time if the substitution $\overline{R} = c(t - \tau)/2$ is made in (32).

3.2 ENVELOPE SAMPLING

Suppose we define a sequence of discrete times $\{t_N\}$ such that

$$\begin{aligned} t_1 &\equiv 2R_o/c + \tau/2 \\ t_2 &\equiv 2R_o/c + 3/2\,\tau \\ &\cdots \\ t_N &\equiv 2R_o/c + (N - 1/2)\,\tau \end{aligned} \tag{34}$$

Corresponding to this time sequence we define a range sequence $\{\overline{R}_N\}$

$$\begin{aligned} \overline{R}_1 &\equiv ct_1/2 = R_o + c\tau/4 \\ \overline{R}_2 &\equiv ct_2/2 = R_o + 3/4c\tau \\ &\cdots \\ \overline{R}_N &\equiv ct_N/2 = R_o + (N - 1/2)\, c\tau/2 . \end{aligned} \tag{35}$$

From the sketch in Fig. 10 we see that the scattering layer can be divided up into non-overlapping shells, Accordingly, the time "t_N" represents the time at which a pulse shell at a range "$\overline{R}_N$" causes an average intensity level $\overline{I}_N = \overline{I}_R(t_N)$ to be

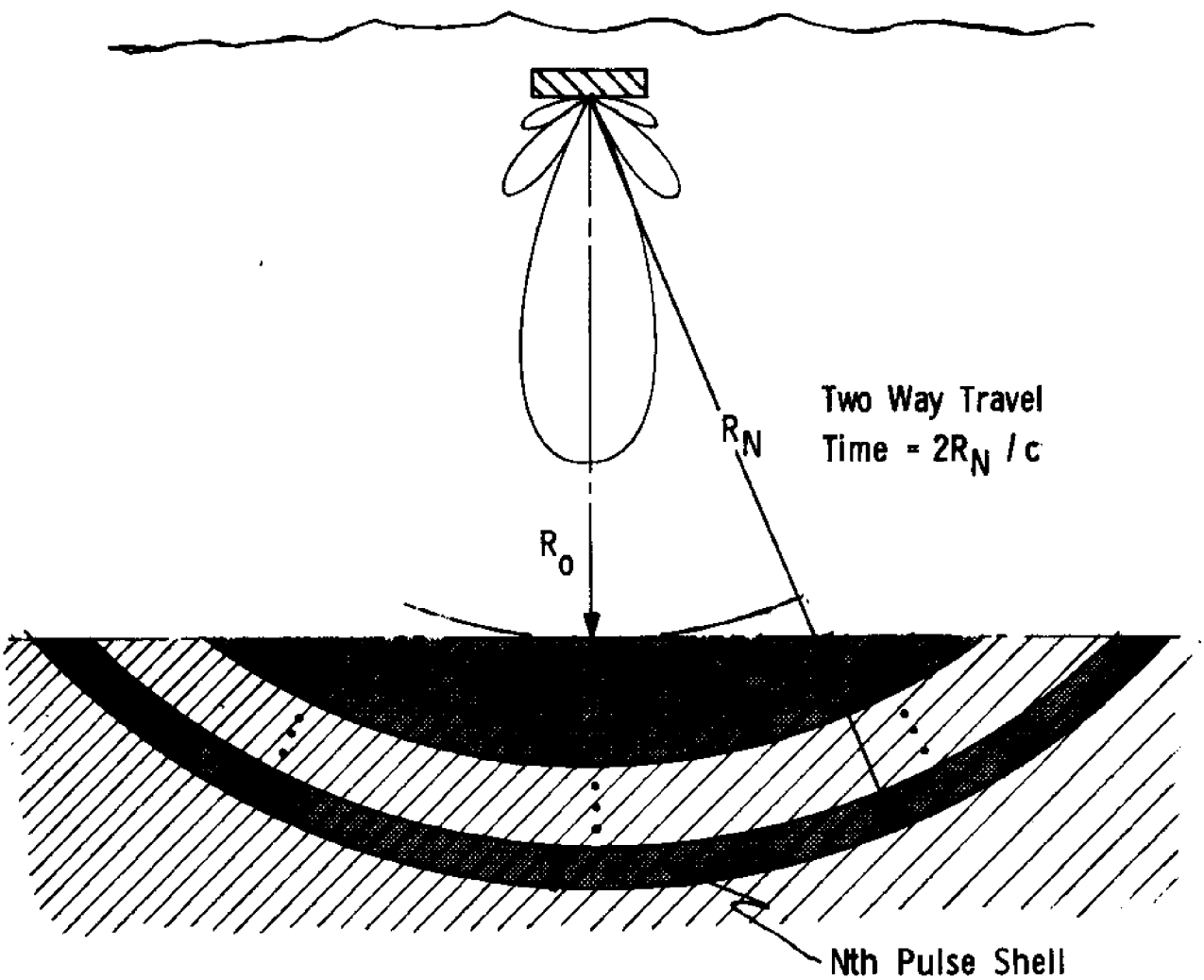

Figure 10 Pulse Shell Geometry for Echo Envelope Sampling

present at the transducer. Substituting (35) into (32) generates a sequence of mean intensity levels $\{\bar{I}_N\}$ where

$$\bar{I}_1 \equiv \bar{I}_R(t_1) = \rho I_o \overline{TS}\,\frac{c\tau}{2}\,\frac{e^{-2\alpha(R_o + c\tau/4)}}{(R_o + c\tau/4)^2}\int_0^{2\pi}\int_0^{\mathrm{Cos}^{-1}(R_o/R_o + c\tau/4)} G^2(\theta,\phi)\,\mathrm{Sin}\phi\,d\phi\,d\theta$$

$$\vdots \qquad \vdots \qquad \vdots \qquad \vdots \qquad \vdots \qquad (36)$$

$$\bar{I}_N \equiv \bar{I}_R(t_N) = \rho I_o \overline{TS}\,\frac{c\tau}{2}\,\frac{e^{-2\alpha(R_o + \frac{(N-1/2)c\tau}{2})}}{\left(R_o + (N-1/2)c\tau/2\right)^2}\int_0^{2\pi}\int_0^{\mathrm{Cos}^{-1}(R_o/R_o + (N-1/2)c\tau/2)} G^2(\theta,\phi)\,\mathrm{Sin}\phi\,d\phi\,d\theta \quad .$$

For ease in handling we define a quantity "ψ_N" such that

$$\psi_N \equiv \int_0^{2\pi}\int_0^{\mathrm{Cos}^{-1}(R_o/R_o + (N-1/2)c\tau/2)} G^2(\theta,\phi)\,\mathrm{Sin}\phi\,d\phi\,d\theta \quad . \qquad (37)$$

Thus, the N^{th} member of the sequence (36) can be written more compactly as

$$\bar{I}_N = \frac{\rho I_o \overline{TS}\, c\tau}{2\bar{R}_N^2}\, e^{-2\alpha\bar{R}_N} \cdot \psi_N \quad , \qquad (38)$$

$$\text{where } \bar{R}_N = R_o + (N-1/2)\,c\tau/2 \quad .$$

It should be remembered that expression (38) represents only the statistical average or expected value of the random variable $\tilde{I}_N$. Moreover, the members of the sequence $\{\tilde{I}_N\}$ are uncorrelated since the associated times are at least a pulselength apart by construction (see expressions (34) and (21)). If we plot the expected value of the intensity level $\bar{I}_R$ vs. time, the shape should be identical to the mean echo level presented in Fig. 7. The only difference is the scale factor "ZK^2" relating echo level S to intensity level $\bar{I}_R$.

In Fig. 11 we have illustrated the variation between the mean intensity, $\bar{I}$, and the intensity level of a single typical signal, $\tilde{I}$, at pulselength intervals. Suppose we now solve equation (38) for the density ρ in terms of the quantities $\tilde{I}_N$. Then

$$\rho = \frac{2\bar{R}_N^2\, e^{+2\alpha\bar{R}_N}}{I_o\,\overline{TS}\,c\tau\,\psi_N}\;\bar{I}_N \quad . \qquad (39)$$

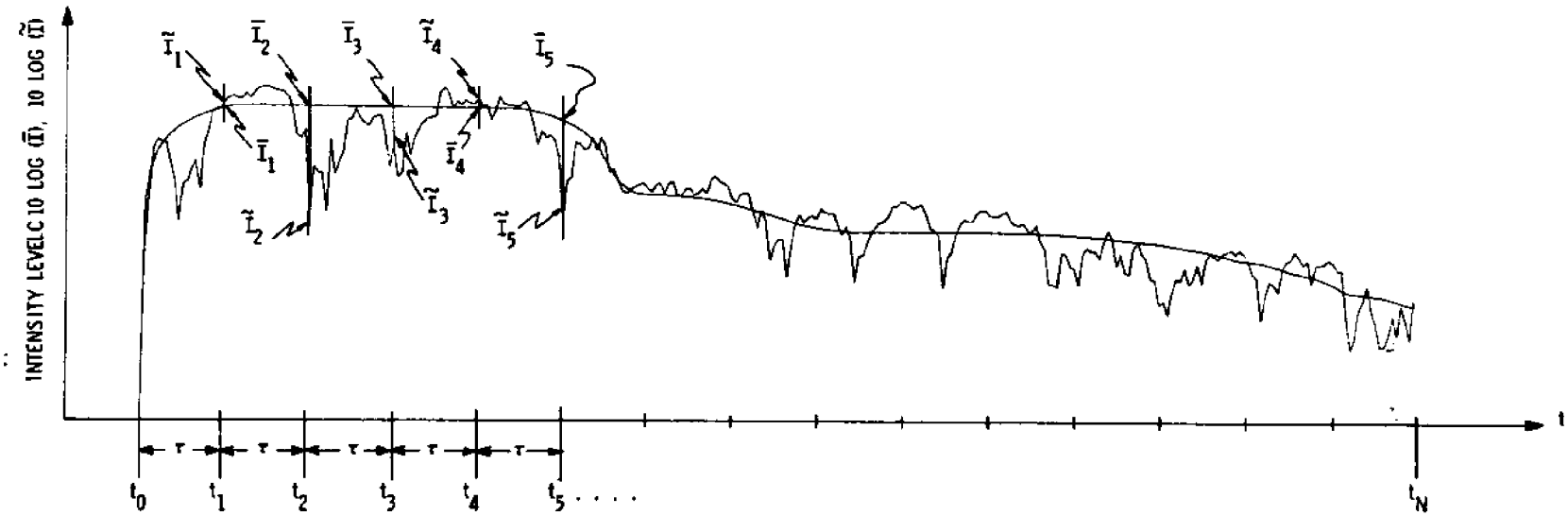

Figure 11 Variation Between Mean Intensity and Typical Intensity at Pulse Length Intervals

Expression (39) implies that if any member of the sequence $\{\bar{I}_N\}$ is weighted by suitable parameters, the quantity ρ will be obtained. Unfortunately in real situations we do not have access to the sequence $\{\bar{I}_N\}$, but rather the random sequence $\{\tilde{I}_N\}$. Thus, the best estimate we can get for ρ on the N^{th} data point $\tilde{I}_N$ is given by

$$\hat{\rho}_N = \frac{2\bar{R}_N^2 e^{+2\alpha \bar{R}_N}}{I_o \overline{TS}\, c\tau\, \psi_N} \cdot \tilde{I}_N \quad , \tag{40}$$

where the circumflex "$\wedge$" over the quantity ρ indicates its estimated value. Taking the expected value of both sides of (40) of course, yields (39). A simple way of combining the discrete data $\{\tilde{I}_N\}$ is to multiply each member of this sequence over the calculated volume of the corresponding pulse shell and sum the results. That is, we let V_N represent the volume of the N^{th} pulse shell responsible for the N^{th} intensity level $\tilde{I}_N$. Define a quantity $\hat{Q}$ where

$$\hat{Q} \equiv \sum_{\substack{\text{all} \\ N}} \hat{\rho}_N V_N \quad . \tag{41}$$

Then the expected value of $\hat{Q}$ becomes

$$E\{\hat{Q}\} = \sum_{\substack{\text{all} \\ N}} E\{\hat{\rho}_N\} V_N = \sum_{\substack{\text{all} \\ N}} \rho V_N = \rho \sum_{\substack{\text{all} \\ N}} V_N \quad . \tag{42}$$

Since the sum $\sum V_N$ is actually the summation of the volumes of the non-overlapping pulse shells, it is therefore equal to the total volume insonified. Thus, with ρ equal to the number of targets or fish per unit volume, the quantity $\hat{Q}$ is seen to be an unbiased estimate of the total number of fish in the insonified volume.

The quantity V_N can be calculated from expression (30) by substituting $\bar{R}_N$ for $\bar{R}$ and integrating to the appropriate limits. Thus,

$$\begin{aligned} V_N &= (c\tau/2)\bar{R}_N^2 \int_0^{2\pi} \int_0^{\mathrm{Cos}^{-1}(R_o/\bar{R}_N)} \mathrm{Sin}\phi\, d\phi\, d\theta \\ &= \pi c\tau \bar{R}_N [\bar{R}_N - R_o] \\ &= \pi c\tau \bar{R}_N (N - 1/2)\, c\tau/2 \quad . \end{aligned} \tag{43}$$

Substituting expressions (40) and (43) into (41) yields an explicit expression for the quantity $\hat{Q}$:

$$\hat{Q} = \frac{\pi c \tau}{\overline{TS}I_o} \sum_{\substack{\text{all} \\ N}} \left(\frac{(N - 1/2)\overline{R}_N^3 \; e^{+2\alpha \overline{R}_N}}{\psi_N} \; \tilde{I}_N \right) \quad . \tag{44}$$

Equation (44) can be written in terms of the time sequence $\{t_N\}$ by a direct substitution of $ct_N/2$ for $\overline{R}_N$ in expression (44).

3.3 ENVELOPE INTEGRATION

It has been shown that sampling, and properly weighting the intensity level at every pulse length in time leads to an unbiased estimate $\hat{Q}$ (expression (44)) of the abundance in an insonified volume. The first sample time, t_1, occurred at $t_1 = \tau$, the second at $t_2 = 2\tau$ and so on. It has also been shown that the resulting sequence of terms $\{\tilde{I}_N\}$ were uncorrelated because they were due to a set of adjoining pulse shells within the scattering layer. Since the only requirement for $\{\tilde{I}_N\}$ to be uncorrelated is that the sample times be taken a pulse length apart we might create another uncorrelated sequence say $\{I'_N\}$ by sampling at times $t'_1 = t_o + \tau + \epsilon$, $t'_2 = t_o + 2\tau + \epsilon$, ... $t'_n = t_o + N\tau + \epsilon$, where ϵ is chosen arbitrarily from a range $0 < \epsilon < \tau$. It should be noted that the cross correlation between the Nth respective terms, $\tilde{I}_N$ and $\tilde{I}'_N$ is $\neq 0$ since there is overlap between the respective pulse shells associated with $\tilde{I}'_N$ and $\tilde{I}_N$. We might make two unbiased estimates based on the sequences $\{\tilde{I}_N\}$ and $\{\tilde{I}'_N\}$ namely $\hat{Q}$ and $\hat{Q}'$. From (44)

$$\hat{Q} = \frac{\pi c \tau}{TSI_o} \sum_{\substack{\text{all} \\ N}} \left(\frac{\left(N - \frac{1}{2}\right)\overline{R}^3_N \; e^{2\alpha \overline{R}_N}}{\psi_N} \; \tilde{I}_N \right) \tag{44}$$

and

$$\hat{Q}' = \frac{\pi c \tau}{\overline{TS}I_o} \sum_{\substack{\text{all} \\ N}} \left(\frac{(N - \frac{1}{2} + \frac{\epsilon}{\tau})\,\overline{R}'^3_N \; e^{2\alpha \overline{R}'_N}}{\psi'_N} \; \tilde{I}'_N \right) \tag{45}$$

the primed quantities R'_N and ψ'_N are defined

$$R'_N \equiv R_o + \frac{c}{2}(N\tau - \epsilon)$$

$$\psi'_N \equiv \int_0^{2\pi} \int_0^{\cos^{-1} R_o/\overline{R}'_N} G^2(\theta, \phi) \sin\phi \, d\phi \, d\theta \tag{46}$$

We now have two quantities $\hat{Q}$ and $\hat{Q}'$ which are estimates of the same number of fish. Though they are not based on independent data (i.e. $\left\{\tilde{I}_N\right\}$ and $\left\{\tilde{I}'_N\right\}$ are correlated), it may be shown that from a statistical standpoint the sample mean is given by

$$\frac{1}{2}\ (\hat{Q} + \hat{Q}') = \text{sample mean} \tag{47}$$

is a better estimate than either $\hat{Q}$ or $\hat{Q}'$ respectively.

We might create yet another sequence say $\left\{I''_N\right\}$ by selecting times $t''_1 = t_o + \tau + 2\epsilon$, $t''_2 = t_o + 2\tau + 2\epsilon$, ... $t''_N = t_o + N\tau + 2\epsilon$. This then leads to another estimate, $\hat{Q}''$, in addition to $\hat{Q}'$ and $\hat{Q}$, and a sample mean

$$\frac{1}{3}\ (\hat{Q}+\hat{Q}'+\hat{Q}'') \tag{48}$$

Obviously this process may be extended indefinitely with the sample mean giving even better estimates. In the limit, the intensity level profile is divided up an infinite number of times giving an infinite number of unbiased, but correlated estimates. This may be shown mathematically as follows. Instead of the primed notation as in (47) and (48) it is convenient to order the estimates by subscripting them. That is $\hat{Q}_1 = \hat{Q}'$, $\hat{Q}_2 = \hat{Q}''$, $\hat{Q}_3 = \hat{Q}'''$... etc. The data sequences will be double subscripted where the second subscript will correspond to the subscript on the $\hat{Q}_i$'s. Thus $\hat{Q}_1$ will depend on the sequence $\left\{\tilde{I}_{N,1}\right\}$, $\hat{Q}_2$ on the sequence $\left\{\tilde{I}_{N,2}\right\}$ and so on. Thus a component $\tilde{I}_{N,K}$ will be the Nth data point of the Kth sequence. Fig. 12 is a sketch of an intensity level profile of which each interval a pulse length wide has been partitioned M times. Each sample component $\tilde{I}_{N,K}$ is a time step $\Delta t = \tau/M$ from the adjacent points $\tilde{I}_{N,K-1}$, and $\tilde{I}_{N,K+1}$. Here we must also impose a double subscript notation on $\overline{R}_N$ and ψ_N of the basic expression (46). Let

$$\begin{aligned} \overline{R}_{N,K} &\equiv R_o + \frac{c\tau}{2}\ \left(N - \frac{1}{2} + K\frac{\Delta t}{\tau}\right) \\ \psi_{N,K} &\equiv \int_0^{2\pi}\int_0^{\overline{R}_{N,K}} G^2(\theta,\phi)\ \sin\phi\, d\phi\, d\theta \end{aligned} \tag{49}$$

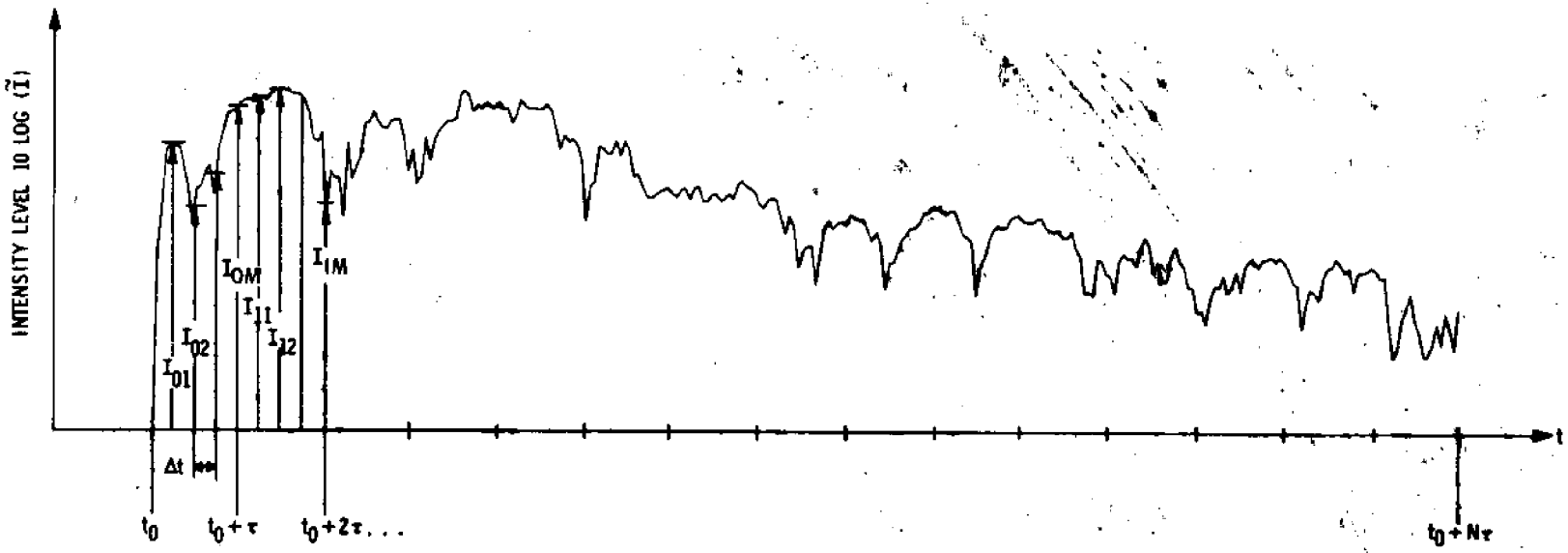

Figure 12 Intensity Level Profile Partitioning Within A Pulse Length For Echo Envelope Integration

Then the Kth estimate $\hat{Q}_K$ may be expressed as

$$\hat{Q}_K = \frac{\pi c \tau}{\overline{TS} I_o} \sum_{\substack{\text{all} \\ N}} \left(N - \frac{1}{2} + \frac{K \Delta t}{\tau}\right) \frac{R_N^3, K \, e^{2\alpha \overline{R}_{N,K}}}{\psi_{N,K}} \tilde{I}_{N,K} \qquad (50)$$

The sample mean, $\tilde{Q}_M$, may be defined as the average of the $\hat{Q}_K$'s, thus

$$\tilde{Q}_M = \frac{1}{M} \sum_{k=1}^{M} \hat{Q}_K \qquad (51)$$

but since $M = \tau/\Delta t$, $\tilde{Q}_M$ may be expressed as

$$\tilde{Q}_M = \frac{1}{\tau} \sum_{k=1}^{\tau/\Delta t} \hat{Q}_K \cdot \Delta t \qquad (52)$$

If we let $\Delta t \to 0$ by forcing $M \to \infty$, the sum on K multiplied by the quantity Δt approaches an integral. That is, the limit as $\Delta t \to 0$ of the right hand side of (52) with expression (50) inserted for $\hat{Q}_K$, is given by

$$\hat{Q} \equiv \lim_{\Delta t \to 0} \tilde{Q}_M = \frac{\pi c^4}{8 \overline{TS} I_o} \cdot \frac{1}{\tau} \int_{t_o + \frac{\tau}{2}}^{\infty} \frac{e^{\alpha c \left(t - \frac{\tau}{2}\right)} \left(t - \frac{\tau}{2}\right)^3 \left(t - t_o - \frac{\tau}{2}\right)}{\psi(t)} \tilde{I}(t) \, dt$$

where (53)

$$\psi(t) = \int_0^{2\pi} \int_0^{\cos^{-1}\left(t_o / \left(t - \frac{\tau}{2}\right)\right)} G^2(\theta, \phi) \sin\phi \, d\phi \, d\theta$$

If we compare expression (53) with its discrete counterpart (44) it is seen that the equations are basically the same except that integration with respect to time has replaced summation over discrete sampled points. The advantage of echo integration (53) over counting or summation (44) is a smaller error variance.

3.4 THIN SCATTERING LAYER

A thin scattering layer may be described as a large expanse of scatterers of thickness much less than $c\tau/2$. The pulse reflection from this type of layer is envisioned as an expanding circular ring in the plane of the scatterers. These rings are analagous to the hemispherical shells of the preceding section. The geometry is sketched in Fig. 13. The incremental area of the Nth ring dS_N is given by

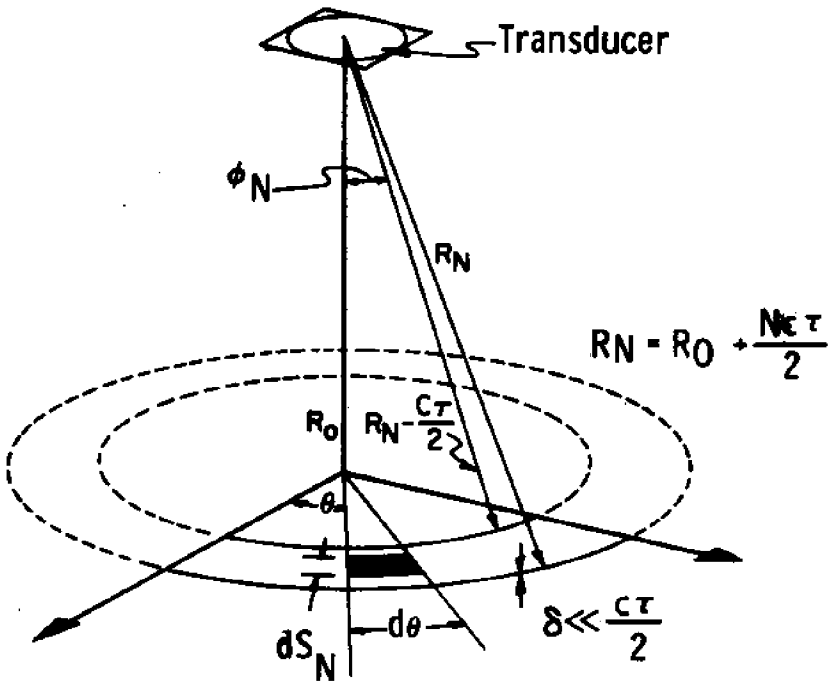

Figure 13 Geometry of Thin Scattering Layer

$$dS_N = R_o^2 \tan\phi_N \sec^2\phi_N \, d\phi \, d\theta \quad . \tag{54}$$

The total area of the Nth ring is

$$S_N = R_o^2 \int_0^{2\pi} \int_{\cos^{-1}\left(\frac{R_o}{R_N - \frac{c\tau}{2}}\right)}^{\cos^{-1}\left(\frac{R_o}{R_N}\right)} \tan\phi \sec^2\phi \, d\phi \, d\theta$$

$$= \pi c\tau \left[R_N - c\tau/4\right] \tag{55}$$

$$\approx \pi c\tau R_N \quad .$$

Since the scatterers lie in the plane, the density ρ is a surface density in units of meters^{-2}. The differential form of the received average intensity from the Nth ring is given by

$$dI_N = \frac{I_o \rho \overline{TS} \, e^{-2\alpha R_N}}{R_N^4} \, G^2(\theta, \phi_N) \, dS_N \tag{56}$$

Substituting $R_N = R_o \sec\phi_N$, and (54) into (56) yields the integral form

$$I_N = \frac{I_o \overline{TS}}{R_o^2} \int_0^{2\pi} \int_{\cos^{-1}\left\{\min\left(1; \frac{R_o}{R_N - \frac{c}{2}}\right)\right\}}^{\cos^{-1}\left(\frac{R_o}{R_N}\right)} e^{-2\alpha R_o \sec\phi} G^2(\theta, \phi) \sin\phi\cos\phi \, d\phi \, d\theta \tag{57}$$

If we define ψ'_N

$$\psi'_N \equiv \int_0^{2\pi} \int_{\cos^{-1}\left\{\min\left(1; \frac{R_o}{R_N - \frac{c\tau}{2}}\right)\right\}}^{\cos^{-1}\left(\frac{R_o}{R_N}\right)} e^{-2\alpha R_o \sec\phi} G^2(\theta, \phi) \sin\phi\cos\phi \, d\phi \, d\theta \tag{58}$$

and manipulate terms in a manner consistent with the procedure for determining the "$\hat{Q}$" of the thick scattering layer (expression 44), we arrive at

$$\hat{Q} = \frac{\pi c\tau R_o^2}{I_o \overline{TS}} \sum_{\substack{\text{all} \\ N}} \frac{R_N I_N}{\psi'_N} \quad . \tag{59}$$

An integrated form of (59) is found to be

$$\hat{Q} = \frac{\pi R_o^2 c^2}{2 I_o \overline{TS}} \left[\int_{t_o}^{t_o+\tau} \frac{t_o (t - t_o)}{\tau} \frac{\tilde{I}(t)}{\psi'(t)} \, dt + \int_{t_o+\tau}^{\infty} t \frac{\tilde{I}(t)}{\psi'(t)} \, dt \right] \tag{60}$$

where

$$\psi'(t) \equiv \int_0^{2\pi} \int_{\cos^{-1}\left\{\min\left(1;\, t_o/t-\tau\right)\right\}}^{\cos^{-1}(t_o/t)} e^{-\alpha c t_o \sec\phi} G^2(\theta,\phi) \sin\phi\cos\phi \, d\phi \, d\theta$$

3.5 VARIANCE ERROR - THICK SCATTERING LAYER

We have by means of (44) and (53) an unbiased estimate of the number of targets in a portion of the thick scattering layer. It remains to be seen how good an estimate this is. We define the error, $\tilde{\varepsilon}_Q$, as follows

$$\tilde{\varepsilon}_Q \equiv \frac{\hat{Q} - \bar{Q}}{\bar{Q}} \qquad \text{where} \quad \bar{Q} = E\{\hat{Q}\} \quad . \tag{61}$$

The mean or expected value of $\tilde{\varepsilon}_Q$ is zero, consistent with the fact that $\hat{Q}$ is an unbiased estimate of $\bar{Q}$. Determining the variance of $\tilde{\varepsilon}_Q$ is not a trivial problem (see Appendix D). The final results are*

$$\sigma_Q^2 = \frac{\sum_{\substack{\text{all} \\ N}} V_N^2 + \left(\frac{1}{\rho}\right) \frac{\overline{TS}^2}{\overline{TS}^2} \sum_{\substack{\text{all} \\ N}} \frac{\overline{G_N}^4}{\overline{G}^{2^2}} V_N}{\left(\sum_{\substack{\text{all} \\ N}} V_N\right)^2} \tag{62}$$

where

$$\sum_{\substack{\text{all} \\ N}} V_N^2 = \left(\frac{\pi}{2}\right)^2 (c\tau)^4 \sum_{N=1}^{2\delta/c\tau} \left(N - \frac{1}{2}\right)^2 \left(R_o + \frac{\left(N - \frac{1}{2}\right) c\tau}{2}\right)^2$$

$$\sum_{\substack{\text{all} \\ N}} V_N = \frac{\pi}{2} (c\tau)^2 \sum_{N=1}^{2\delta/c\tau} \left(N - \frac{1}{2}\right) \left(R_o + \left(N - \frac{1}{2}\right) \frac{c\tau}{2}\right) \tag{63}$$

---

* The variance σ_Q^2 is sometimes called the mean squared error.

δ = layer thickness

τ = pulse length

c = sound velocity

and

$$\text{a)}\quad \overline{TS} = \frac{1}{4\pi}\int_0^{2\pi}\int_0^{\pi} TS(\theta',\phi')\sin\phi'\,d\phi'\,d\theta'$$

$$\text{b)}\quad \overline{TS}^2 = \frac{1}{4\pi}\int_0^{2\pi}\int_0^{\pi} TS^2(\theta',\phi')\sin\phi'\,d\phi'\,d\theta' \qquad (64)$$

$$\text{c)}\quad \overline{G_N}^2 = \frac{R_N}{\pi\left(N-\frac{1}{2}\right)C\tau}\int_0^{2\pi}\int_0^{\cos^{-1}(R_o/R_N)} G^2(\theta,\phi)\sin\phi\,d\phi\,d\theta$$

$$\text{d)}\quad \overline{G_N}^4 = \frac{R_N}{\pi\left(N-\frac{1}{2}\right)C\tau}\int_0^{2\pi}\int_0^{\cos^{-1}(R_o/R_N)} G^4(\theta,\phi)\sin\phi\,d\phi\,d\theta$$

Expression (55) can be broken down into two components of variance. For high densities, expression (55) is given approximately by

$$\sigma_Q^2\Big)_{\rho\to\infty} \approx \sum_{\substack{\text{all}\\ N}} V_N^2 \Big/ \left(\sum_{\substack{\text{all}\\ N}} V_N\right)^2 \qquad (65)$$

$$= \sum_{N=1}^{2\delta/c\tau}\left(N-\frac{1}{2}\right)^2\left(R_o+\left(N-\frac{1}{2}\right)\frac{c\tau}{2}\right)^2 \Bigg/ \left(\sum_{N=1}^{2\delta/c\tau}\left(N-\frac{1}{2}\right)\left(R_o+\left(N-\frac{1}{2}\right)\frac{c\tau}{2}\right)\right)^2,$$

which, if $R_o >> \delta$ and $2\delta/c\tau > 1$ is approximately

$$\sigma_Q^2\Big)_{\rho\to\infty} \approx \frac{\frac{2}{3}\left(2\,\frac{2\delta}{c\tau}+1\right)}{\frac{2\delta}{c\tau}\left(\frac{2\delta}{c\tau}+1\right)} \qquad (66)$$

Thus, at high densities, the variance of the error is a function of the ratio of pulse length to scattering layer thickness. This portion of the error can be attributed to the random phases of the echo components. The fact that the error decreases with larger δ/τ is indicative of the fact that with smaller pulse lengths we base our estimate on more uncorrelated data points for a given insonified volume. For example, suppose we were implementing a scheme based on expression (44) to estimate the number of fish in a highly dense, 5 meter thick scattering layer. If a 1/2 millisecond pulse were used then based on expression (66), $\sigma_Q^2 \approx 0.1$. For a pulse length of about 6.6 milliseconds we can calculate $\sigma_Q^2 \approx 1.0$. Since we have only one significant data point, it is expected that the results

of (66) should be in agreement with expression (18). A plot of expression (66) is shown in Fig. 14. At low densities, $\rho \to 0$, the second component of variance predominates:

$$\sigma_Q^2\Big)_{\rho \to 0} \approx \frac{1}{\rho} \frac{\overline{TS}^2}{\overline{TS}^2} \sum_{\substack{\text{all} \\ N}} \left(\frac{\overline{G_N}^4}{\overline{G_N}^2} \right) V_N \Big/ \left(\sum_{\substack{\text{all} \\ N}} V_N \right)^2 \quad . \tag{67}$$

The ratio of the mean squared to the squared mean target strengths contributes directly to the variance. This is because of the fact that the estimate, expression (44), uses a target strength averaged over all orientations. The members of the target aggregate generally have scattering strengths which, at different orientations, fluctuate significantly about the mean. Mathematically, this will be reflected in the ratio $\overline{TS}^2/\overline{TS}^2$ which can vary from 1, for spherical isotropic scatterers, to larger numbers for more complex scatterers. Unfortunately, there seems to be little in the way of analytical techniques to aid in the calculation of the first and second moments, $\overline{TS}$ and $\overline{TS}^2$ respectively, for a given fish. Estimates would probably have to be made on the basis of experimental investigation. For example, one could numerically integrate the experimental data published in page 4 of Reference 2 for the POMOXIS NIGROMACULATUS (black crappie). A polar plot for this data is shown in Fig. 15. For this example we assume that the target strength $TS(\theta', \phi')$ does not vary with θ' (cylindrical symmetry) so that the polar plot of Fig. 15 fully defines the aspect behavior of TS (i.e. $TS(\theta', \phi') = TS(\phi')$). In this instance equations 64 (a) and (b) reduce to

$$\begin{aligned} &\text{(a)} \quad \overline{TS} = \frac{1}{2} \int_0^{\pi} TS(\phi') \sin\phi' \, d\phi' \\ &\text{(b)} \quad \overline{TS}^2 = \frac{1}{2} \int_0^{\pi} TS^2(\phi') \sin\phi' \, d\phi' \quad . \end{aligned} \tag{68}$$

Two integrations of the data in the polar plot of Fig. 3(a) corresponding to the expressions of 68 (a) and (b) resulted in the ratio

$$\frac{\overline{TS}^2}{\overline{TS}^2} \approx 2.7 \quad , \tag{69}$$

for a 20.6 cm black crappie at a frequency of 30 kHz.

The ratio of the transducer moments $\overline{G_N}^4/(\overline{G_N}^2)^2$ also contributes directly

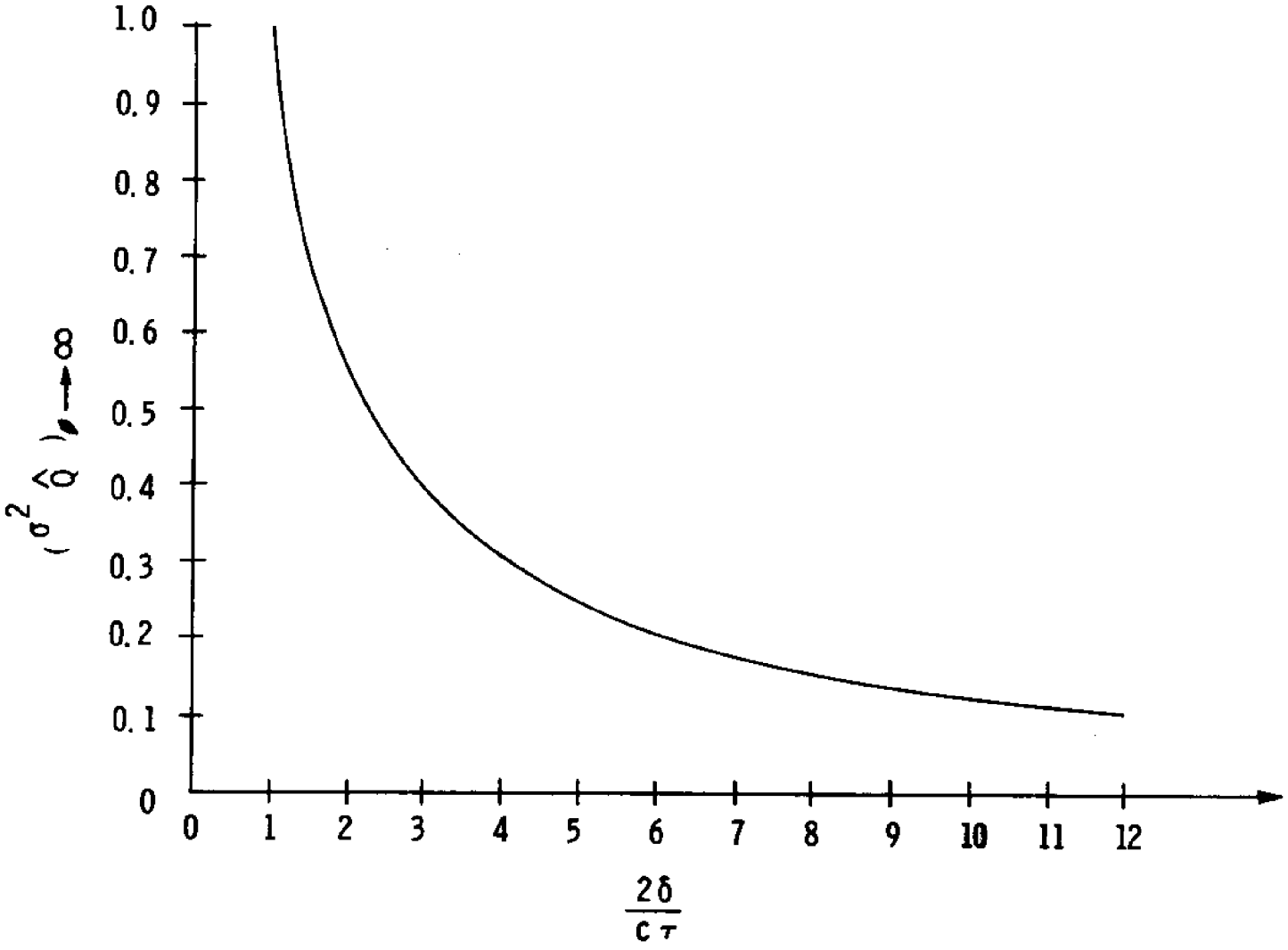

Figure 14 Variance Error in Estimated Number of Targets Versus Ratio of Scattering Layer Thickness and Pulse Length

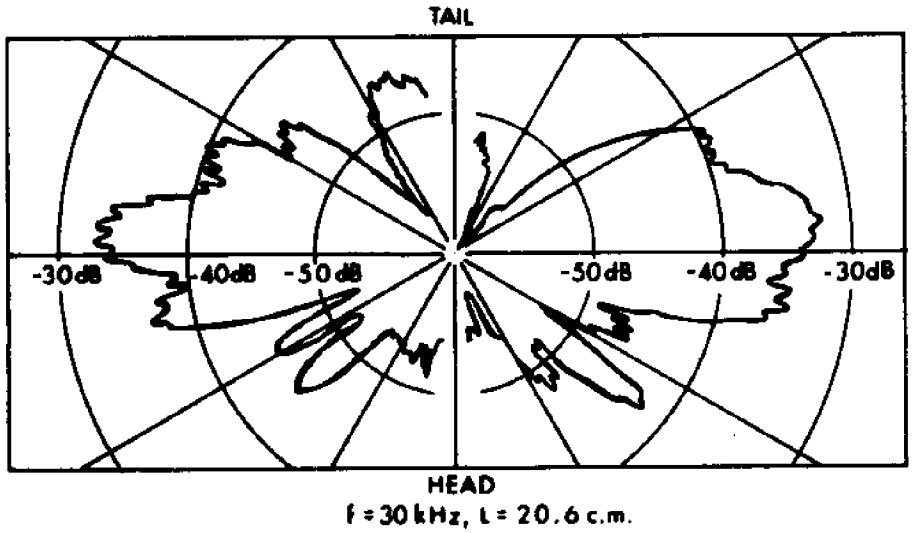

Figure 15 Variation of Target Strength of Black Crappie About X Axis (Ref. 2)

to the variance at low densities (equation (60)). Generally, this ratio is about unity for $N = 1$ and becomes larger with greater N at a rate dependent upon the depth of the scattering layer (R_o) and the aperture size of the transducer. Smaller R_o and narrower beam widths result in larger quantities for the sequence $\left\{\overline{G_N^4}/(\overline{G_N^2})^2\right\}$. As an example, these ratios were calculated for a few specific cases and are shown in Figs. 16 (a), (b), and (c). A circular directivity pattern (equation 6A) with $d/\lambda = 2, 4, 6, 8$ was integrated with the aid of a digital computer. The other parameters were set at τ(pulselength) $= 10^{-3}$ seconds and R_o (layer depth) = 100 meters (Fig. 16(a)), $R_o = 50$ meters (Fig 16 (b)), and $R_o = 25$ meters (Fig. 16 (c)).

Equation (67) was evaluated with the aid of a digital computer using the data in Fig. 16 (a), (b), and (c). Figure 17 (a), (b), and (c) depicts the variance error in the estimated number of fish σ_Q^2 versus layer depth R_o. For various circular transducer aperture sizes. The results in Fig. (17) are merely representative values based upon arbitrarily selected parameters.

Note that in all situations presented the variance error decreases with increasing depth R_o and increases with larger transducer apertures d/λ, e.g., smaller half power beam width angles. It is shown in Appendix C that the variance of the integration estimate is given by

$$\sigma_Q^2 = \frac{\sum_N \left(\frac{1}{2}+\frac{1}{2N}\right) V_N^2 + \left(\frac{1}{\rho}\right) \frac{\overline{TS^2}}{\overline{TS}^2} \sum_N \left(\frac{2}{3}+\frac{2}{3N}\right) \frac{\overline{G_N^4}}{\overline{G_N^2}^2} V_N}{\left(\sum_N V_N\right)^2} \quad . \tag{70}$$

Comparison between (70) and (62) shows that the difference lies in the coefficients $(1/2+1/2N)$ and $(2/3+2/3N)$. Since,

$$\frac{1}{2} + \frac{1}{2N} \to \frac{1}{2}$$

$$\frac{2}{3} + \frac{2}{3N} \to \frac{2}{3} \quad , \qquad (N = 1, 2, \ldots)$$

it is seen that integration reduces the variance of the error, σ_Q^2, by approximately $1/2$ in the high density component and by $1/3$ for the low density component.

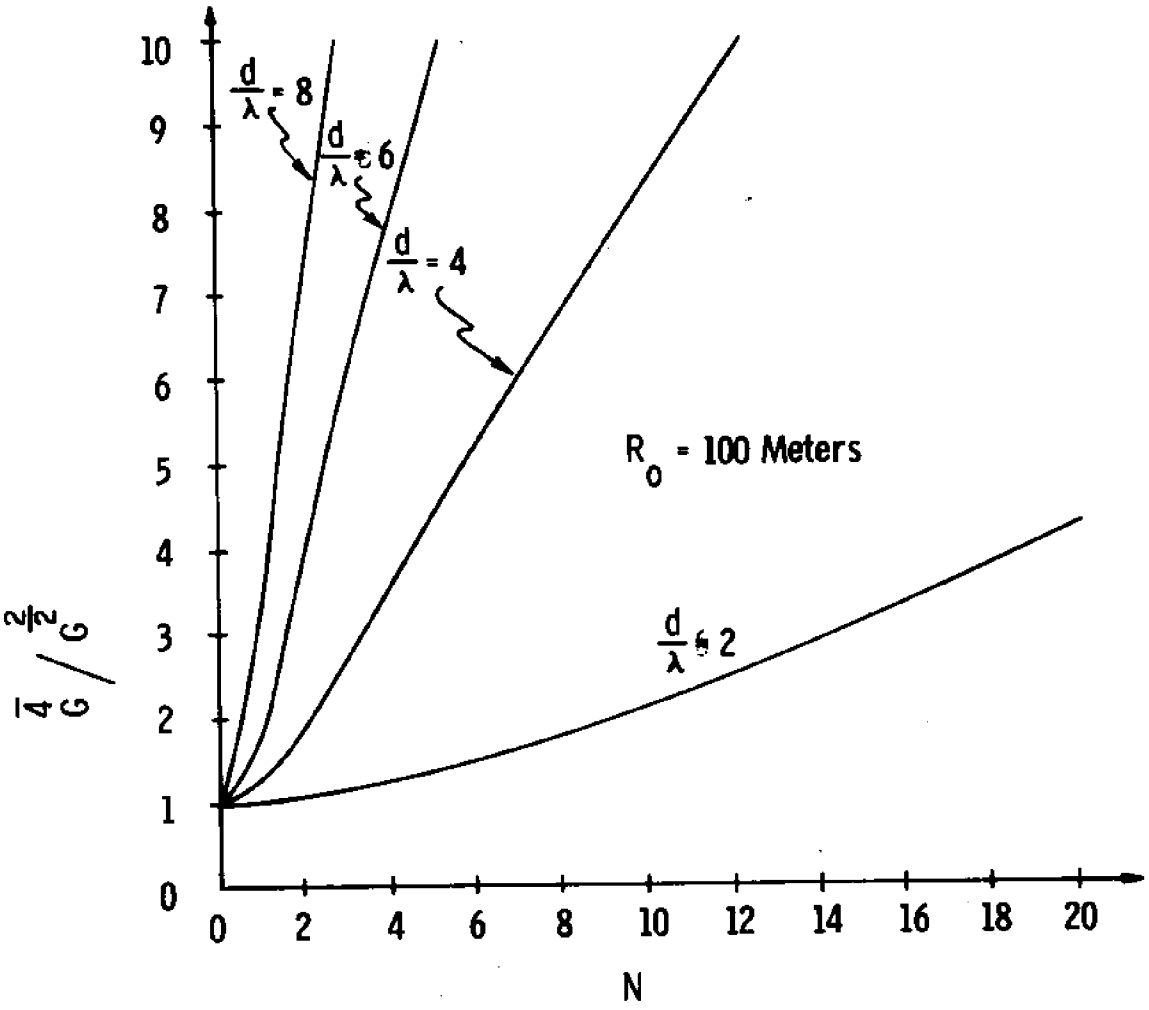

Figure 16a Normalized Fourth Moment of Transducer Directivity Function Versus Sampling Index

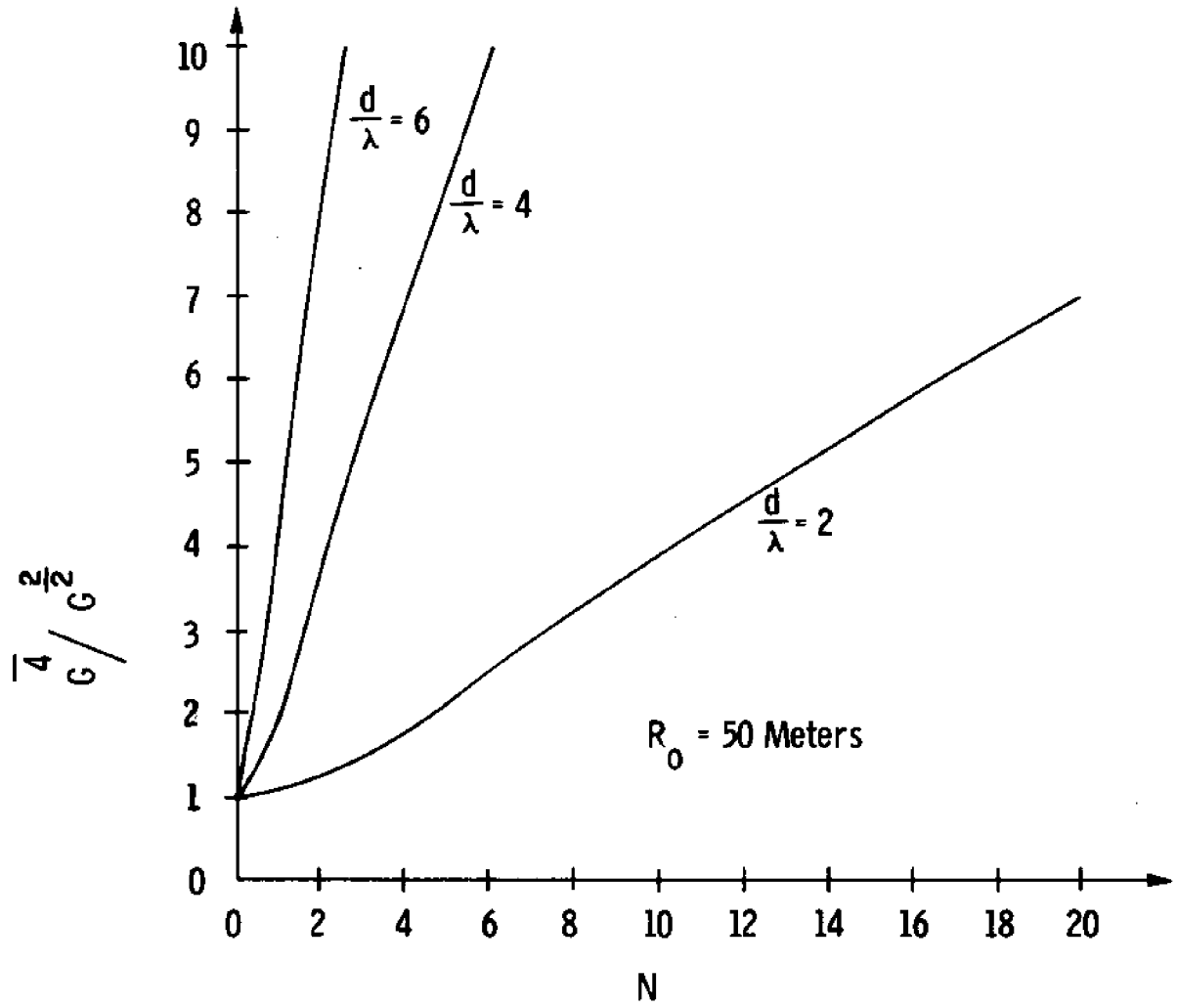
10
9
8
7
6
5
4
3
2
1
0
$\overline{G_4}/G_2^2$
$\frac{d}{\lambda} = 6$
$\frac{d}{\lambda} = 4$
$\frac{d}{\lambda} = 2$
R_0 = 50 Meters
0
2
4
6
8
10
12
14
16
18
20
N

Figure 16 (b)

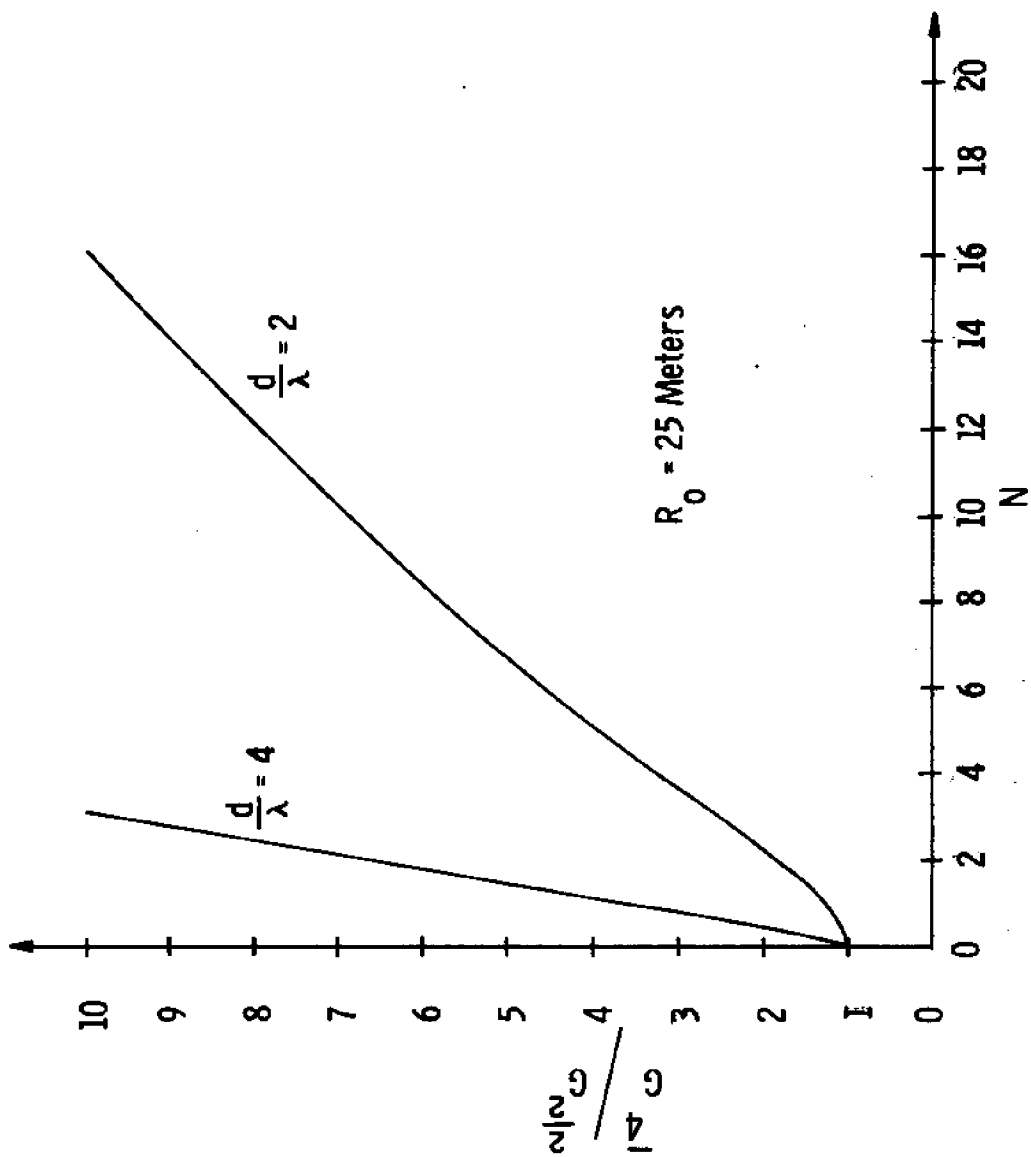
$\frac{d}{\lambda} = 4$
$\frac{d}{\lambda} = 2$
$R_o = 25$ Meters
$\sigma_{\Delta I}^4 / \sigma_{nI}^2$
N
0
1
2
3
4
5
6
7
8
9
10
0
2
4
6
8
10
12
14
16
18
20

Figure 16 (c)

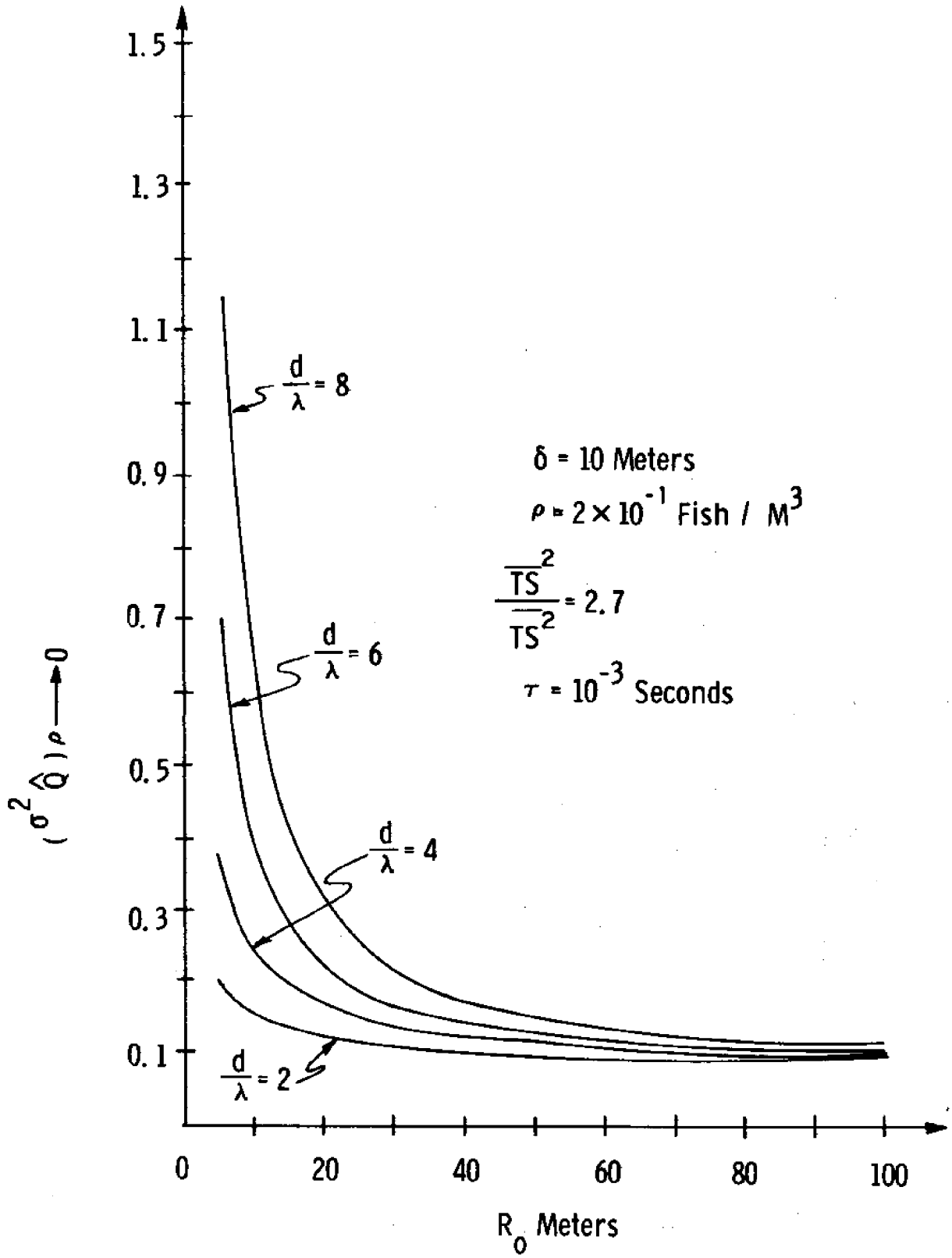

Figure 17(a) Variance Error in Estimated Number of Fish in Insonified Volume Versus Range to Scattering Layer for Various Circular Aperture Transducer Sizes

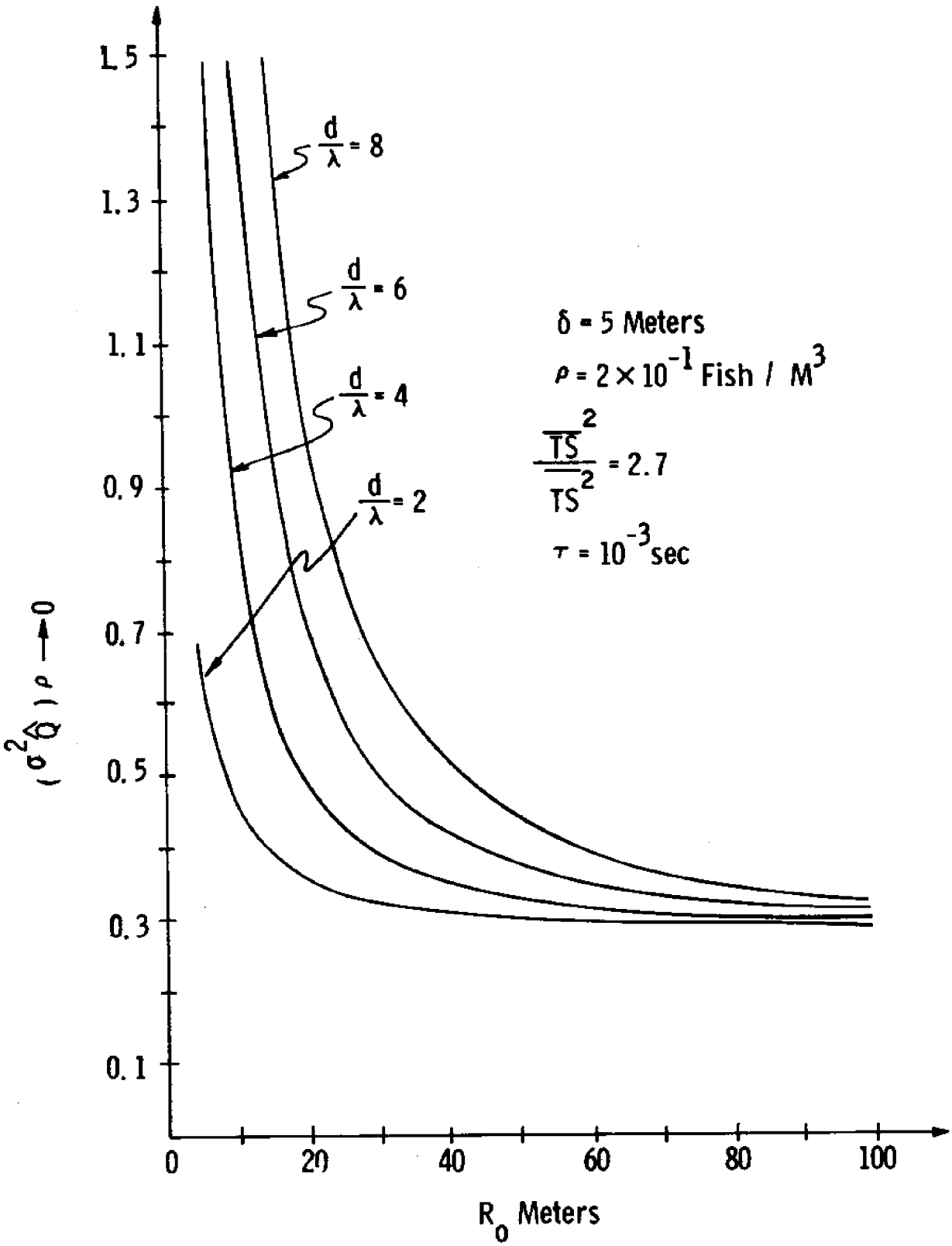
1.5
1.3
1.1
0.9
0.7
0.5
0.3
0.1
$(\sigma^2_{\hat{Q}})_{\rho \to 0}$
$\frac{d}{\lambda} = 8$
$\frac{d}{\lambda} = 6$
$\frac{d}{\lambda} = 4$
$\frac{d}{\lambda} = 2$
$\delta = 5$ Meters
$\rho = 2 \times 10^{-1}$ Fish / M^3
$\frac{\overline{TS}^2}{\overline{TS^2}} = 2.7$
$\tau = 10^{-3}$ sec
0
20
40
60
80
100
R_0 Meters

Figure 17 (b)

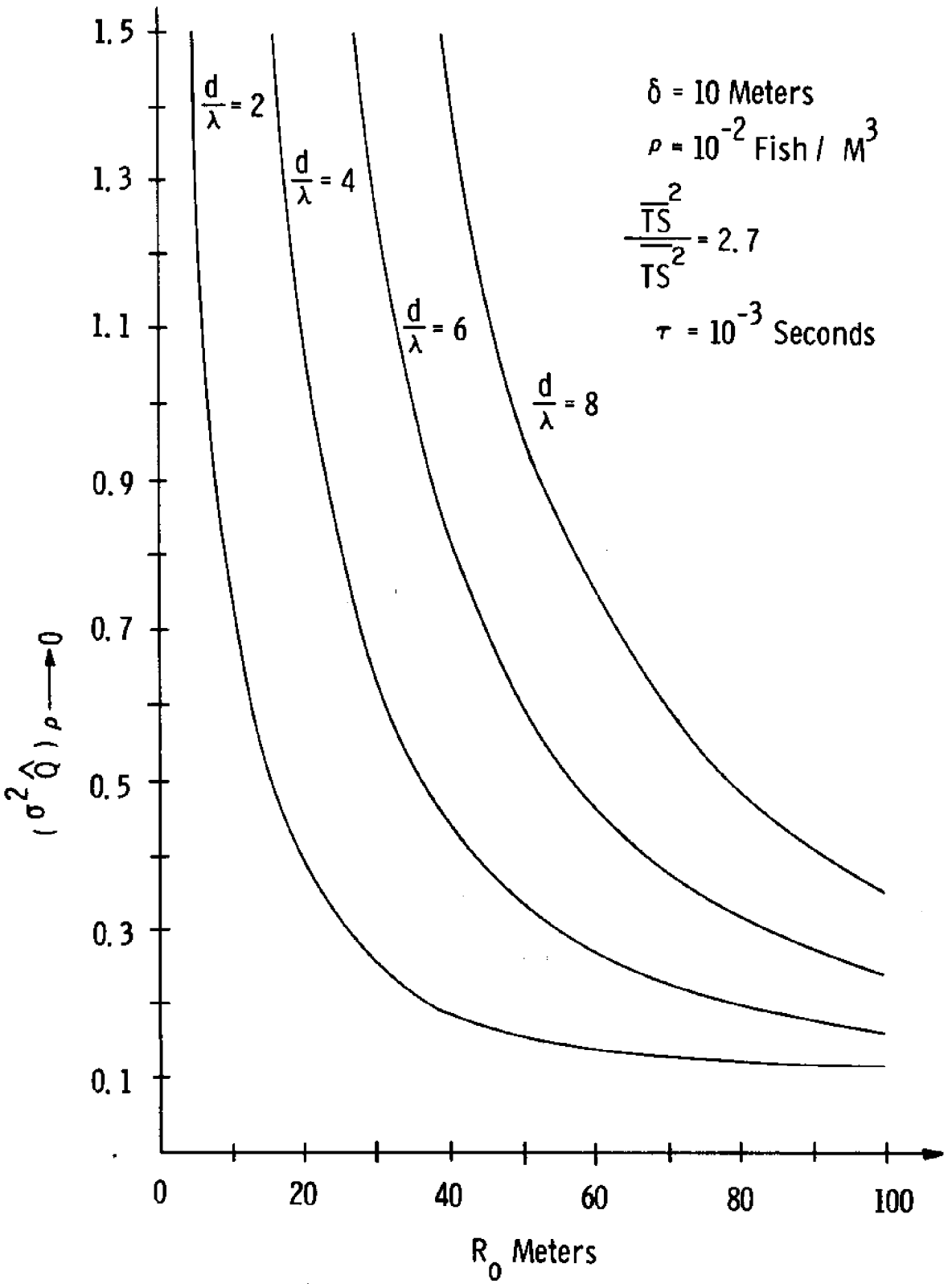
1.5
1.3
1.1
0.9
0.7
0.5
0.3
0.1
$(\sigma^2\hat{Q})_{\rho \to 0}$
$\frac{d}{\lambda} = 2$
$\frac{d}{\lambda} = 4$
$\frac{d}{\lambda} = 6$
$\frac{d}{\lambda} = 8$
δ = 10 Meters
$\rho = 10^{-2}$ Fish / M^3
$\frac{\overline{TS}^2}{\overline{TS^2}} = 2.7$
$\tau = 10^{-3}$ Seconds
0
20
40
60
80
100
R_0 Meters

Figure 17 (c)

It is interesting to modify (53) by means of the following approximation; let

$$\int_{t_o+\frac{\tau}{2}}^{\infty} e^{\alpha c\left(t-\frac{\tau}{2}\right)} \frac{\left(t-\frac{\tau}{2}\right)^3 \left(t-t_o-\frac{\tau}{2}\right)}{\psi(t)} \tilde{I}(t)\,dt \simeq e^{\alpha c t_o} t_o^3 \sum_N e^{\alpha c\left(N-\frac{1}{2}\right)\tau} \frac{\left(N-\frac{1}{2}\right)\tau}{\psi N} \int_{t_o+\left(N-\frac{1}{2}\right)\tau}^{t_o+\left(N+\frac{1}{2}\right)\tau} \tilde{I}(t)$$

Then by multiplying by τ/τ we get from (63):

$$Q \simeq \frac{\pi c^4 \tau t_o^3 e^{\alpha c t_o}}{8 \overline{TS} I_o} \sum_N e^{\alpha c\left(N-\frac{1}{2}\right)} \frac{\left(N-\frac{1}{2}\right)}{\psi N} \frac{1}{\tau} \int_{t_o+\left(N-\frac{1}{2}\right)\tau}^{t_o+\left(N+\frac{1}{2}\right)\tau} \tilde{I}(t)\,dt \,. \quad (71)$$

We observe that the term $\frac{1}{\tau} \int_{t_o+\left(N-\frac{1}{2}\right)\tau}^{t_o+\left(N+\frac{1}{2}\right)\tau} \tilde{I}\,dt$ is simply the time average of the intensity over a pulse length. Thus, it is not surprising that the variance of the high density error component approaches $1/2 \sum_N V_N^2 / \left(\sum_N V_N\right)^2$, since this is consistent with out investigation of time averaging over a pulse length (equations 22 and 23 with Δt set equal to τ).

3.6 VARIANCE ERROR — THIN LAYER

The error analyses for the thin scattering layer configuration can be carried out in a manner similar to those for the thick scattering layer. The results are nearly identical to expression (62) for echo sampling.

The variance for echo sampling of a thin layer is

$$\sigma_Q^2 = \frac{\sum_{\substack{\text{all}\\N}} S_N^2 + \frac{1}{\rho} \frac{\overline{TS^2}}{\overline{TS}^2} \sum_{\substack{\text{all}\\N}} \frac{\overline{G_N^4}}{\overline{G_N^2}} S_N}{\left(\sum_{\substack{\text{all}\\N}} S_N\right)^2} \quad (72)$$

and for integration

$$\sigma_Q^2 = \frac{\frac{1}{2} \sum_N S_N^2 + \frac{1}{\rho} \frac{\overline{TS^2}}{\overline{TS}^2} \frac{2}{3} \sum_N \frac{\overline{G_N^4}}{\overline{G_N^2}} S_N}{\left(\sum_N S_N\right)^2} \quad (73)$$

where

$$S_N = \pi c \tau R_N$$

$$\overline{G_N}^2 = \frac{1}{2\pi} \int_0^{2\pi} G^2 \left[\cos^{-1} \left(\frac{R_o}{R_N} \right), \theta \right] d\theta$$

$$\overline{G_N}^4 = \frac{1}{2\pi} \int_0^{2\pi} G^4 \left[\cos^{-1} \left(\frac{R_o}{R_N} \right), \theta \right] d\theta \quad .$$

4.0 SUMMARY

In this note we have employed a series of mathematical expressions, beginning with a form of the basic sonar equation, and developed methods for estimating the number of independent random scatterers contributing to a single hydroacoustical echo signal.

This analysis has been limited to an examination of the echo signal as it appears at the terminals of an electro-acoustic transducer.

We have assumed a static environment, i.e., within the time interval between a transmitted hydroacoustical pulse and the received echo from the targets of interest there is no relative motion between the transducer and the insonified targets.

We have defined the positions of the targets of interest to be based upon an average number per unit volume. If the concept of average target density is acceptable for fish distributions in a natural environment then the error models developed in this note are valid. If, however, fish in the wild are in an ordered array then a different distribution and corresponding error model would be required. For the present, the concept of average target density appears applicable for situations where fish are separated to a point where the mean distance between them approaches their individual length.

A detailed discussion, concerning the basic concepts of linear hydroacoustics* as it relates to biomass measurement, has been developed.

We have devoted a considerable amount of discussion to the postulation of random phases of the individual target echo signals as they appear at the transducer. This has been done to illustrate the expected amplitude variation of the echo signal envelope and to provide insight into the information contained therein.

In the derivation of the correlation coefficient we have shown that it is necessary, if the echo signal envelope is to be sampled at discrete intervals, that the amplitude measurement must be at pulse length intervals. This interval is necessary to assure statistical independence of the measurement of signal amplitude in order to avoid bias error.

---

* Linear acoustics assumes that the density and compressibility of sea water and the targets of interest are not affected by the acoustic intensities resulting from the pulse time durations employed in simple echo sounding equipment. Non-linear hydroacoustical techniques are not within the scope of this note.

It has also been shown that if measurements of the echo signal amplitude is averaged over a time interval (integrated), the amplitude variations can be smoothed without introducing measurement bias error.

We have developed two echo signal envelope amplitude processing methods which produce a quantity which is the estimated number of fish targets within the sea volume insonified by a single hydroacoustical pulse. These methods are defined as echo signal envelope sampling and echo signal envelope integration.

The geometrical configuration of the target aggregation we have examined may be loosely defined as a scattering layer. We have defined the scattering layer as "thick" or "thin" according to the mathematical manipulations required to estimate the number of targets from the insonified volume. It should be noted that our definition of the thickness of the scattering layer implies no biological significance.

The variance error models derived include the effects of the transducer directivity function, the density of the targets, target strength, transmitted hydroacoustical pulse length and layer thickness. Arbitrary and perhaps typical situations are presented from computer aided solutions of the echo envelope sampling variance error model.

It is shown that in all cases the variance error is minimized when a small aperature transducer and a short transmitted pulse length is employed.

It should be noted that the variance errors given are the absolute minimum that may be obtained under ideal conditions. The significance of this result suggests that considerable investigation and thought into a particular hydroacoustic equipment configuration must precede a decision to commence measurements at sea.

For example, it is shown that if the ratio of the transducer aperture to the wave length of the transmitted carrier frequency is small (resulting in a large half power beam width) the variance error is minimized, theoretically at least. Practically speaking a small aperture transducer will receive more unwanted noise signal than a large aperture transducer. This noise will reduce the signal to noise ratio at the receiver input terminals. The point at which the noise signal introduces significant error into the measurement must be known in order to evaluate the usefulness of any data which may be obtained.

In this note fish targets are treated as individual point sources of scattered hydroacoustical energy. In Appendix E, we have combined the theoretical work of others with our own to support this thesis.

It will be noted that we have ignored the effect of multiple scattering. Multiple scattering is presumed to exist in dense aggregations of fish and is related to the scattering of acoustic intensity from one fish to another. In addition, we have ignored the effect of acoustic absorption by the aquatic animal. The analyses of these effects in Appendix E suggests that multiple scattering and absorption have no significant effect upon the results of the work we have done to date. If, however, appropriate modifications can be identified the mathematical model described in Appendix E and the corresponding environment simulation described in Appendix F will be changed.

Appendix F contains a brief description of the digital computer aided simulations and analyses we have developed in the course of our engineering investigations to support the conclusions presented in this note.

5.0 CONCLUSION

It has been demonstrated that there are many factors interacting in the simple hydroacoustical environment we have examined and the precision of the measurement of biomass or fish quantification is related to the following:

1. The average target strength of an individual fish.
2. The density and spatial distribution of the individual fish.
3. The geometrical shape of an aggregation of the fish.
4. The characteristics of the hydroacoustical equipment employed.
5. The characteristics of the surrounding sea environment.

Any attempt to apply pulsed hydroacoustical signals for aquatic biomass or resource assessment measurements which does not properly account for the factors listed above can hardly be expected to yield useful results.

As stated in the preface we have avoided analytical short cuts which can lead to erroneous conclusions concerning the applicability of hydroacoustics to aquatic biomass measurements.

It is our considered opinion that it is impractical to predict or estimate errors in a particular hydroacoustical biomass or fish quantification scheme without first performing careful analyses.

The analyses we refer to here are the kinds which deal with a clearly defined situation.

The detailed specification of such a situation and the subsequent description by mathematical modeling, supported by computer aided simulation techniques, is a form of systems analysis. The overall objective of systems analysis, in this context, is to examine specific situations in order to determine the performance of a postulated system.

It is obvious that, if a postulated situation or environment cannot be defined in some detail, the concept of systems analysis is of doubtful value.

Realistic models of a biomass measurement system, including the man-machine combination, must be clearly defined in order to apply systems analysis effectively.

In view of the above, the analysis we have presented in this note is by no

means complete, however, we believe it to provide a sound basis from which to continue further investigations.

The reader will note that we have not considered the effects of transducer motion, target motion and noise, therefore, we are suggesting that effort should be expended in examining, by analytical techniques, the probable effects of these upon hydroacoustical measurements.

We are also suggesting that a hydroacoustical measurement program be initiated to verify the analytically derived echo signal processing methods described in this note. This program should be carefully planned and executed in order that any hydroacoustic biomass measurement system that may result will be verified for concept, accuracy and cost to benefit criteria.

REFERENCES

1. A. Papoulis, "Probability, Random Variables and Stochastic Processes", McGraw-Hill, 1965.

2. R. Love, "An Emperical Equation for the Determination of the Maximum Side-Aspect Target Strength of an Individual Fish", Naval Oceanographic Office, Washington, D.C., 1969.

3. R. Urick, "Principles of Underwater Sound for Engineers", McGraw-Hill, 1967.

4. K. Norton, L. Vogler, W. Mansfield and P. Short, "The Probability Distribution of the Amplitude of a Constant Vector Plus a Rayleigh-Distributed Vector", Proceedings of the IRE, October 1955.

APPENDIX A

DISTRIBUTION OF THE SPACING BETWEEN UNIFORMLY DISTRIBUTED POINTS

Let N+1 objects be randomly distributed throughout a volume enclosed by a sphere of radius "R". We concentrate on any one of the objects located at say position "P_o" and proceed to determine the probability distribution of the distance to its closest neighbor. Let "D" be an arbitrary, fixed distance from P_o. The probability of the remaining N objects being greater than distance "D" from P_o can be found by considering each object separately. Define the following quantities:

$$V_T = \text{total volume enclosing all objects} = \frac{4}{3}\pi R^3 \quad ,$$

$$V_D = \text{volume enclosed by sphere of radius D} = \frac{4}{3}\pi D^3 \quad .$$

Thus any given object, other than that located at P_o of course, say the "i^{th}" one, has a probability of being located outside V equal to:

$$P\left\{i^{th} \text{ object located outside } V_D\right\} = \frac{V_T - V_D}{V_T} \qquad \text{(A-1)}$$

and the probability that all N objects have locations outside V_D, since these are independent events, is given by:

$$P\left\{\text{all N objects located outside } V_D\right\} = \left(\frac{V_T - V_D}{V_T}\right)^N \quad . \qquad \text{(A-2)}$$

It then follows that the probability of at least one object falling within V_D is given by:

$$P\left\{\text{at least one object falling within } V_D\right\} = 1 - \left(\frac{V_T - V_D}{V_T}\right)^N \qquad \text{(A-3)}$$

Thus, the distribution function $F_N(D)$ of the random variable $\tilde{D}$, is given by:

$$F_N(D) \equiv P\left\{\tilde{D} \le D\right\} = 1 - \left(\frac{V_T - V_D}{V_T}\right)^N \quad , \qquad \text{(A-4)}$$

or

$$F_N(D) = 1 - \left(1 - \frac{D^3}{R^3}\right)^N \quad . \qquad (D > 0) \quad . \qquad \text{(A-5)}$$

Define the volume density ρ to be:

$$\rho \equiv \frac{N}{V_T} = \frac{N}{\frac{4}{3}\pi R^3} \quad . \qquad \text{(A-6)}$$

Then $F_N(D)$ may be written:

$$F_N(D) = 1 - \left(1 - \frac{\frac{4}{3}\pi \rho D^3}{N}\right)^N \qquad (D > 0) \quad . \qquad \text{(A-7)}$$

Equation (7) is cumbersome and difficult to work with. The following relation may be used to alleviate the probelm:

$$\lim_{x \to \infty} \left(1 - \frac{a}{x}\right)^x = e^{-a} \quad . \qquad \text{(A-8)}$$

Since $N = V_T \rho = 4/3 \pi R^3 \rho$, we may let $R \to \infty$ while holding ρ constant and

$$\lim_{R \to \infty} F_N(D) = \lim_{N \to \infty} F_N(D) = 1 - e^{-\frac{4}{3}\pi \rho D^3} \qquad (D > 0) \quad . \qquad \text{(A-9)}$$

Therefore, for large N the distribution function of the random variable $\tilde{D}$ may be approximated by

$$F_\infty(D) = \lim_{N \to \infty} F_N(D) \qquad \text{(A-10)}$$

or

$$F_\infty(D) = 1 - e^{-\frac{4}{3}\pi \rho D^3} \qquad (D > 0) \quad . \qquad \text{(A-11)}$$

The mean of $\tilde{D}$ is given by:

$$\langle \tilde{D} \rangle = \int_0^\infty D \left(\frac{d F_\infty}{d D}\right) \cdot d D \quad , \qquad \text{(A-12)}$$

but

$$\frac{d F_{\infty}}{d D} = 4 \pi \rho D^2 \, e^{-\frac{4}{3} \pi \rho D^3} \quad ,$$

and

$$\int_0^{\infty} D \cdot (4 \pi \rho D^2) \, e^{-\frac{4}{3} \pi \rho D^3} \, d D = \frac{\left(\frac{1}{3}\right)!}{\left(\frac{4}{3} \pi \rho\right)^{1/3}} \approx \frac{.55}{\rho^{1/3}} \quad .$$

or

$$\langle \tilde{D} \rangle \approx \frac{.55}{\rho^{1/3}} \quad .$$

The second moment of $\tilde{D}$ is given by:

$$\langle \tilde{D}^2 \rangle = \int_0^{\infty} D^2 \cdot \left(\frac{d F_{\infty}}{d D} \right) d D = \frac{\left(\frac{2}{3}\right)!}{\left(\frac{4}{3} \pi \rho\right)^{2/3}} \approx \frac{.342}{\rho^{2/3}} \quad . \qquad \text{(A-13)}$$

Therefore, the variance is:

$$\sigma_D^2 = \langle \tilde{D}^2 \rangle - \langle \tilde{D} \rangle^2 \approx \frac{.037}{\rho^{2/3}} \quad .$$

It is important to note that the probability of the following events are easily calculated:

I. The probability that $\tilde{D}$ will be less than any number $D_1 > 0$:

$$P \left\{ \tilde{D} < D_1 \right\} = F_{\infty} (D_1) = 1 - e^{-\frac{4}{3} \pi \rho D_1^3}$$

II. The probability that $\tilde{D}$ will be greater than any number $D_2 > 0$:

$$P \left\{ \tilde{D} > D_2 \right\} = 1 - F_{\infty} (D_2) = e^{-\frac{4}{3} \pi \rho_v D_2^3} \quad .$$

III. The probability that $\tilde{D}$ will lie between D_1 and D_2 where $D_1 \leq D_2$:

$$P\left\{D_1 \leq \tilde{D} \leq D_2\right\} = F_\infty(D_2) - F_\infty(D_1) = \left(e^{-\frac{4}{3}\pi\rho D_1^3}\right) - \left(e^{-\frac{4}{3}\pi\rho D_2^3}\right) .$$

APPENDIX B

CORRELATION COEFFICIENT FOR THICK SCATTERING LAYER

The coherence between two distinct points on the echo level is described by its correlation coefficient. Suppose $\tilde{I}(t_1)$ is the value of the intensity level at time t_1, and $\tilde{I}(t_2)$ is the value at time t_2, and $0 \le t_2 - t_1 \le \tau$. The correlation coefficient $r(t_1, t_2)$ is given by:

$$r(t_1, t_2) = \frac{\overline{\left[\tilde{I}(t_1) - \bar{I}(t_1)\right]\left[\tilde{I}(t_2) - \bar{I}(t_2)\right]}}{\left[\overline{\left[\tilde{I}(t_1) - \bar{I}(t_1)\right]^2}\,\overline{\left[\tilde{I}(t_2) - \bar{I}(t_2)\right]^2}\right]^{1/2}} \quad . \qquad \text{(A-14)}$$

As before we assume that the targets are dispersed uniformly throughout the thick scattering layer with an average density ρ. In figure B-1 a portion of the scattering layer has been broken up into three distinct volumes designated A, B, and C. The intensity level $\tilde{I}(t_1)$ is defined to be that produced by the scatterers contained in volumes A and B which comprise a complete pulse shell. The intensity level $\tilde{I}(t_2)$ is produced by scatterers contained in volumes B and C which also comprise a complete pulse shell. The volume B is therefore the overlap region which couples $\tilde{I}(t_1)$ and $\tilde{I}(t_2)$. Since $\tilde{I}(t_1)$ and $\tilde{I}(t_2)$ are the squared magnitudes of vector or phasor sums, they may be expressed mathematically as:

$$\tilde{I}(t_1) = \frac{I_o}{\bar{R}^4}\left[\left(\sum_{i=1}^{\tilde{N}_A} \tilde{\beta}_i \sin\tilde{\phi}_i + \sum_{j=1}^{\tilde{N}_B} \tilde{\beta}_j \sin\tilde{\phi}_j\right)^2 + \left(\sum_{i=1}^{\tilde{N}_A} \tilde{\beta}_i \cos\tilde{\phi}_i + \sum_{j=1}^{\tilde{N}_B} \tilde{\beta}_j \cos\tilde{\phi}_j\right)^2\right]$$

$$\tilde{I}(t_2) = \frac{I_o}{\bar{R}^4}\left[\left(\sum_{j=1}^{\tilde{N}_B} \tilde{\beta}_j \sin\tilde{\phi}_j + \sum_{k=1}^{\tilde{N}_C} \tilde{\beta}_k \sin\tilde{\phi}_k\right)^2 + \left(\sum_{j=1}^{\tilde{N}_B} \tilde{\beta}_j \cos\tilde{\phi}_j + \sum_{k=1}^{\tilde{N}_C} \tilde{\beta}_k \cos\tilde{\phi}_k\right)^2\right] \qquad \text{(A-15)}$$

where

I_o = source level

$\bar{R}$ = average range to volumes A, B, and C

$\tilde{N}_A$, $\tilde{N}_B$, $\tilde{N}_C$ = random number of scatterers in volumes A, B, and C, respectively

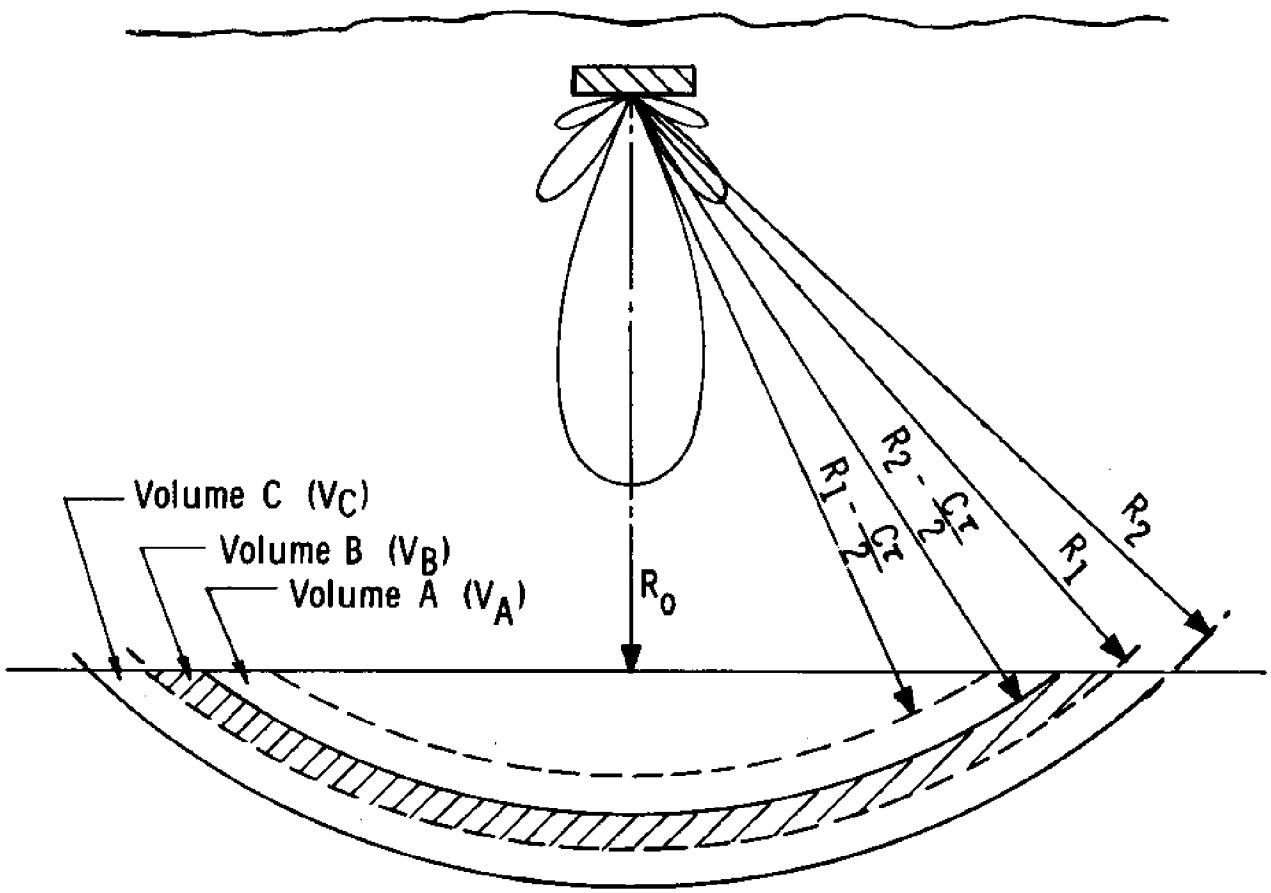
Volume C (V_C)
Volume B (V_B)
Volume A (V_A)
R_0
$R_1 - \frac{c\tau}{2}$
$R_2 - \frac{c\tau}{2}$
R_1
R_2

Figure B-1

$$\tilde{\beta}_i = \left[\tilde{TS}_i\, G^2\,(\tilde{\theta}_i, \tilde{\phi}_i)\right]^{\frac{1}{2}} = \left[\text{Target strength} \times \text{directivity function}^2\right]^{\frac{1}{2}}$$

$\tilde{\phi}_i$ = random phase of an individual acoustical wave .

We note that in (A-15) there are sums of random variables to limits which are themselves random variables, namely $\tilde{N}_A$, $\tilde{N}_B$, and $\tilde{N}_C$. These are Poisson distributed random variables with first and second moments given by:

$$\begin{aligned}
E\left\{\tilde{N}_A\right\} &= \rho V_A, \quad E\left\{\tilde{N}_A^2\right\} = \rho V_A (1 + \rho V_A), \\
E\left\{\tilde{N}_B\right\} &= \rho V_B, \quad E\left\{\tilde{N}_B^2\right\} = \rho V_B (1 + \rho V_B), \\
E\left\{\tilde{N}_C\right\} &= \rho V_C, \quad E\left\{\tilde{N}_C^2\right\} = \rho V_C (1 + \rho V_C),
\end{aligned} \tag{A-16}$$

where

$E\{\ \}$ = expected value

$V_A = 2\pi\bar{R}(R_2 - R_1)(\bar{R} - R_o)$

$V_B = 2\pi\bar{R}(R_1 - R_2 + C\tau/2)(\bar{R} - R_o)$

$V_C = 2\pi\bar{R}(R_2 - R_1)(\bar{R} - R_o)$.

An important relationship involving random sums may be found on pp. 248-249 of Reference 1. It states that if we have a random variable $\tilde{N}$ of discrete type, taking on values 1, 2, ... n ..., and a sequence of random variables $\tilde{x}_1, \tilde{x}_2, \ldots \tilde{x}_n, \ldots$ that are uncorrelated and independent of $\tilde{N}$, the first and second moments random sum

$$\tilde{S} = \sum_{k=1}^{\tilde{N}} \tilde{x}_K \tag{A-17}$$

are

$$E\left\{\tilde{S}\right\} = E\left\{\tilde{N}\right\}\, E\left\{\tilde{X}_K\right\}$$

$$E\left\{\tilde{S}^2\right\} = E\left\{\tilde{N}^2\right\}\, E\left\{\tilde{X}_K\right\}^2 + \sigma_x^2\ E\left\{\tilde{N}\right\}$$

where

$$\sigma_x^2 \equiv E\left\{\tilde{X}_K^2\right\} - E\left\{\tilde{X}_K\right\}^2 \quad .$$

Finally, we make the assumption that the random phases, $\tilde{\phi}_i$, are independent and uniformly distributed between 0 and 2π. Thus, the moments of the trigonometric functions are given by:

$$E\left\{\sin^n \phi_i\right\} = \frac{1}{2\pi} \int_0^{2\pi} \sin^n \phi \, d\phi \quad .$$

$$E\left\{\cos^n \phi_i\right\} = \frac{1}{2\pi} \int_0^{2\pi} \cos^n \phi \, d\phi \quad . \qquad \text{(A-18)}$$

We now multiply the right hand sides of equations (A-15) and square the indicated terms. After much algebra and application of (A-17) and (A-18) we find

$$E\left\{\tilde{I}(t_1)\tilde{I}(t_2)\right\} = \frac{I_o}{\bar{R}^8}\left[\overline{TS}^2\,\overline{G}^{2\,2}\,(\bar{N}_A\bar{N}_B + \bar{N}_A\bar{N}_C + \bar{N}_B\bar{N}_C) + \bar{N}_B\,\overline{TS}^2\,\overline{G}^4 + 2\,(\overline{N_B}^2 - \bar{N}_B)\,\overline{TS}^2\,\overline{G}^{2\,2}\right] \quad , \qquad \text{(A-19)}$$

but, from (A-16)

$$\bar{N}_A \equiv E\left\{\tilde{N}_A\right\} = \rho \cdot 2\pi\,\bar{R}\,(R_2 - R_1)\,(\bar{R} - R_o) \quad ,$$

$$\bar{N}_B \equiv E\left\{\tilde{N}_B\right\} = \rho \cdot 2\pi\,\bar{R}\,(R_1 - R_2 + C\tau/2)\,(\bar{R} - R_o) \quad ,$$

$$\bar{N}_C \equiv E\left\{\tilde{N}_C\right\} = \rho \cdot 2\pi\,\bar{R}\,(R_2 - R_1)\,(\bar{R} - R_o) \quad ,$$

$$\overline{N_B^2} \equiv E\left\{\tilde{N}_B^2\right\} = \rho \cdot 2\pi\,\bar{R}(R_1 - R_2 + C\tau/2)(\bar{R} - R_o) \cdot \left[1 + \rho \cdot 2\pi\,\bar{R}(R_1 - R_2 + C\tau/2) \cdot (\bar{R} - R_o)\right]$$

Since t_1 and t_2 are related to R_1 and R_2 by $t_1 = 2R_1/C$, and $t_2 = 2R_2/C$, (A-19) becomes, with Δt substituted for $t_2 - t_1$,

$$\overline{\tilde{I}(t_1)\,\tilde{I}(t_2)} = \frac{I_o^2}{\bar{R}^8}\left[\pi^2 c^2 \rho^2 \bar{R}^2 (\bar{R} - R_o)^2\left((\Delta t - \tau)^2 + \tau^2\right) \overline{TS}^2\, \overline{G^2}^2 + \pi c \rho \bar{R} (\bar{R} - R_o)(\tau - \Delta t)\, \overline{TS}^2\, \overline{G}^4\right] . \tag{A-20}$$

The second moment of $\tilde{I}(t)$ can be found by setting $\Delta t = 0$ in (A-20):

$$\overline{\tilde{I}^2} = \frac{2 I_o^2}{\bar{R}^8}\left[\pi^2 c^2 \rho^2 \bar{R}^2 (\bar{R} - R_o)^2 \tau^2\, \overline{TS}^2\, \overline{G^2}^2 + \frac{1}{2}\pi c \rho \bar{R} \cdot (\bar{R} - R_o)\, \tau\, \overline{TS}^2\, \overline{G}^4\right] . \tag{A-21}$$

The first moment of $\tilde{I}(t)$ can be found by taking the expected value of either equation in (A-15),

$$\bar{I} = \bar{\tilde{I}}(t_1) = \bar{\tilde{I}}(t_2) = \frac{I_o}{\bar{R}^3}\, \pi c \rho \tau\, \overline{TS}\, \overline{G}^2 (\bar{R} - R_o) . \tag{A-22}$$

We may now expand the numerator and denominator of (A-14):

$$\overline{\left[\tilde{I}(t_1) - \bar{I}(t_1)\right]\left[\tilde{I}(t_2 - \bar{I}(t_2)\right]} = \overline{\tilde{I}(t_1)\,\tilde{I}(t_2)} - \overline{\tilde{I}(t_1)\,\bar{I}(t_2)} - \overline{\bar{I}(t_1)\,\tilde{I}(t_2)} + \overline{\bar{I}(t_1)\,\bar{I}(t_2)}$$

$$= \overline{\tilde{I}(t_1)\,\tilde{I}(t_2)} - \bar{I}^2$$

$$\left[\overline{\left[\tilde{I}(t_1) - \bar{I}(t_1)\right]^2 \cdot \left[\tilde{I}(t_2) - \bar{I}(t_2)\right]^2}\right]^{\frac{1}{2}} = \left[(\bar{\tilde{I}}_1^2 - \bar{I}^2)(\bar{\tilde{I}}_2^2 - \bar{I}^2)\right]^{\frac{1}{2}} = \bar{\tilde{I}}^2 - \bar{I}^2 .$$

Thus, for $0 \le t_1 - t_2 \le \tau$,

$$r(t_1, t_2) = \frac{\overline{\tilde{I}(t_1)\tilde{I}(t_2)} - \bar{I}^2}{\bar{\tilde{I}}^2 - \bar{I}^2} = \frac{\rho \pi c \bar{R}(\bar{R}-R_o)(\Delta t-\tau)^2\, \overline{TS}^2 \overline{G^2}^2 + (\tau-\Delta t)\, \overline{TS}^2 \overline{G}^4}{\rho \pi c \bar{R}(\bar{R}-R_o)\, \tau^2\, \overline{TS}^2 \overline{G^2}^2 + (\tau-\Delta t)\, \overline{TS}^2 \overline{G}^4} , \tag{A-23}$$

where

$$\Delta t = t_2 - t_1 .$$

Expression (A-23) was derived assuming $0 \le t_2 - t_1 \le \tau$. It is easy to show that if we assumed that $0 \le t_1 - t_2 \le \tau$, the results would be identical to (A-23) except that Δt would be replaced by $-\Delta t$. Thus, for $|\Delta t| \le \tau$,

$$r(t_1, t_2) = \begin{cases} \dfrac{\rho \pi c \bar{R}(\bar{R}-R_o)(|\Delta t| - \tau)^2 \overline{TS}^2 \overline{G}^{2\,2} + (\tau - |\Delta t|)\overline{TS}^2 \overline{G}^4}{\rho \pi c \bar{R}(\bar{R}-R_o)\, \tau^2 \overline{TS}^2 \overline{G}^{2\,2} + (\tau - |\Delta t|)\, \overline{TS}^2 \overline{G}^4} \\ \\ 0 \quad \text{for} \quad |\Delta t| \ge 0 \ . \end{cases} \tag{A-24}$$

For high densities $(\rho \to \infty)$, (A-24) reduces to

$$r(t_1, t_2) \underset{\rho \to \infty}{\approx} \begin{cases} \left(\dfrac{|\Delta t|}{\tau} - 1 \right)^2 & |\Delta t| \le \tau \\ 0 & \text{Otherwise.} \end{cases} \tag{A-25}$$

For low densities (A-24) is approximately

$$r(t_1, t_2) \underset{\rho \to 0}{\approx} \begin{cases} 1 & |\Delta t| \le \tau \\ \\ 0 & \text{Otherwise.} \end{cases}$$

APPENDIX C

DETERMINATION OF VARIANCE ERROR OF INTEGRATION

The quantity $\hat{Q}$ given by equation (53) in the text is a method of thick scattering layer quantification by echo integration. In this method $\hat{Q}$ is given by:

$$\hat{Q} = \frac{\pi c^4}{8 \overline{TS} I_o} \frac{1}{\tau} \int_{t_o + \tau/2}^{\infty} e^{\alpha c(t - \tau/2)} \frac{(t - \tau/2)^3 (t - t_o - \tau/2)}{\psi(t)} \tilde{I}(t)\, dt \quad . \tag{53}$$

The error $\tilde{\varepsilon}_Q$ is given by (61)

$$\tilde{\varepsilon}_Q = \frac{\hat{Q} - \bar{Q}}{\bar{Q}} \quad , \tag{61}$$

where

$$\bar{Q} = E\left\{\hat{Q}\right\} \quad .$$

The variance of (49) is,

$$\sigma_Q^2 = E\left\{\tilde{\varepsilon}_Q^2\right\} \quad . \tag{A-43}$$

In order to evaluate (A-43) we make some initial simplifications. In expression (67) the integral may be expressed as a sum of integrals

$$\int_{t_o + (\tau/2)}^{\infty} e^{\alpha c(t - \tau/2)} \frac{\left(t - \frac{\tau}{2}\right)^3 \left(t - t_o - \frac{\tau}{2}\right)}{\psi(t)} \tilde{I}(t)\, dt = \sum_{N=1}^{\infty} \int_{t_o + (N - 1/2)\tau}^{t_o + (N + 1/2)\tau} e^{\alpha c(t - \tau/2)} \cdot \left(t - \frac{\tau}{2}\right)^3 \frac{\left(t - t_o - \frac{\tau}{2}\right)}{\psi(t)} \tilde{I}(t)\, dt \quad . \tag{A-44}$$

We may assume for present purposes the terms $e^{\alpha c(t - \tau/2)}$, $(t - \tau/2)^3$ and $\psi(t)$ vary slowly over a short time interval so that they may be taken out from under the integral signs. Then, to a first order approximation

$$\int_{t_o+(N-1/2)\tau}^{t_o+(N+1/2)\tau} e^{\alpha c(t-\tau/2)} \frac{\left(t-\frac{\tau}{2}\right)^3 \left(t-t_o-\frac{\tau}{2}\right)}{\psi(t)} \tilde{I}(t)\,dt \simeq \frac{e^{\alpha c\left[t_o+(N-1/2)\tau\right]}\left[t_o+\left(N-\frac{1}{2}\right)\tau\right]^3}{\psi(t_o+N\tau)}$$

$$\cdot \int_{t_o+(N-1/2)\tau}^{t_o+(N+1/2)\tau} \left(t-t_o-\frac{\tau}{2}\right) \tilde{I}(t)\,dt \quad . \tag{A-45}$$

Therefore, expression (53) may be rewritten

$$\hat{Q} \simeq K \sum_N X_N \frac{1}{\tau} \int_{t_o+(N-1/2)\tau}^{t_o+(N+1/2)\tau} \left(t-t_o-\frac{\tau}{2}\right) \tilde{I}(t)\,dt \quad ,$$

where

$$K \equiv \frac{\pi c^4}{8\,\overline{TS}\,I_o}$$

$$X_N \equiv \frac{e^{\alpha c\left[t_o+(N-1/2)\tau\right]}\left[t_o+\left(N-\frac{1}{2}\right)\tau\right]^3}{\psi(t_o+N\tau)} \quad .$$

The expected value of $\hat{Q}$ is given by:

$$\bar{Q} = K \sum_N X_N \frac{1}{\tau} \int_{t_o+(N-1/2)\tau}^{t_o+(N+1/2)\tau} \left(t-t_o-\frac{\tau}{2}\right) \bar{I}(t)\,dt \quad . \tag{A-47}$$

Substituting (A-46) and (A-47) into (61) yields

$$\tilde{\varepsilon}_Q = \frac{K \sum_N X_N \frac{1}{\tau} \int_{t_o+(N-1/2)\tau}^{t_o+(N+1/2)\tau} \left(t-t_o-\frac{\tau}{2}\right)\left(\tilde{I}(t)-\bar{I}(t)\right) dt}{\bar{Q}} \quad . \tag{A-48}$$

Since our goal is to evaluate (A-43) we must first square both sides of (A-48). Then taking the expected value of the quantity $\tilde{\varepsilon}_Q^{\,2}$, we are left with

$$\sigma_Q^2 = E\left\{\tilde{\varepsilon}_Q^2\right\} = \frac{K^2}{\bar{Q}^2} \sum_{M=1}^{\infty} \sum_{N=1}^{\infty} X_M X_N \cdot \frac{1}{\tau^2} \overline{\int_{t_o+(N-1/2)\tau}^{t_o+(N+1/2)\tau} \left(t - t_o - \frac{\tau}{2}\right)\left(\tilde{I}(t) - \bar{I}(t)\right) dt \int_{t_o+(M-1/2)\tau}^{t_o+(M+1/2)\tau} \left(t - t_o - \frac{\tau}{2}\right)\left(\tilde{I}(t) - \bar{I}(t)\right) dt} \quad . \tag{A-49}$$

The product of the integrals can be written as a double integral and the averaging can be carried out under the integral signs. Thus,

$$\overline{\int_{t_o+(N-1/2)\tau}^{t_o+(N+1/2)\tau} (\quad) dt \int_{t_o+(M-1/2)\tau}^{t_o+(M+1/2)\tau} (\quad) dt} = \int_{t_o+(N-1/2)\tau}^{t_o(N+1/2)\tau} \int_{t_o+(M-1/2)\tau}^{t_o(M+1/2)\tau} \cdot \overline{(\quad)(\quad)}\, dt_1\, dt_2 \quad . \tag{A-50}$$

The integrand of the right hand side of (A-50) is reducible to

$$\overline{\left(t_1 - t_o - \frac{\tau}{2}\right)\left(\tilde{I}(t_1) - \bar{I}(t_1)\right)\left(t_2 - t_o - \frac{\tau}{2}\right)\left(\tilde{I}(t_2) - \bar{I}(t_2)\right)}$$

$$= \begin{cases} \left(t_1 - t_o - \frac{\tau}{2}\right)\left(t_2 - t_o - \frac{\tau}{2}\right)\left(\overline{\tilde{I}(t_1)\tilde{I}(t_2)} - \bar{I}^2\right) & |t_1 - t_2| \le \tau \\ 0 & |t_1 - t_2| > \tau \end{cases} \quad . \tag{A-51}$$

The reason that the mean of the integrand of (A-50) is zero for $|t_1 - t_2| \ge \tau$ is a consequence of the fact that $\tilde{I}(t_2)$ and $\tilde{I}(t_1)$ are uncorrelated for $|t_1 - t_2| \ge \tau$. (See Appendix B, equation (A-24).) Thus, for $|t_1 - t_2| > \tau$,

$$\overline{\left(\tilde{I}(t_1) - \bar{I}(t_1)\right)\left(\tilde{I}(t_2) - \bar{I}(t_2)\right)} = \overline{\left(\tilde{I}(t_1) - \bar{I}(t_1)\right)} \cdot \overline{\left(\tilde{I}(t_2) - \bar{I}(t_2)\right)} = 0 \, . \tag{A-52}$$

It follows that from (A-50) and (A-51) that the double sum in (A-49) reduces to a single sum and the variance of $\tilde{\varepsilon}_Q$ is given by

$$\sigma_Q^2 = \frac{K^2}{\bar{Q}^2} \sum_N X_N^2 \frac{1}{\tau^2} \int_{t_o+(N-1/2)\tau}^{t_o+(N+1/2)\tau} \int \left(t_1 - t_o - \frac{\tau}{2}\right)\left(t_2 - t_o - \frac{\tau}{2}\right)\left(\overline{\tilde{I}(t_1)\,\tilde{I}(t_2)} - \bar{I}^2\right) \cdot dt_1\, dt_2 \quad . \tag{A-53}$$

Analytic expressions for the terms $\overline{\tilde{I}(t_1)\,\tilde{I}(t_2)}$ and $\bar{I}$ are developed in Appendix B and are given by equations (A-20) and (A-22), respectively. These may be substituted into the right hand side of (A-53) and the integration may then be carried out. The results after integration and substitution are:

$$\sigma_Q^2 = \frac{\sum_N \left(\frac{1}{2} + \frac{1}{2N} + \frac{13}{90N^2}\right) V_N^2 + \frac{1}{\rho}\frac{\overline{TS}^2}{\bar{TS}^2} \sum_N \left(\frac{2}{3} + \frac{2}{3N} + \frac{11}{60N^2}\right) \frac{\overline{G_N}^4}{\overline{G_N}^2} V_N}{V_T^2} , \tag{A-54}$$

where

$$V_N = \pi c T \bar{R}_N \left(N - \frac{1}{2}\right) \frac{c\tau}{2}$$

$$V_T = \sum_N V_N \quad .$$

Note that V_N is the volume of the N^{th} pulse shell given by expression (43) of the text.

APPENDIX D

DETERMINATION OF VARIANCE OF $\tilde{\varepsilon}_Q$ (SAMPLING ERROR)

The quantity $\hat{Q}$ given by expression (44) in the text was seen to be an unbiased estimate of the total number of targets in the insonified portion of a thick scattering layer. The error $\tilde{\varepsilon}_Q$ was defined by (61) such that

$$\tilde{\varepsilon}_Q = \frac{\hat{Q} - \bar{Q}}{\bar{Q}} \quad , \tag{61}$$

where

$$\bar{Q} = E\left\{\hat{Q}\right\} \quad .$$

The mean of $\tilde{\varepsilon}_Q$ is seen to be zero and the variance is given by:

$$\sigma_Q^2 = E\left\{\tilde{\varepsilon}_Q^2\right\} \quad . \tag{A-27}$$

In order to evaluate (A-27) we proceed with the definition of $\hat{Q}$ given by (44)

$$\hat{Q} = \frac{\pi c \tau}{\overline{TS}\, I_o} \sum_{\text{All } N} \frac{\left(N - \frac{1}{2}\right) \overline{R}_N^3 \, e^{2\alpha \overline{R}_N} \, \tilde{I}_N}{\psi_N} \tag{44}$$

But, $\tilde{I}_N$, the random variable representing the received intensity from the Nth pulse shell, may be written:

$$\tilde{I}_N = \frac{e^{-2\alpha \overline{R}_N} I_o}{\overline{R}_N^4} \left[\left(\sum_{i=1}^{\tilde{K}_N} \tilde{\beta}_{N_i} \sin \phi_i \right)^2 + \left(\sum_{i=1}^{\tilde{K}_N} \tilde{\beta}_{N_i} \cos \phi_i \right)^2 \right] \tag{A-28}$$

where

$\tilde{K}_N$ = random number of scatterers contained in N^{th} pulse shell

ϕ_i = random phase of an individual acoustical wave .

The double subscripted random variables $\tilde{\beta}_{N_i}$ are defined as

$$\tilde{\beta}_{N_i} = \left[\tilde{TS}_i \, G_N^2 \, (\tilde{\theta}_i, \tilde{\phi}_i)\right]^{\frac{1}{2}} . \tag{A-29}$$

$\tilde{TS}_i$ is the random quantity which represents the target strength of the i^{th} fish in the N^{th} pulse shell. Its first and second moments are defined by equations (64-a) and (64-b) in the text.

The term $G_N(\tilde{\theta}_i, \tilde{\phi}_i)$ refers to the directivity function of the transducer as a function of the directional angles $(\tilde{\theta}_i, \tilde{\phi}_i)$ of the i^{th} fish in the N^{th} pulse shell. These angles are assumed to be independent random variables with a joint probability density function given by:

$$P(\tilde{\theta}_i, \tilde{\phi}_i) = \frac{\sin \phi_i}{2\pi\left[1 - \frac{R_o}{\bar{R}_N}\right]} , \quad 0 < \theta_i < 2\pi , \; 0 < \phi_i < \cos^{-1}(R_o/\bar{R}_N) . \tag{A-30}$$

The second and fourth moments of the directivity function associated with the N^{th} shell are found by averaging over all θ_i and ϕ_i, and are given by equations (64-c) and (64-d) in the text. It follows that

$$\begin{aligned} \overline{\beta_N^2} &= \overline{TS} \cdot \overline{G_N^2 \, (\tilde{\theta}_i, \tilde{\phi}_i)} , \\ \overline{\beta_N^4} &= \overline{TS^2} \cdot \overline{G_N^4 \, (\tilde{\theta}_i, \tilde{\phi}_i)} . \end{aligned} \tag{A-31}$$

In evaluating (A-27) we will need the first and second moments of (A-28). First,

$$E\left\{\tilde{I}_N\right\} = \frac{e^{-2\alpha \bar{R}_N} I_o}{\bar{R}_N^4} \left[\overline{\left(\sum_{i=1}^{\tilde{K}_N} \tilde{\beta}_{N_i} \sin \tilde{\Phi}_i\right)^2 + \left(\sum_{i=1}^{\tilde{K}_N} \tilde{\beta}_{N_i} \cos \tilde{\Phi}_i\right)^2}\right] . \tag{A-32}$$

Since the random quantities $\tilde{K}_N$, $\tilde{\beta}_{Ni}$, and $\tilde{\Phi}_i$ are independent, and $\tilde{\Phi}_i$ is assumed to be uniformly distributed between 0 and 2π, it is easily shown that

$$\overline{\left[\left(\sum_{i=1}^{\tilde{K}_N} \tilde{\beta}_{N_i} \sin\tilde{\phi}_i\right)^2 + \left(\sum_{i=1}^{\tilde{K}_N} \tilde{\beta}_{N_i} \cos\tilde{\phi}_i\right)^2\right]} = \overline{K_N}\,\overline{\beta_N}^2 \quad . \tag{A-33}$$

Thus,

$$E\left\{\tilde{I}_N\right\} = \frac{e^{-2\alpha\overline{R_N}}\, I_o}{\overline{R_N}^4}\ \overline{K_N}\,\overline{\beta_N}^2 \quad . \tag{A-34}$$

For the second moment:

$$E\left\{\tilde{I}_N^{\,2}\right\} = \frac{e^{-4\alpha\overline{R_N}}\, I_o^{\,2}}{\overline{R_N}^8}\ \overline{\left[\left(\sum_{i=1}^{\tilde{K}_N} \tilde{\beta}_{N_i} \sin\tilde{\phi}_i\right)^2 + \left(\sum_{i=1}^{\tilde{K}_N} \tilde{\beta}_{N_i} \cos\tilde{\phi}_i\right)^2\right]^2} \quad . \tag{A-35}$$

It is shown after much arithmetic that,

$$\overline{\left[\left(\sum_{i=1}^{\tilde{K}_N} \tilde{\beta}_{N_i} \sin\tilde{\phi}_i\right)^2 + \left(\sum_{i=1}^{\tilde{K}_N} \tilde{\beta}_{N_i} \cos\tilde{\phi}_i\right)^2\right]^2} = 2\,\overline{K_N}^2\,\overline{\beta_N}^{2^2} + \overline{K_N}\left(\overline{\beta_N}^4 - 2\,\overline{\beta_N}^{2^2}\right) \quad . \tag{A-36}$$

Thus,

$$E\left\{\tilde{I}_N^{\,2}\right\} = \frac{e^{-4\alpha\overline{R_N}}\, I_o^{\,2}}{\overline{R_N}^8}\ \left[2\,\overline{K_N}^2\,\overline{\beta_N}^{2^2} + \overline{K_N}\left(\overline{\beta_N}^4 - 2\,\overline{\beta_N}^{2^2}\right)\right] \quad . \tag{A-37}$$

Now $\tilde{\varepsilon}_Q$ may be expressed as

$$\tilde{\varepsilon}_Q = \frac{\sum_N \frac{\left(N - \frac{1}{2}\right)}{\psi_N}\, \overline{R_N}^3\, e^{2\alpha\overline{R_N}}\, \left(\tilde{I}_N - \overline{I_N}\right)}{\sum_N \frac{\left(N - \frac{1}{2}\right)}{\psi_N}\, \overline{R_N}^3\, e^{2\alpha\overline{R_N}}\, \overline{I_N}} \tag{A-38}$$

and squaring the above and taking the expected value of both sides yields:

$$E\left\{\tilde{\varepsilon}_Q^{\,2}\right\} = \frac{\sum_N \frac{\left(N-\frac{1}{2}\right)^2}{\psi_N^{\,2}}\,\overline{R_N}^{6}\; e^{4\alpha\overline{R_N}}\left[E\left\{\tilde{I}_N^{\,2}\right\} - E^2\left\{\tilde{I}_N\right\}\right]}{\left[\sum_N \left(N-\frac{1}{2}\right)\frac{\overline{R_N}^{3}}{\psi_N}\; e^{2\alpha\overline{R_N}}\,\overline{I_N}\right]^2} \quad . \tag{A-39}$$

We recall that $\tilde{K}_N$ is a random variable with assumed Poisson distribution with first and second moments given by

$$\begin{aligned} \overline{K_N} &= \rho V_N \quad , \\ \overline{K_N}^{\,2} &= \rho V_N\,(1 + \rho V_N) \quad . \end{aligned} \tag{A-40}$$

where ρ is the target density and V_N is the volume of the N^{th} pulse shell. Also comparing ψ_N, equation (37) in the text, with $\overline{G_N}^{\,2}$ (64-c) we see that

$$\overline{G_N}^{\,2} = \frac{\overline{R_N}}{\pi c \tau\left(N-\frac{1}{2}\right)}\quad \psi_N \quad . \tag{A-41}$$

Substituting expressions (A-31), (A-34), (A-37), (A-40) and (A-41) into (A-39) yields:

$$\sigma_Q^{\,2} = \frac{\sum_N V_N^{\,2} + \frac{1}{\rho}\,\frac{\overline{TS}^2}{\overline{TS}^2}\sum\left(\frac{\overline{G_N}^{\,4}}{\overline{G_N}^{\,2\,2}}\right)V_N}{\left(\sum_N V_N\right)^2} \quad . \tag{A-42}$$

APPENDIX E

PROPAGATION OF SOUND THROUGH A SCATTERING LAYER

REFERENCES:

1. L. L. Foldy: The Multiple Scattering of Waves, Physics Revue, 67, 1945.

2. E. L. Corstensen and L. L. Foldy: Propagation of Sound Through a Liquid Containing Bubbles; The Journal of the Acoustical Society of America, 19, 1947.

3. R. H. Love: An Empirical Equation for the Determination of the Maximum Side-Aspect Target Strength of an Individual Fish; Naval Oceanographic Office, 1969.

4. D. E. Weston: Sound Propagation in the Presence of Bladder Fish; Underwater Acoustics-2, Plenum Press, N. Y.

SUMMARY

The problem of wave scattering by large (random) ensembles of scatterers has been dealt with in some detail in the scientific literature. For a layer consisting of absorption and/or scattering bodies of high density the problem is extemely complex due to the multiple scattering phenomena, and may be approached by a painstaking statistical treatment of scalar wave theory. With some suitable approximations the latter method has yielded results (References 1 and 2) which will be discussed. On the other hand, for a layer where the number per unit volume of significant scatterers is sufficiently small, each scatterer may be treated independently of the other and it is a simple task to derive an expression for the attenuation effect. Also of interest is the measure of density, i.e., when does a scattering layer appear "dense" to an impinging sound wave. This question is directly related to the propagation velocity in the scattering layer, i.e., if the velocity in the scatterer-free medium is very different from that in the layer, the layer appears dense and multiple scattering cannot be neglected.

A. Scattering Parameters

It is useful to introduce a quantity (generally complex) called the scattering coefficient that contains all the information concerning the scattering and absorption characteristics of a point target. The scattering coefficient can be used as a basis to calculate "scattering cross section", "extinction cross section", etc. Consider a (plane) pressure wave $\hat{P}_i$ incident on a point target (Figure 1). If the incident pressure is written:

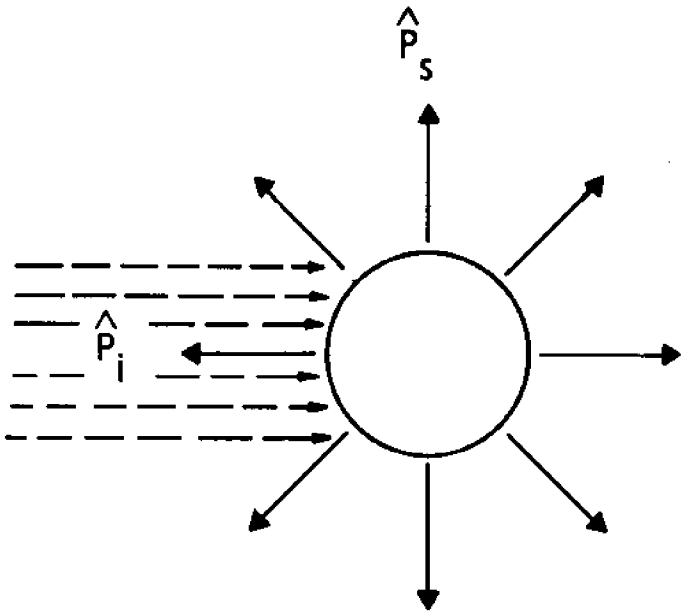

Figure E-1

$$\hat{P}_i = A_i \, e^{-j(\omega_o t + \theta)} \tag{1}$$

where

A_i = peak amplitude of incident pressure

ω_o = frequency

θ = electrical phase of incident wave

The scattered field $\hat{P}_s$ may be written as a function of distance r away from the scatterer:

$$\hat{P}_s(r) = \frac{\hat{G}(\omega_o) \, Ai}{r} \, e^{-j(\omega_o t + k_o r + \theta)} \tag{2}$$

where

$\hat{G}(\omega_o)$ = scattering coefficient

$K_o = \omega_o / c_o$, sound velocity = c_o

r = distance from scatterer

The quantity $\hat{G}(\omega_o)$ is the scattering coefficient written as a function of frequency ω_o and characterizes the properties of the point target by making the strength of the scattered field (pressure) proportional to the incident field acting on it. The quantity $\hat{G}(\omega_o)$ is in general complex*. Mathematically, this results in an amplitude and phase change in the scattered field expression (2), relative to the incidnet field (1). It is shown in Reference 1 that at a frequency ω_o, the scattering cross section σ_s is given by:

$$\sigma_s = 4\pi \left| \hat{G}(\omega_o) \right|^2 \tag{3}$$

The quantity σ_s represents the fraction of the total scattered power to the incident intensity. The target strength TS is given by:

$$TS = \left. \frac{\sigma_s}{4\pi r^2} \right]_{r=1} = \left| \hat{G}(\omega_o) \right|^2 \tag{4}$$

---

* A complex quantity is implied by circumflex ($\hat{}$).

The target strength is the ratio of scattered intensity at unit distance from the target to the incident intensity. The extinction cross section σ_e is given by:

$$\sigma_e = -\frac{4\pi}{K_o} \, IM\left[\hat{G}(\omega_o)\right] \tag{5}$$

where

$$IM\left[\ \right] = \begin{array}{l}\text{imaginary} \\ \text{- part - of}\end{array} \left[\ \right] .$$

σ_e represents the ratio of power absorbed and scattered to the incident intensity. The absorption cross section σ_A is given by:

$$\sigma_A = \sigma_e - \sigma_s \tag{6}$$

represents the ratio of the power absorbed to the incident intensity.

The specification $\hat{G}(\omega_o)$ is sufficient for a single scatterer or group of identical scatterers. Now suppose there are many scatterers of different "size" which though they may be considered point targets cannot each be represented by the scattering function $\hat{G}(\omega_o)$. Usually there is some unique physical dimension associated with each scatterer which determines a $\hat{G}(\omega_o)$ for each scatterer. For example, in the case of a spherical bubble, the scattering coefficient is uniquely determined by its radius. In any case, we will denote this physical quantity by "β" and now express the scattering parameter $\hat{G}$ as

$$\hat{G}(\omega_o) \rightarrow \hat{G}(\omega_o ; \beta) \tag{7}$$

Suppose we are concerned about a uniform layer of scatterers distributed in size over a range of β. (For example, β might be the radius of the swim bladders if we are working with a school of fish.) It is particularly useful to define a set of averaged scattering parameters analogous to equations (3), (4), (5), (6) and (7). In particular, let the average number of scatterers per unit volume (volume density) in a given scattering layer be ρ. Let the average number of scatterers per unit volume with parameter β' lying between β and $\beta + \Delta\beta$ be specified by $N(\beta)\Delta\beta$. Then the following average scattering parameters may be used assuming the distribution function $N(\beta)$ to be defined for all values of β. The average scattering coefficient $\bar{\sigma}_s$ is defined (see equation 3)

$$\bar{\sigma}_s \equiv \frac{1}{\rho} \int_0^\infty 4\pi \left| \hat{G}(\omega_o ; \beta) \right|^2 N(\beta)\, d\beta \qquad (3\text{-A})$$

Likewise, for the other parameters (see equations 4, 5, 6 and 7)

$$\overline{TS} \equiv \frac{1}{\rho} \int_0^\infty \left| \hat{G}(\omega_o ; \beta) \right|^2 N(\beta)\, d\beta \qquad (4\text{-A})$$

$$\bar{\sigma}_e \equiv \frac{1}{\rho} \int_0^\infty - \frac{4\pi}{k_o} IM \left[\hat{G}(\omega_o ; \beta) \right] N(\beta)\, d\beta \qquad (5\text{-A})$$

$$\bar{\sigma}_A \equiv \sigma_e - \sigma_s \qquad (6\text{-A})$$

$$\overline{\hat{G}}(\omega_o) \equiv \frac{1}{\rho} \int_0^\infty \hat{G}(\omega_o ; \beta)\, N(\beta)\, d\beta \qquad (7\text{-A})$$

Using the above averaged quantities we will proceed to examine scattering layers of the simplest shapes.

B. Independent vs Multiple Scattering

Intuitively one feels that if the density and strength of scatterers in a cloud or layer is sufficiently small the multiple scattering effects are negligible and one can proceed to analyze the total effect by treating each scatterer as if it were independent of its neighbors. This is of course the situation and is rigorously shown to be true on the average in many published articles (see References 1 and 2 for example). A pertinent question is how small is "sufficiently small". The work done by L. Foldy (Reference 1), sheds some light on this. It follows from examination of expressions (54) and (55) in Reference 1 that the value of the wave propagation parameter $K_o = 2\pi/\lambda_o$ is subject to change in scattering layers of high density and scattering strengths. Physically, this change in the wave parameter implies a change in sound velocity through the medium. More specifically, the average value of the wave parameter $\hat{K}$ in a scattering layer is related to that of the incident sound wave K_o by the expression:

$$\hat{K}^2 = K_o^2 + 4\pi \int_0^\infty \hat{G}(\omega_o ; \beta)\, N(\beta)\, d\beta \qquad (8)$$

The velocity of sound in the scattering layer is given by:

$$\hat{C} = \frac{\omega_o}{\hat{K}} = \frac{\omega_o}{\left[K_o^2 + 4\pi \int_0^\infty \hat{G}(\omega_o ; \beta)\, N(\beta)\, d\beta\right]^{1/2}} \tag{9}$$

But since $C_o = \omega_o / K_o$, and $K_o = 2\pi/\lambda_o$, it follows from equation (9) that:

$$\hat{C} = \frac{C_o}{\left[1 + \frac{\lambda_o^2}{\pi} \int_0^\infty \hat{G}(\omega_o ; \beta)\, N(\beta)\, d\beta\right]^{1/2}} \tag{10}$$

It has been shown that as $C \to C_o$ the effects of multiple scattering become negligible. Thus, theoretically at least, the magnitude of the term $\hat{\Gamma}$, where:

$$\hat{\Gamma} \equiv \frac{\lambda_o^2}{\pi} \int_0^\infty \hat{G}(\omega_o ; \beta)\, N(\beta)\, d\beta \tag{11}$$

is indicative of the measure of multiple scattering. As defined, $\hat{\Gamma}$ is complex since $\hat{G}(\omega_o ; \beta)$ is in general complex. Examination of expressions (53) through (56) of Reference 1 leads to a range of $\hat{\Gamma}$ for which there is no interference between scatterers (i.e., multiple scattering is negligible). That is, if $\hat{\Gamma}$ is sufficiently small so that we may expand the square root:

$$\frac{1}{\left[1 + \hat{\Gamma}\right]^{1/2}} \approx 1 - \frac{\hat{\Gamma}}{2} \tag{12}$$

then we can ignore the effects of multiple scattering. Expression (12) is good to within a few percent for $|\hat{\Gamma}| < 1/4$, so let us set $1/4$ as a limit on the magnitude of $\hat{\Gamma}$ for which we can ignore the effects of multiple scattering. Since the target strength TS, of most scatterers is usually more accessible than is the scattering coefficient $\hat{G}(\omega_o)$, it is useful to rework condition (13),

$$|\hat{\Gamma}| \leq \frac{1}{4} \qquad \text{(for independent scattering)} \tag{13}$$

in terms of the average target strength $\overline{TS}$ (Equation 4-A). To do this we can use the "Schwarz Inequality" which states that for any two functions $L(\beta)$ and $M(\beta)$:

$$\left| \int_a^b L(\beta)\, M(\beta)\, d\beta \right| \leq \left| \int_a^b |L(\beta)|^2\, d\beta \cdot \int_a^b |M(\beta)|^2\, d\beta \right|^{\frac{1}{2}} . \quad (14)$$

If we let

$$a = 0 \quad , \quad b = +\infty$$
$$L(\beta) \equiv \hat{G}(\omega_o ; \beta)\, N^{1/2}(\beta)$$
$$M(\beta) \equiv N^{1/2}(\beta)$$

and substitute in (14) we get:

$$|\hat{\Gamma}| = \left| \int_0^\infty \hat{G}(\omega_o ; \beta)\, N(\beta)\, d\beta \right| \leq \left| \int_0^\infty |\hat{G}(\omega_o ; \beta)|^2\, N(\beta)\, d\beta \cdot \int_0^\infty N(\beta)\, d\beta \right|^{\frac{1}{2}} \quad (15)$$

but by definitions of $N(\beta)$ and average target strength (Equation 4-A)

$$\int_0^\infty N(\beta)\, d\beta = \rho \qquad (\rho = \text{number of scatterers per unit volume}) \quad (16)$$

$$\int_0^\infty |\hat{G}(\omega_o ; \beta)|^2\, N(\beta)\, d\beta = \overline{TS}\, \rho \quad .$$

Thus it follows from (13) through (16) that if

$$|\hat{\Gamma}| \leq \frac{\lambda_o^2\, \rho}{\pi} \sqrt{\overline{TS}} \leqq \frac{1}{4} \quad (17)$$

expression (17) is sufficient to satisfy (13). Rearranging (17) we have:

$$\rho \sqrt{\overline{TS}} \leq \frac{\pi}{4 \lambda_o^2} \quad . \quad (18)$$

Thus by the inequality (18) we may judge whether the number of scatterers per unit volume, (ρ), is sufficiently small when the average target strength, $\overline{TS}$, is known.

Example: A hypothetical scattering layer of nearly identical fish at a frequency of 50 kHz.

Equation (7) of Reference 3 gives a deterministic expression for the scattering strength σ_s of an individual fish. In MKS units this expression is

$$\sigma_s \simeq .58 \frac{L^{2.41}}{\lambda_o{}^{.41}}$$

where

L = length of fish in meters

λ_o = wavelength in meters

The target strength therefore is:

$$TS = \frac{\sigma_s}{4\pi} = .046 \frac{L^{2.41}}{\lambda_o{}^{.41}}$$

at a frequency of 50 kHz in seawater (C_o = 1500 m/sec) the wavelength is:

$$\lambda_o = 3 \times 10^{-2} \text{ meters}$$

For a fish of $L = .3$ meters

$$TS = \frac{.046\ (.3)^{2.41}}{(3 \times 10^{-2})^{.41}} = 1.1 \times 10^{-2}$$

and by expression (18) the maximum allowable number of fish per cubic meter (ρ) is:

$$\rho = \frac{\pi}{4(3 \times 10^{-2})^2 \left(1.1 \times 10^{-2}\right)^{1/2}} = 8.7 \times 10^3.$$

Obviously 8,700 fish per cubic meters each .3 meters in length is a physical impossibility. However the mathematics is founded on a "point source"

representations of targets and therein, lies the reason for such an unrealistic number. Most of the fish in the sea possess a swim bladder comprising about 1/20 of the total volume. Since the acoustic parameters of fish tissue are practically identical to those of sea water, the point source representation is a very reasonable model. The fact is that the swim bladder dominates acoustic scattering and absorption even away from the low frequency resonant point (see Reference 4).

C. Attenuation Coefficient — Independent Scatter/Absorption

Given the case where the average target strength and density are sufficiently small it is easy to derive the attenuation coefficient for a plane wave propagating through the layer. Consider the situation depicted in Figure 2. The scattering layer is assumed to have thickness δ. A "pencil beam" of itensity I_i is assumed incident on the scattering layer at an angle ϕ. The layer is assumed to be made up of point scatterers, all of which may be represented by an average extinction cross section $\bar{\sigma}_e$ (Equation 5-A). We now proceed to analyze an incremental length "$\Delta \ell$" of the sound beam at an arbitrary point in the layer, (Figure 3). The average number of scatterers ΔN contained in $\Delta \ell$ is

$$\Delta N \simeq \rho A \Delta \ell \tag{19}$$

where

A = cross sectional area of "left" face

ΔA = change in area

The intensity of the power entering $\Delta \ell$ is denoted by "I" and leaving $\Delta \ell$ by $I+\Delta I$. The cross sectional area at the left face is A and the right face $A+\Delta A$.

We may now calculate the power entering, leaving, scattered, and absorbed by the element $\Delta \ell$.

POWER IN THRU RIGHT FACE $= P_{in} = IA$

POWER SCATTERED AND ABSORBED FROM BEAM $= P_{S+A} = I \Delta N \bar{\sigma}_e$

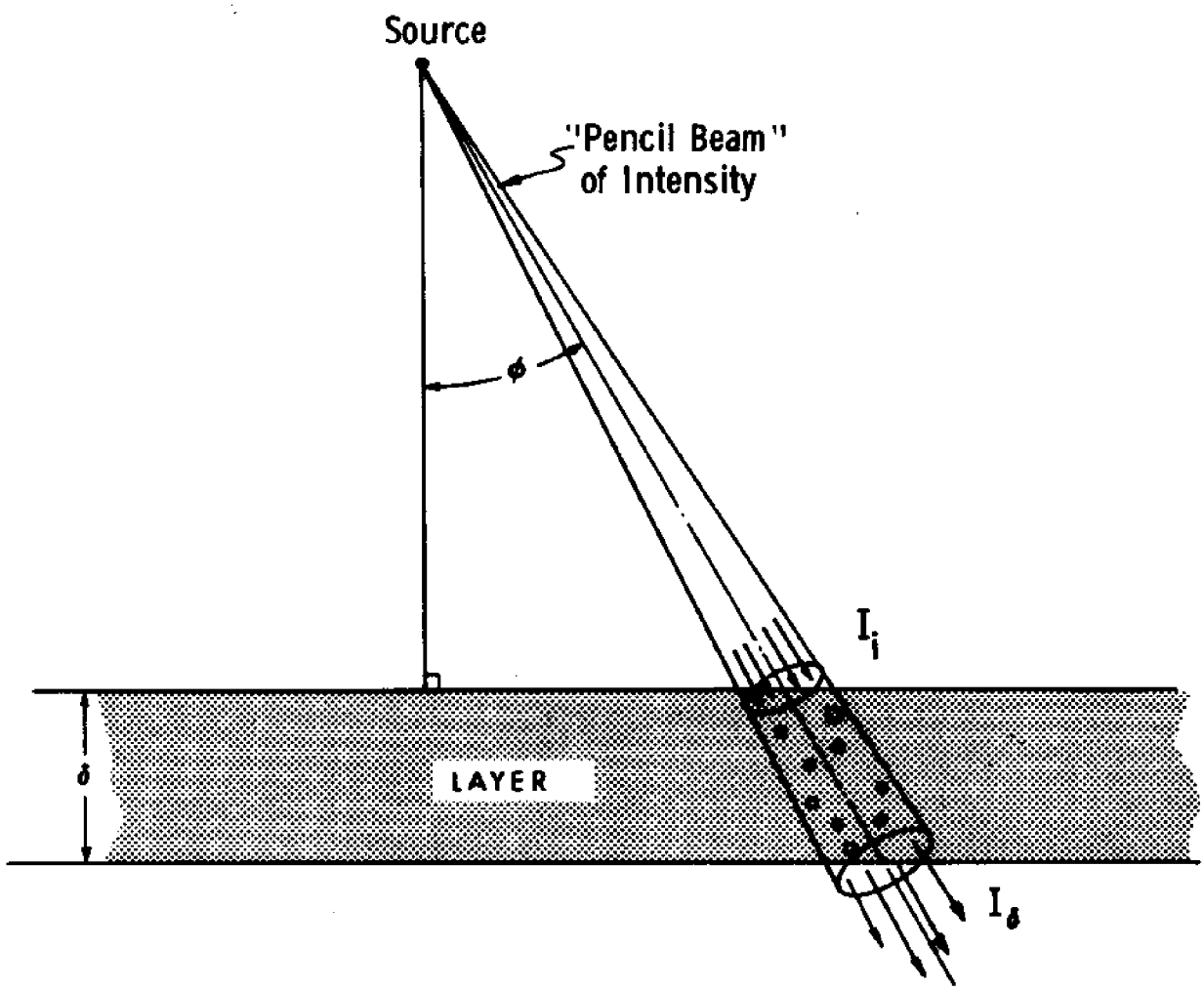

Figure E-2

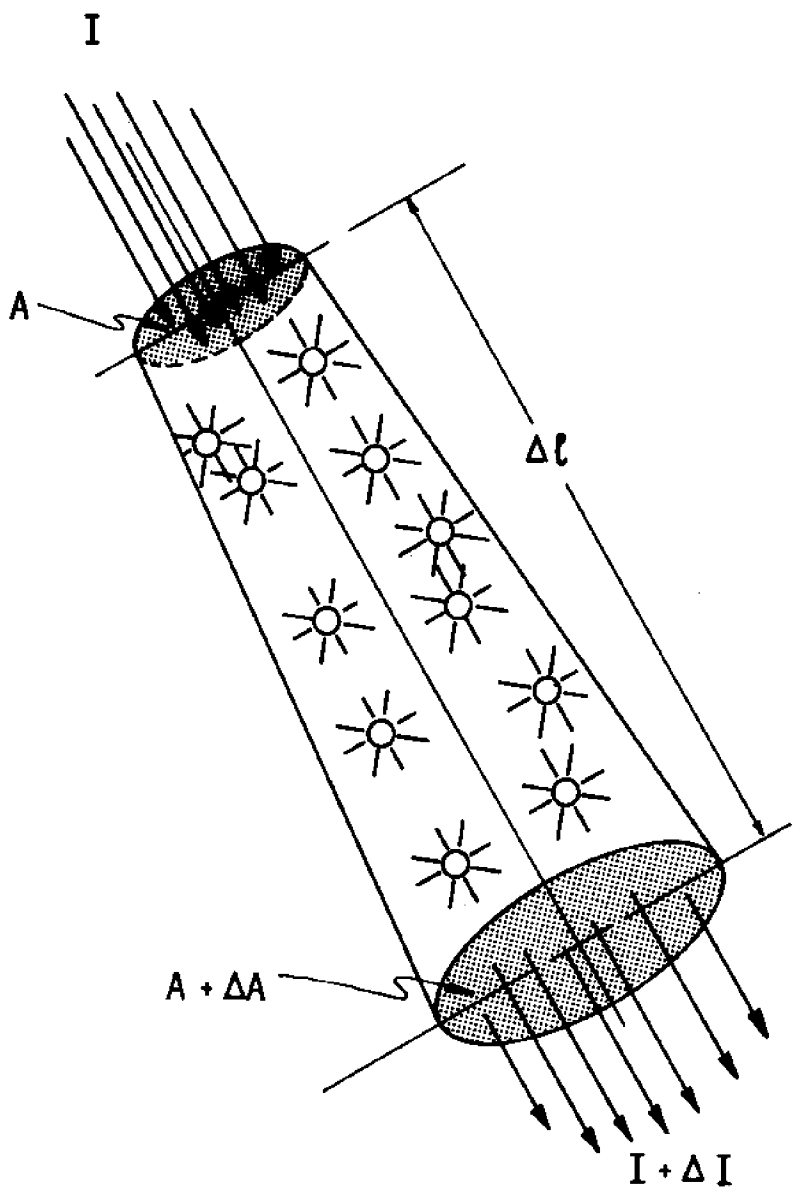

Figure E-3

$$\text{POWER CROSSING LEFT FACE} = P_{out} = (I+\Delta I)(A+\Delta A)$$

By the conservation of energy laws

$$P_{in} = P_{S+A} + P_{out}$$

$$I A = I A \rho \Delta \ell \bar{\sigma}_e + (I+\Delta I)(A+\Delta A) \tag{21}$$

Rearranging terms in (21) and neglecting any Δ^2 (second order) terms we get:

$$\frac{I \Delta A + A \Delta I}{A I} + \rho \bar{\sigma}_e \Delta \ell = 0 \tag{22}$$

Now if we let $\Delta \ell \to 0$, Equation (22) becomes the differential equation:

$$\frac{d\,IA}{IA} = - \rho \bar{\sigma}_e \, d\ell \tag{23}$$

integrating both sides (subscript "δ" denotes for boundary of layer)

$$\int_{I_i A_i}^{I_s A_s} \frac{d\,(IA)}{IA} = - \int_0^{\delta \sec \phi} \rho \bar{\sigma}_e \, d\ell$$

$$\frac{I_\delta}{I_i} = \frac{A_i}{A_\delta} \, e^{- \rho \sigma_e \delta \sec \phi} \tag{24}$$

Since the term A_i/A_δ is the geometric spreading loss, the quantity:

$$\left(e^{- \rho \sigma_e \delta \sec \phi} \right)$$

is that attributable to scattering and absorption out of the sound beam by elements of the scattering layer. This result agrees completely with Foldy's results of a more detailed analysis (Ref. 1, Equation (56)).

D. Attenuation Coefficient – Multiple Scattering Effects

For those scattering layers where the number of scatterers per unit volume and average target strength combine to produce significant multiple scattering, i.e., inequality (18) does not hold, the analysis is extremely complex. It involves solving the scalar wave equation with distinct boundary conditions in a medium of isotropic point scatterers. The reader is referred to References 1 and 2 for the methods of attack and derivation. The results for the same geometry depicted in Figure 2 are:

$$\frac{I_\delta}{I_i} = \frac{A_i}{A_\delta} \; e^{\frac{4\pi\delta}{\lambda_o} \cos\phi \; IM\left[\, 1 + \sec^2\phi \, \hat{\Gamma} \,\right]} \tag{25}$$

where $IM\left[\, 1+\sec^2\phi\,\hat{\Gamma}\,\right]$ denotes the imaginary part of the quantity $\left[\, 1+\sec^2\phi\,\hat{\Gamma}\,\right]$. The term A_i/A_δ merely refers to the geometrical spreading loss. Thus we are left to evaluate the expression $\hat{Q}$ which is defined as:

$$\hat{Q} \equiv \left[\, 1 + \sec^2\phi \, \hat{\Gamma}\right]^{\frac{1}{2}} \quad . \tag{26}$$

Recalling that:

$$\hat{\Gamma} = \frac{\lambda_o^2}{\pi} \int_0^\infty \hat{G}(\omega_o ; \beta)\, N(\beta)\, d\beta \tag{11}$$

and manipulating equations (3) and (5), we can write $\hat{G}(\omega_o ; \beta)$ as:

$$\hat{G}(\omega_o ; \beta) = \left[\frac{\sigma_s}{4\pi} - \frac{\sigma_e^2}{4\lambda_o^2} \right]^{\frac{1}{2}} - j\,\frac{\sigma_e}{2\lambda_o} \quad . \tag{27}$$

Substitution of expression (27) into (11) yields:

$$\hat{\Gamma} = \frac{\lambda_o^2}{\pi} \int_0^\infty \left[\frac{\sigma_s}{4\pi} - \frac{\sigma_e^2}{4\lambda_o^2} \right]^{\frac{1}{2}} N(\beta)\, d\beta - j\rho\lambda_o \frac{\bar{\sigma}_e}{2\pi} \quad . \tag{28}$$

If we define α and γ such that

$$\alpha \equiv \mathrm{Re}\,(\hat{\Gamma}) = \frac{\lambda_o^2}{\pi} \int_0^{\infty} \left[\frac{\sigma_s}{4\pi} - \frac{\sigma_e^2}{4\lambda_o^2} \right] N(\beta)\, d\beta \tag{29}$$

$$\gamma \equiv \mathrm{Im}\,(\hat{\Gamma}) = \lambda_o \rho \frac{\bar{\sigma}_e}{2\pi} \quad .$$

Then Equation (26) becomes:

$$\hat{Q} = \left[1 + \alpha \sec^2\phi + j\gamma \sec^2\phi \right]^{\frac{1}{2}} \tag{30}$$

It can then be shown by algebraic manipulations that:

$$IM(\hat{Q}) = \left[\frac{\left[(\alpha \sec^2\phi + 1)^2 + \gamma^2 \sec^4\phi \right]^{\frac{1}{2}}}{2} - \frac{\alpha \sec^2\phi + 1}{2} \right]^{\frac{1}{2}}. \tag{31}$$

Equation (31) then may be substituted into (25) to give the value of the attenuation coefficient, since by definition:

$$IM(\hat{Q}) = IM\left[\left(1 + \sec^2\phi\, \hat{\Gamma} \right)^{\frac{1}{2}} \right]$$

and thus:

$$\frac{I_\delta}{I_i} = \frac{A_i}{A_\delta}\, e^{(4\pi\delta/\lambda_o)\cos\phi\, IM(\hat{Q})} \tag{32}$$

RESULTS

Expressions (29) through (32) offer a direct, if somewhat laborious method for estimating the average loss of intensity of a sound beam passing through a dense scattering layer of thickness δ. What must be specified are the scattering cross section $\sigma_s(\beta)$, the extinction cross section $\sigma_e(\beta)$ as well as the size distribution $N(\beta)$. If we compared equations (24) and (32) we find that (24) is merely a special case of (32) when the quantity $|\hat{\Gamma} \sec^2\phi| << 1$.

APPENDIX F

COMPENDIUM OF SIMULATIONS AND SUPPORTING ANALYSES

This Appendix briefly describes a number of simulations and analyses developed in the course of an engineering investigation of the application of pulsed hydroacoustic techniques for aquatic biomass measurements.

The simulations and supporting analyses described below have been performed with the aid of an IBM 360-75 Digital Computer. They are coded in the MAC-360 program language. MAC-360 is an algebraic compiler developed at MIT, C. S. Draper Laboratory, for use in digital computations in fields such as dynamics and control theory. MAC is a programming language, designed to simplify the task of describing the mathematics of space mechanics. It features a three-line format, permitting the use of superfields and subfields while preserving their readability. The use of superfields which define vectors and matrices allows a concise and powerful notation of complicated algebraic expressions.

1.0 SIMULATIONS

1.1 FISHSPY II-A

This program synthesizes the echo received from an aggregation of identical or nearly identical point sources of scattered hydroacoustical energy.

The scatterers are assumed to be uniformly distributed between two parallel planes located perpendicular to the acoustic axis of a hydroacoustic transducer. The received echo is assumed to provide a single square pulse of acoustic energy at the working face of the transducer.

The thickness criteria of the scattering layer in this simulation is defined as "thick" if the layer is greater than one half of the transmitted pulse length. The accuracy of this program is optimal for situations where the thickness of layer is not less than twice the length of the transmitted hydroacoustical pulse in water.

Arbitrary inputs to this program include transmitted acoustic source level, transducer voltage response, transmitted pulse time duration, transducer directivity characteristics, average target strength and target array configuration.

The output of this program includes the average incoherent (summation of hydroacoustic intensities) echo signal, an estimate of the peak coherent (summation of hydroacoustic pressures) echo signal and a typical stochastic incoherent echo signal which is the result of a Rayleigh Power distribution generated by a random number routine. A typical program output listing is illustrated in Figure F-1.

The plotted output of this program is the mean or average incoherent intensity and a typical stochastic incoherent intensity versus time. A typical plotted output is illustrated in Figure F-2.

1.2 FISHSPY II-B

This program is similar to FISHSPY II-A except that it operates on a scattering layer of thickness less than the transmitted pulse duration.

The input and output characteristics are identical to FISHSPY II-A.

1.3 FISHSPY II-C

This program is similar to FISHSPY II-A and II-B except that the targets are uniformly distributed throughout a spherical volume of arbitrary dimension located at an arbitrary range from a transducer.

The input and output characteristics are identical to FISHSPY II-A and II-B.

TRANSDUCER APERTURE RAD. 4.1 LAMBDA,TARGET EXTINCTION STRENGTH -50.94 DB.,TARGET STRENGTH -33.00 DB.,TARGET DENSITY 2.0 PER CUBIC METER,SOURCE LEVEL 119.00 DB.,TRANSDUCER VOLTAGE RESPONSE -88.59 DB.,PULSE LENGTH 0.0006 SEC.,RANGE TO SCATTERING LAYER 7 METERS,SCATTERING LAYER THICKNESS 2.0 METERS,EQUIVALENT CONICAL BEAM ANGLE 2.9 DEG.,EST. CRITICAL RANGE 340 METERS,ATTENUATION IN SCATTERING LAYER 0.000 DB. PER METER,COHERENT REFLECTION COEFFICIENT- 120.7 DB.,EST. TRANSDUCER RMS VOLTAGE(COHERENT REFLECTION)- 114.8 DB.,EST. TRANSDUCER RMS VOLTAGE FROM 10 LOG PSI(URICK) - 42.3 DB.,TRANSMITTING FREQUENCY 121.99 KHZ.

$$G(\theta,\phi) = G(\phi) = \left| \frac{2J_1(\frac{\pi d}{\lambda}\sin\phi)}{\frac{\pi d}{\lambda}\sin\phi} \right|^2$$

TIME(2R/C +...) (PULSE LENGTHS)	RECEIVED INTENSITY (DB.)	RMS.VOLTS IN DB. (XDUCER TERMINALS)	MEAN INTENSITY (DB.)	REC.INT./MEAN INT. (DB.)	RANGE VARIATION (AS IN N LOG(R))
0.050	22.289	- 66.310	31.267	- 8.97	24.4573
0.100	31.113	- 57.486	35.278	- 4.16	22.1574
0.150	39.711	- 48.888	37.359	2.35	21.4054
0.200	41.117	- 47.482	38.757	2.36	20.9753
0.250	40.499	- 48.100	39.808	0.69	20.7013
0.300	40.332	- 48.267	40.648	- 0.31	20.5252
0.350	37.547	- 51.052	41.349	- 3.80	20.3968
0.400	34.638	- 53.961	41.949	- 7.31	20.2943
0.450	26.763	- 61.836	42.473	- 15.71	20.2062
0.500	23.098	- 65.501	42.939	- 19.84	20.1297
0.550	27.676	- 60.923	43.357	- 15.68	20.0619
0.600	30.164	- 58.435	43.736	- 13.57	20.0012
0.650	37.184	- 51.415	44.083	- 6.89	19.9460
0.700	33.109	- 55.490	44.402	- 11.29	19.8941
0.750	38.646	- 49.953	44.698	- 6.05	19.8462
0.800	42.042	- 46.557	44.973	- 2.93	19.8012
0.850	45.673	- 42.926	45.231	0.44	19.7586
0.900	46.028	- 42.571	45.472	0.55	19.7180
0.950	45.963	- 42.636	45.700	0.26	19.6791
1.000	47.523	- 41.076	45.915	1.60	19.6416
1.050	48.014	- 40.585	45.974	2.04	19.4799
1.100	48.132	- 40.467	45.957	2.17	19.3342
1.150	47.166	- 41.433	45.932	1.23	19.2729
1.200	47.216	- 41.383	45.908	1.30	19.2175
1.250	48.400	- 40.199	45.883	2.51	19.1618
1.300	47.239	- 41.360	45.859	1.38	19.1070
1.350	48.659	- 39.940	45.834	2.82	19.0466
1.400	49.407	- 39.192	45.910	3.59	18.9924
1.450	49.785	- 38.814	45.785	4.00	18.9370
1.500	49.787	- 38.812	45.760	4.02	18.8833
1.550	49.428	- 39.171	45.736	3.69	18.8299
1.600	48.925	- 39.674	45.711	3.21	18.7768
1.650	48.790	- 39.809	45.687	3.10	18.7240
1.700	48.568	- 40.031	45.662	2.90	18.6716
1.750	47.493	- 41.106	45.638	1.85	18.6194
1.800	44.747	- 43.852	45.614	- 0.86	18.5676
1.850	39.598	- 49.001	45.590	- 5.99	18.5151
1.900	39.037	- 49.562	45.566	- 6.52	18.4639
1.950	40.821	- 47.778	45.542	- 4.72	18.4129
2.000	24.607	- 63.992	45.518	- 20.91	18.3622
2.050	32.936	- 55.663	45.494	- 12.55	18.3112
2.100	31.565	- 57.034	45.470	- 13.90	18.2610
2.150	31.474	- 57.125	45.446	- 13.97	18.2111
2.200	23.642	- 64.957	45.422	- 21.78	18.1613
2.250	38.651	- 49.948	45.399	- 6.74	18.1119
2.300	31.508	- 57.091	45.375	- 13.86	18.0628

Figure F-1. Input and Output Listing-FISHSPY II-A

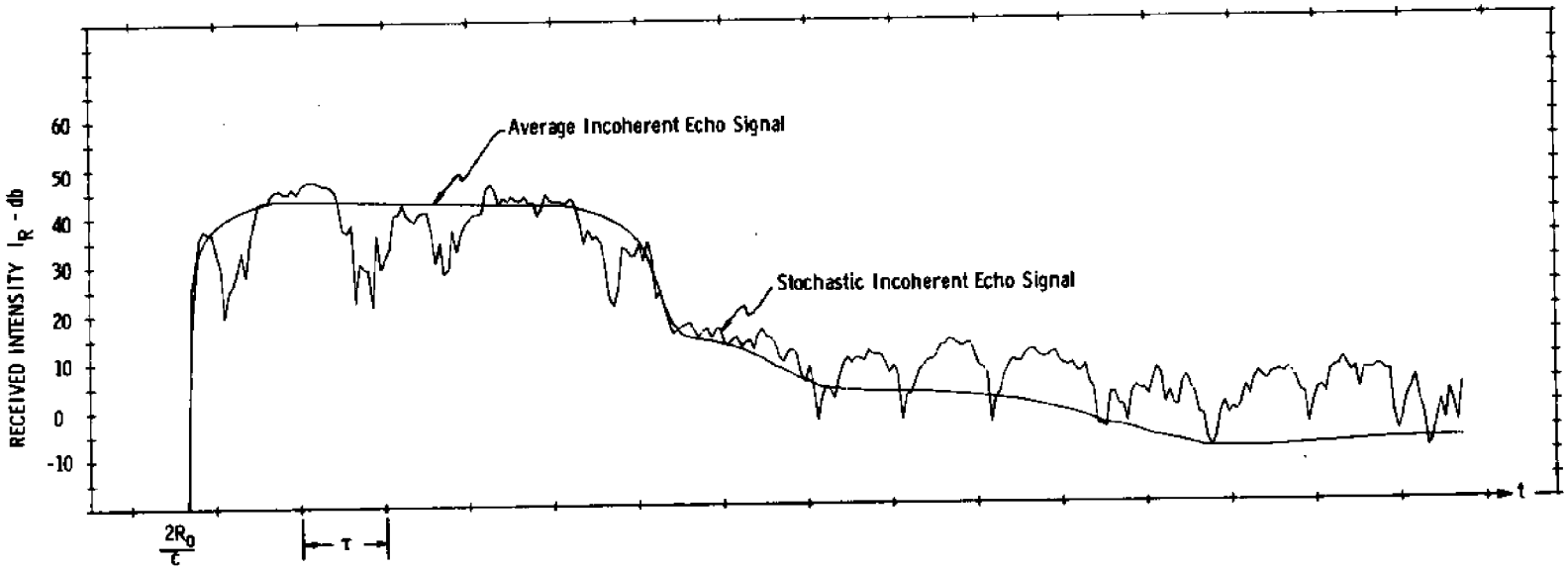

Figure F-2. Output Plot- FISHSPY II-A

2.0 SUPPORTING ANALYSES

2.1 $\hat{Q}$-PROGRAM

This program reduces the voltage data produced by a hydroacoustic echo signal from a scattering layer of infinite expanse. The output consists of an unbiased estimate of the density of the layer and the estimated number of scatterers.

The input to the program includes the average target strength of the scatterers and the transducer characteristics, such as directivity function, source level, pulse length and voltage response.

The voltage data to be reduced must be in a digital sequence either on cards or on magnetic tape.

2.2 ERROR PROGRAM

This program computes the mean squared error associated with the $\hat{Q}$ estimators presented in the note.

The output consists of a printout of the normalized variance error for echo envelope sampling and integration techniques.

The input includes scattering layer depth, transducer directivity, target strength variance and transmitted pulse time duration.